PLOS ONE

RESEARCH ARTICLE

Distinct microglial transcriptomic signatures within the hippocampus

Sana Chintamen[1☯], Pallavi Gaur[2☯], Nicole Vo[2], Elizabeth M. Bradshaw[2], Vilas Menon[2], Steven G. Kernie[1,2]*

1 Department of Pediatrics, Columbia University College of Physicians and Surgeons, New York, New York, United States of America, **2** Department of Neurology, Columbia University College of Physicians and Surgeons, New York, New York, United States of America

☯ These authors contributed equally to this work.
* sk3516@cumc.columbia.edu

Citation: Chintamen S, Gaur P, Vo N, Bradshaw EM, Menon V, Kernie SG (2024) Distinct microglial transcriptomic signatures within the hippocampus. PLoS ONE 19(1): e0296280. https://doi.org/10.1371/journal.pone.0296280

Editor: Giuseppe Biagini, University of Modena and Reggio Emilia, ITALY

Received: June 10, 2023

Accepted: December 8, 2023

Published: January 5, 2024

Peer Review History: PLOS recognizes the benefits of transparency in the peer review process; therefore, we enable the publication of all of the content of peer review and author responses alongside final, published articles. The editorial history of this article is available here: https://doi.org/10.1371/journal.pone.0296280

Data Availability Statement: All relevant data are within the manuscript and its Supporting information files.

Funding: This research was supported by National Institutes of Health/National Institute of

Abstract

Microglia, the resident immune cells of the brain, are crucial in the development of the nervous system. Recent evidence demonstrates that microglia modulate adult hippocampal neurogenesis by inhibiting cell proliferation of neural precursors and survival both *in vitro* and *in vivo*, thus maintaining a balance between cell division and cell death in the neural stem cell pool. There are increasing reports suggesting these microglia found in neurogenic niches differ from their counterparts in non-neurogenic areas. Here, we present evidence that hippocampal microglia exhibit transcriptomic heterogeneity, with some cells expressing genes associated with neurogenesis. By comprehensively profiling myeloid lineage cells in the hippocampus using single cell RNA-sequencing, we have uncovered a small, yet distinct population of microglia which exhibit depletion in genes associated with homeostatic microglia and enrichment of genes associated with phagocytosis. Intriguingly, this population also expresses a gene signature with substantial overlap with previously characterized phenotypes, including disease associated microglia (DAM), a particularly unique and compelling microglial state.

Introduction

The hippocampus is important for memory consolidation as well as declarative and spatial memory and learning [1–3]. Hippocampal function is also known to be affected early or more severely in a variety of neurodegenerative and psychiatric diseases. These include Alzheimer's disease (AD), epilepsy, and major depressive disorder, which all are known to exhibit alterations in immune activity and each manifest hallmark traits of inflammation [4–7]. Subsets of immune cells show proclivity towards disease progression in both the rodent and human brain [8–10]. Thus, characterizing various immune subsets in the hippocampus is crucial for uncovering mechanisms of disease development and progression.

Under resting conditions, the immune compartment of the central nervous system (CNS) is comprised of myeloid lineage cells, microglia and other macrophages which contain distinct transcriptomic and phenotypic properties [11, 12]. The latter of the two are typically found in the meninges, perivascular regions, and choroid plexus [13]. Collectively, these non-microglial

Neurological Disorders and Stroke Grants R01-NS-095803 (SGK) and the Paul Allen Foundation (SGK), and National Institute of Aging Grant R01-AG-066831 (VM). This research was funded in part through the National Institute of Health and National Cancer Institute (NIH/NCI) Cancer Center Support Grant P30CA013696 and used the Genomics and High Throughput Screening Shared Resource. Research reported in this publication was performed in the CCTI Flow Cytometry Core, supported in part by the Office of the Director, National Institutes of Health under awards S10OD020056. The content is solely the responsibility of the authors and does not necessarily represent the official views of the National Institutes of Health. Images were collected and/or image processing and analysis for this work was performed in the Confocal and Specialized Microscopy Shared Resource of the Herbert Irving Comprehensive Cancer Center at Columbia University, supported by NIH grant #P30 CA013696 (National Cancer Institute). The funders had no role in study design, data collection and analysis, decision to publish, or preparation of the manuscript.

Competing interests: The authors have declared that no competing interests exist.

macrophages are termed CNS-associated macrophages (CAMs) or Border Associated Macrophages (BAMs) [11, 12]. However, as microglia are the primary macrophage in the brain parenchyma and found to be actively interacting with neurons, they are more widely studied and characterized compared to macrophages in non-parenchymal tissue, particularly in the context of neurodevelopmental processes. During early postnatal development, the brain is highly plastic and microglia exhibit a great degree of heterogeneity. In contrast, previous studies in the adult rodent brain have shown limited heterogeneity, corresponding to a time point when the brain is less plastic [10, 14, 15]. However, since neurogenic niches undergo life-long development, immune cells show phenotypic differences that correlate with a specialized need to support these regions [16–18]. Increasing evidence demonstrates that microglia actively regulate adult hippocampal neurogenesis [19, 20], and in fact, immune input has been shown to alter neurogenesis during injury, stroke, and aging [21]. Importantly, adult hippocampal neurogenesis (AHN) is key in certain forms of spatial memory and learning, memory consolidation, and recovery from injury [22]. Deficits in AHN in the murine and human brain have been found in a host of neurodegenerative diseases such as depression, Alzheimer's Disease, and age-associated cognitive deficits [23–26]. This suggests that attenuating reductions in neurogenesis may prevent the cognitive decline associated with aging or neurodegeneration [27].

Bulk sequencing experiments show subtle differences in various genes between subregions in the hippocampus [16]. Single cell transcriptomic profiling of cells in the dentate gyrus has demonstrated that immune cells minimally express common microglia markers and more highly express some genes associated with microglial activation [28]. This necessitates a direct comparison between various populations within the hippocampus at the single-cell level to provide relative information on how immune cells are specialized to support the neurogenic niche. In this study, we leverage transcriptomic profiles from myeloid lineage cells in the hippocampus at the level of single cells to resolve heterogeneity previously obscured in bulk sequencing/profiling.

Our experimental paradigm profiles over 18,000 cells from twelve murine hippocampi to resolve heterogeneity in the myeloid landscape of the adult hippocampus. In doing so, we have a substantially higher number and resolution of hippocampal myeloid cells than previously reported [14, 16, 28]. Consequently, we uncovered rare populations that reside in the hippocampus and have previously not been identified. Here, we identify a unique subset or population of cells that correspond to myeloid cells in the subgranular zone, which shape, regulate and/or support the pool of hippocampal neural progenitor cells. By examining these cells within the myeloid cell pool in the hippocampus, not only are we able to make a direct comparison to other subsets of microglia, but we also can examine other populations that may influence the neurogenic niche, even when not in direct contact with stem/progenitor cells in this region. This novel and comprehensive transcriptomic study, with single cell resolution, uniquely highlights genes involved in immune activation and neuronal development and support that provides insight into how the neurogenic niche is regulated in development and disease.

Materials and methods

Animals

All experimental procedures were in accordance with the Guide for the Care and Use of Laboratory Animals of the National Institutes of Health and approved by the Institutional Animal Care and Use Committee at Columbia. Experimental animals were humanely housed and cared for under the supervision of the Institute of Comparative Medicine at Columbia University. For generation of the dual reporter mice, Cx3Cr1CreERT2+/+ (Jackson stock no. 021160)

males were bred with Rosa26-loxp-stop-tdtomato+/+ females, resulting in progeny (F1) that were heterozygous for both the Cre recombinase and the flox-stop tdTomato reporter (Jackson stock 007914). Mice from F1 were crossed mice from F2 that were homozygous for the CreERT2 and tdTomato were selected as breeders. Finally, these mice were crossed with Nestin-GFP mice developed by us (Jackson stock no. 02967), resulting in progeny (F3) that were heterozygous for each of the 3 alleles of interest, the Cx3Cr1CreERT2, Rosa26-tdtomato, and TK-Nestin-eGFP. See S1 Fig [29].

Microglial isolation

Seven-week old dual reporter mice were injected with Tamoxifen (100mg/kg) intraperitoneally once a day for four consecutive days. Each sequencing sample replicate comprised of four bilateral hippocampi from two female and two male, eight week old mice. We had a total of three replicates for single cell RNA-sequencing, resulting in cells analzyed from twelve bilateral hippocampi. Our data set consists of cells from hippocampi originating from a total of six male mice and six female mice. Mice were perfused with approximately 25–30 mL of ice-cold sterile PBS (Corning Cellgro REF 21-040-CV) under general isoflurane anesthesia to minimize pain and suffering. Each brain was extracted whole and placed in 5 mL of homogenization buffer (see buffers list) at 4˚ while other mice were being perfused. After all brains were extracted, hippocampi were dissected on a sterile petri dish placed atop a cold metal platform on top of ice brick to ensure brains remain cold throughout. Each brain was hemisected along the midline using a sterile scalpel. Using curved forceps with sharpened ends, bilateral hippocampi were dissected from each hemisphere of each mouse and bilateral hippocampi from each of the four mice were pooled together in a 2 mL dounce with 1 ml of sample buffer (see buffer list). Cortical tissue was also dissected to be used for setting up sample gates during FACS.

Following homogenization, we adapted the isolation protocol from Bohlen et. al. 2018 [30]. In brief, cell suspensions were filtered by passing through a 70um filter. Samples were transferred to 2 mL eppendorf tubes coated with 10% sterile filtered FBS in PBS (to prevent cell adhesion on tubes) and centrifuged. Pellets were suspended in 1.8 mL myelin removal buffer. Myelin removal beads were briefly vortexed. 200 μL of myelin removal beads were added to each sample and incubated over ice for 15 minutes with gentle flicking every 5 minutes to mix settled beads. The reaction was stopped after incubation period by diluting with 2 mL of myelin buffer per sample. Samples were transferred to 2 mL Eppendorf tubes and centrifuged. Pellets were resuspended in MACS buffer (1ml buffer/pellet). After LS columns were washed twice with flow through discarded, cell suspension was applied to columns (1 tube/LS column). LS columns were washed to elute remaining cells adhering to columns. Flow through containing demyelinated cells were transferred to 2 mL eppendorf tubes and centrifuged. Pellets were resuspended in 1 mL Sterile PBS and incubated with 1 μl Live/Dead Violet per sample for 5 minutes covered from light over ice. Samples were centrifuged, resuspended in flow buffer (containing RNAsin and DNase), and transferred to 5 mL polypropylene tubes for FACS.

Flow cytometry

Samples were sorted on BD Influx at the Columbia Center for Translational Immunology Flow Cytometry core. Between 113,00–132,000 cells were retrieved per sort sample. Samples were of high viability and yield. Gates were established as illustrated in Fig 1B. Cells were first selected by size and granularity (FSC and SSC, respectively). Next cells were gated to exclude doublets. Subsequently, cells were gated for viability and finally gated for td-Tomato

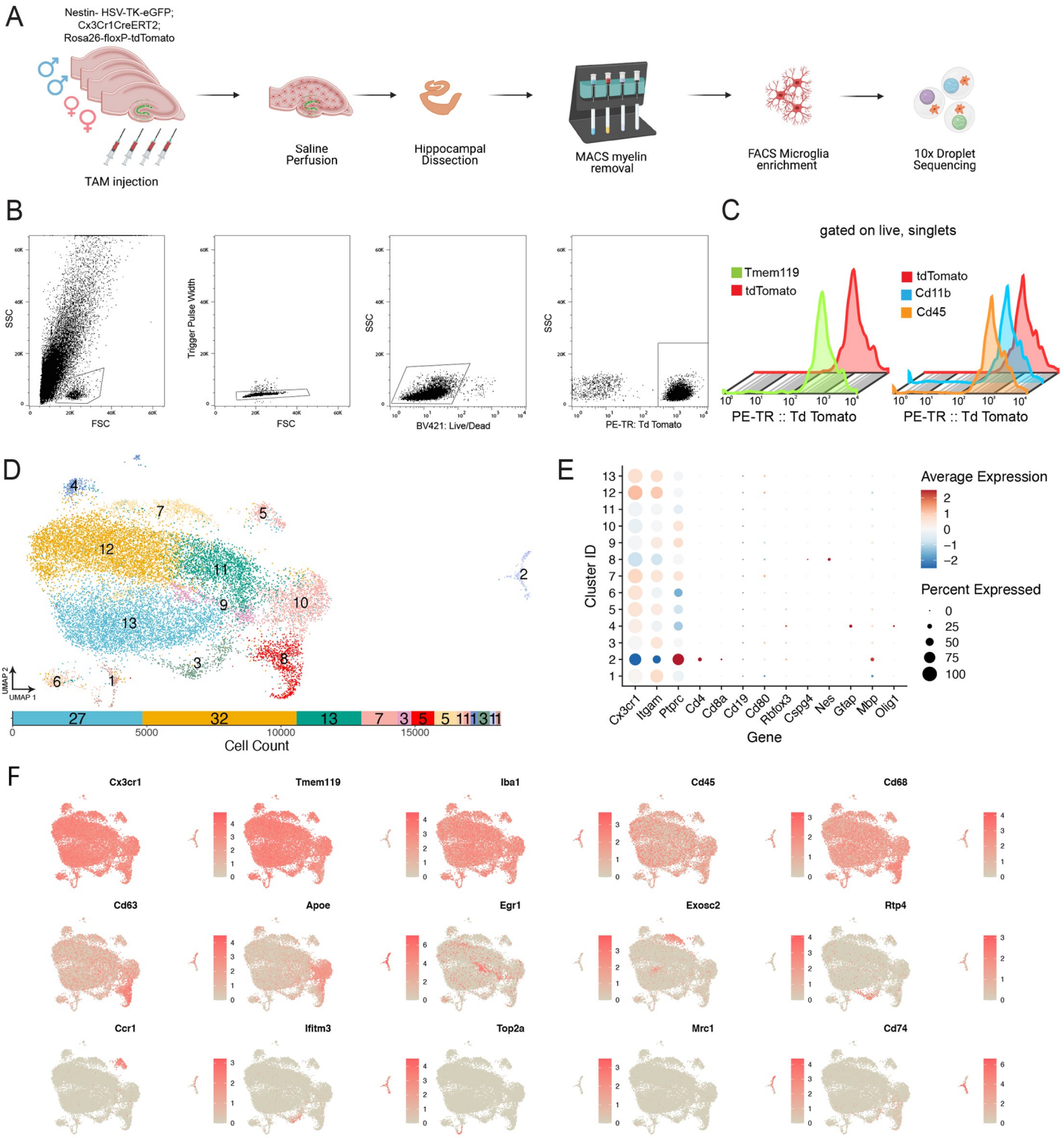

Fig 1. Transcriptomic Heterogeneity of myeloid population in the hippocampus. (A) Schematic illustrating experimental workflow and double reporter mouse model used in single cell sequencing experiments. (B) Fluorescent Activated Cell Sorting (FACS) gating scheme to isolate tdTomato+ cells. (C) Flow cytometry analysis of cells expressing Tdtomato with Tmem119 antibody(left) or CD11b/CD45 (right). (D) Top: UMAP Plot showing dimensionality reduction, colored by Seurat clusters. Each dot represents a cell. Bottom: Bar Plot showing distribution of cells across clusters to show cell count in each cluster (right to left starting with cluster 1). Percentage of cells in each cluster labeled within bar. (E) Dot Plot displaying expression of marker genes for cell types found in the brain across clusters. Each row represents a cluster while each column represents the level of expression of a selected gene marker. The fraction of cells in a given cluster is represented by the size of

the dot. The color of the dot represents the average expression of the cells within a given cluster. (F) UMAP projection displaying scaled expression of previously identified gene markers to investigate heterogeneity in hippocampal myeloid cells.

https://doi.org/10.1371/journal.pone.0296280.g001

expression. TdTomato+ cells were validated using cd11b (1:100 BD biosciences 557396) and cd45 (1:50 BD Biosciences 59864) and Tmem119 (1:100 abcam ab225495). Antibodies serving as isotype controls against both FITC (BD 400607) and APC (BD 402205) were used to determine nonspecific binding of antibodies.

Sequencing

Single-cell 3′ library construction and library pooling. After samples were sorted, suspensions were spun down and resuspended at a final concentration of 1000 cells /μL with between 90,000–13,000 cells. Cell viability was confirmed with trypan blue after resuspension. Between roughly 30,000–40,000 cells were loaded onto 10x Chromium Controller. Libraries were constructed as per manufacturer's (10x Genomics) instructions. Samples were sequenced at the Columbia Sulzberger genomics core. Chemistry Single Cell 3' v3. Cell ranger v 3.0.2 for Run 1, 3.1 for Run 2 and 3. Live cell suspensions were loaded onto GEM droplets. Pooled 3'-end libraries were sequenced on NovaSeq 6000.

Analysis

Single-cell RNA-seq preprocessing and alignment. Read alignment to reference transcriptome mm10 was performed using Cell Ranger v 3.0. At least 94% of reads were mapped to genome. Cells were filtered using default parameters for UMI counts. Counts matrices were generated and further preprocessed as outlined below.

Normalization and integration. Preprocessing of the transcriptomic data was performed using CellRanger version 3.0.2 for the first sample and version 3.1.0 for the subsequent two samples using default parameters. Count matrices were then exported to Seurat version 4.0.0 to create a list of Seurat objects for each sample. To attain this, the raw gene-UMI matrix from each sample was converted to corresponding Seurat object in R 4.0.3 using Read10X function from Seurat package and a list of all Seurat objects was created. To avoid confounding effects due to low quality cells, we used a standard criterion of excluding cells with higher than 20% of total UMIs from mitochondrial genes, less than 1,000 features (nFeature_RNA), and less than 2500 transcripts (nCount_RNA) before proceeding further for normalization and integration (S1 Table).

To remove the potential influence of technical effects in the analyses, we normalized the raw data using function SCTransform separately for each dataset within the Seurat pipeline; this uses Pearson residuals to harmonize the data instead of regular log-normalized expression values. We regressed out percentage of mitochondrial genes expressed this metric from influencing clustering results.

Next, by running PrepSCTIntegration function that calculates all Pearson residuals, we proceeded to identify anchors and integrate the datasets using FindIntegrationAnchors and IntegrateData functions respectively. The anchor as well as integration dimension was set to 30, using 3000 features total.

Dimensionality reduction and clustering. After count normalization and integration, we used the RunPCA function in Seurat for Principal Component Analysis and proceeded with 20 principal components for further clustering and visualization; this value was selected based on the elbow plot cutoff (S3 Fig) for significant components.

The function FindClusters from the Seurat package was used for *K*-nearest neighbor clustering with a resolution parameter of 0.5. For the visualization of integration and clustering onto a 2D space, we used uniform manifold approximation and projection (UMAP) by implementing as implemented in the Seurat functions RunUMAP, DimPlot, and UMAPPlot.

Identification of cluster markers via differential expression analysis. We used Seurat's FindAllMarkers function, which implements the non-parametric Wilcoxon rank sum test, to inspect differentially expressed genes by comparing a single cluster of interest with all others. We only tested the genes that were observed to be positively (up) regulated in minimum fraction of at least 70% cells in the cluster of interested showed at least ~1.5(logfc = 0.5) fold change between cluster of interest and all other groups, with an FDR-adjusted p-value <0.01.

Gene enrichment analysis of differentially expressed genes. We used TopGO to find enriched Gene Ontology (GO) terms for high variance genes obtained in differential expression analysis. We ran TopGO with the Kolmogorov-Smirnov test and considered terms with a statistical significance of <0.05 (adjusted p-value).

Comparison of novel cluster 8 and homeostatic clusters (12 and 13) with Keren-Shaul et al. disease-associated microglia data set. We compared the transcriptomic profiles of SGZ (cluster 8) and homeostatic clusters (cluster 12 and 13) to microglia subtypes signatures found in Keren-Shaul et. al.'s study (GEO: GSE98969). The primary goal of the integration was to compare the unique signature found in SGZ-enriched cluster with the disease-associated microglia (DAM) signature identified by the group.

We used Harmony to integrate our data with the Keren-Shaul et. al. data by passing a merged Seurat object consisting of all selected microglial cells from both datasets and following the standard pipeline through PCA. We then ran the *RunHarmony* function on the normalized data, where we ran 10 rounds of iteration with default values of theta and lambda to achieve the corrected harmony coordinates. We used the first 10 dimensions from the Harmony integration to generate the UMAP and run nearest neighbor analyses, using a resolution of 0.7 with the harmony embeddings rather than PCs. We investigated the expression of genes known to be downregulated in DAM profile to map the cluster associated with unique signature found in SGZ-enriched cluster in the integrated dataset.

Data and code availability. Single cell sequencing analysis was done primarily using Seurat version 4.0.0. Scripts and code are available on GitHub at https://github.com/sanachintamen/HC_myeloid. Raw BAM files and Cell Ranger processed gene expression matrices are available in the NCBI GEO databank with accession number GSE182289.

Brain sectioning and immunohistochemistry

Mice were perfused with PBS followed by 4% paraformaldehyde. Brains were dissected and post-fixed over night at 4˚C. Free floating sections were cut with 50 μm thickness on Leica 1000S vibrating blade microtome. Sections were permeabilized in 0.3% PBST followed by 1 hour incubation with 5% Normal Donkey Serum at RT. Samples were then incubated overnight in primary antibody at the following concentrations 1:500 Iba1 (Wako 019–19741), 1:100 Cd68 (Biorad MCA1957), 1:200 Cd9 (BioLegend 124802) at 4˚C. The next day, sections were washed thrice with PBST for 5 minutes at room temperature. Afterwards, they were incubated with secondary antibody staining solution containing secondary antibodies at a final concentration of 1:200 (Jackson immunoresearch). Sections were incubated in secondary antibody solution for two hours at room temperature after which they were washed thrice in PBST and twice in PBS. Sections were then mounted using LifeTechnologies Prolong mounting medium containing DAPI or NucBlue.

Imaging and analysis

Images for Sholl Analysis were obtained using a Laser Scan confocal microscope (TCS SP8, Leica). Cells for reconstruction were obtained from a single section originating from one eight-old week male mouse. Z-stack images were acquired at 0.5μm intervals. Images were projected across z-planes for representative images. Cells were traced in a semi-automated manner in 3D using Neurolucida. Dendritic complexity was measured using intersections at 10 μm radii were used to determine microglial process ramification. These intersections were summed for each cell to obtain the total number of intersections and compared using an unpaired, Type 2 t-test. For confocal imaging of sections from dual reporter mice, Nikon Ti Eclipse inverted with Yokogawa CSU-X1 spinning disk was used to minimize photobleaching. Images were obtained using 25x water of 40x air objectives. Images were stitched together using NIS-Elements. Epifluorescent images were acquired with a Zeiss microscope (Axio Imager M2, Zeiss) equipped with a Hamamatsu camera (Orca-R2, Hamamatsu).

Results

Single cell sequencing of myeloid cells in the hippocampus

The brain immune compartment consists primarily of innate immune cells which include microglia (the predominant cell type) as well as other CNS-associated macrophages. To dissect cellular interactions between immune cells and neural progenitor/precursor cells in the neurogenic niche, we utilized a double reporter mouse model expressing eGFP under the control of the Nestin promoter and tdTomato conditionally active in cells expressing the fractalkine receptor (CX3CR1) and CreERT2 [31] (S2 and S3 Figs). These double reporter mice were used for both transcriptomic and histology experiments (Fig 1A). We isolated tdTomato+ myeloid lineage cells for single cell RNA-sequencing (Fig 1B). We validated the reporter line using flow cytometry analysis using antibodies common for microglia and showed near complete overlap with $Cd11b^{hi}/Cd45^{lo}$ cells as well as $Tmem119^{+}$ cells (Fig 1C and S1 Fig).

Single cell RNA-sequencing experiments were conducted to determine which cells compose the myeloid landscape of the hippocampus. For each experiment, four hippocampi of tdTomato positive mice (two male, two female) were pooled and enriched for tdTomato-positive myeloid lineage cells, which were then sequenced with three technical triplicates, yielding cells from the hippocampi of twelve mice in total.

The pre-processing of the data yielded 20,376 combined cells from all samples. To filter out cells with low quality, we excluded cells whose UMI counts were fewer than 2,500; comprised of higher than 20 percent of mitochondrial genes; and reflected less than 1,000 unique features (S1 Table and S2A Fig). We checked the percentage of genes encoding ribosomal protein which were consistently acceptable throughout each sample (S2A Fig). The remaining 18,198 cells were included in downstream normalization, analysis, and integration (S2 Fig). We applied Canonical Component Analysis (CCA)-based integration on our integrated dataset to account for batch effects and found that cells from different batches mixed together across all major cell types after applying CCA. Subsequently, we conducted principal component analysis for dimensionality reduction with the number of principal components set using an elbow plot (S2 Fig) in order to cluster myeloid cells based on transcriptome profiles; this approach (see Methods) yielded 14 clusters. However, since two of these clusters yielded virtually no differences in differential gene expression analysis, we merged them which then totaled 13 clusters. These are illustrated in Fig 1D and we refer to these clusters as such for downstream analysis. As further quality control checks, we applied cell cycle scoring to our dataset to determine whether cell proliferation status greatly influenced clustering (S2 Fig). It should be noted

that this scoring method has been developed on human genes as a reference for cell cycle status. This may be a caveat as we converted these lists to their mouse homologs and performed this analysis. As microglia do not rapidly turnover in the homeostatic brain, the majority of cells are not dividing and hence not in S-phase with the exception of cells from cluster 1 [32]. However, we chose to not regress out the cell cycle scores as microglial proliferation itself marks immune activation and the number of proliferating cells at baseline levels may serve as a useful reference to compare with disease and injury model systems. We also used DoubletFinder to check for potential doublets (S2C Fig). Predicted doublets with this method were not restricted to any one cluster, suggesting that their removal would not impact clustering results in a significant manner.

Cells from all clusters expressed common marker genes such as *Cx3cr1*, *Cd11b* (*Itgam*), and *Cd45* (*Ptprc*) that are known to be enriched in myeloid lineage cells such microglia and other macrophages (Fig 1E). We next plotted relative transcript levels of marker genes found broadly in myeloid lineage cells (*Iba1* aka *Aif1*), monocytes (*Ccr2*), and those specific to microglia (*Tmem119, P2ry12, and Hexb*; S3C Fig). Some clusters had small fractions of cells with negligible levels of marker genes from other immune cells such as T cells (*Cd4*, *Cd8a*), B cells (*Cd19*, *Cd80*), neurons (*Rbfox* aka NeuN), NG2 glia (*Cspg4*), neuronal stem cells (*Nes*, *Gfap*), astrocytes (*Gfap*), and oligodendrocytes (*Mbp* and *Olig1*) but in large part these transcripts are not detected at appreciable levels or in most cells (Fig 1E). These may reflect material from adjacent cells in close association with isolated microglia or alternatively transient expression of these genes as is the case in newly formed microglia with *Nestin* expression [33]. In addition, we examined in further detail marker genes to resolve types of myeloid lineage cells. We noted relatively consistent levels of microglial specific genes such as *Tmem119*, *P2ry12*, and *Hexb* (S3 and S4 Figs) across most clusters with the exception of two clusters which we describe in greater detail below.

We next determined whether there were sex-specific differences in the transcriptome profiles of cells originating from male versus female samples. To do this, we plotted *Xist* expression, a gene expressed specifically by the inactivated X chromosome in female cells (S5 Fig). We found that cluster 14 is the only cluster primarily comprising female cells and that *Xist* expression separates cluster 13 from clusters 11 and 12 (S4 Fig). Based on the expression of known genes, we designated these three clusters as homeostatic clusters. We then tested whether there were significant differences in gene expression related to immune function in these putative homeostatic clusters (Table 1). We found that none of the differentially expressed genes reflect significant changes in immune function between cells of male and female origin in these homeostatic populations.

To assess whether these clusters truly distinguish cells based on biological differences, we next performed differential gene expression analysis between clusters (Table 1 and S4 Fig). Due to the high enrichment of classical microglia-specific genes- *Tmem119*, *P2ry12*, *Selplg*- and low numbers of differentially expressed genes, we concluded that clusters 11,12, and 13, which represent about 72 percent of cells in the data set, reflect a homeostatic gene expression profile [34–36]. We also inspected some key genes previously identified to be implicated in immune dynamics (Fig 1F) and then delved deeper into different transcriptomic clusters to determine to what extent these clusters reflect distinct populations [10, 12, 15, 34].

Clusters 4,5, and 6 did not meet the threshold for differential gene expression for gene set enrichment analysis. These clusters failed to show enrichment of at least ten nuclear genes. Cluster 4 shows high expression of mitochondrial genes. While these cells passed the threshold during processing, they may be indicative of cells that are lower quality. Cluster 5 was observed to express high levels of *Ccr1* and upregulate *Tmem176a*. These genes are found in border macrophages transitioning to a microglia-like state [15]. However, in our dataset these cells

Table 1. Differences in gene expression related to immune function in these putative homeostatic clusters.

	p_val	avg_log2FC	pct.1	pct.2	p_val_adj	cluster	gene
Stmn1	1.405487958053E-206	3.07876097378747	0.832	0.131	4.36446175614199E-202	1	Stmn1
Hmgb2	8.60450362450788E-99	2.39413825583662	0.8	0.231	2.67195651051843E-94	1	Hmgb2
Ptma	1.51259994061616E-54	1.07018770963932	0.995	0.898	4.69707659559536E-50	1	Ptma
Dek	2.84321008688058E-51	1.36450422401494	0.805	0.381	8.82902028279026E-47	1	Dek
Tuba1b	2.5211811959346E-44	1.27690413462073	0.935	0.659	7.82902396773573E-40	1	Tuba1b
Tubb5	5.49430629964004E-44	1.45491436717803	0.919	0.674	1.70614693522722E-39	1	Tubb5
Slbp	2.9995279292458E-43	1.13787083025338	0.703	0.289	9.31443407868699E-39	1	Slbp
H2afz	1.67617696783389E-39	1.59162937247635	0.924	0.735	5.20503233821458E-35	1	H2afz
Ran	2.3103161005717E-30	0.932352110222592	0.822	0.488	7.17422458710531E-26	1	Ran
Ppia	9.49734094653465E-30	0.677329773054638	1	0.978	2.9492092841274E-25	1	Ppia
Malat1	2.71503645925915E-26	-0.507907024790841	1	0.999	8.43100271693745E-22	1	Malat1
Fcgr3	1.47579356997005E-24	-0.647677838303455	0.914	0.977	4.58278177282798E-20	1	Fcgr3
Srsf7	1.12323083988607E-23	0.627731663609143	0.751	0.37	3.48796872709823E-19	1	Srsf7
Hsp90aa1	9.03067923283368E-22	0.966906173083516	0.789	0.484	2.80429682217184E-17	1	Hsp90aa1
Gapdh	1.96374437187526E-21	0.663395978278371	0.968	0.83	6.09801539798425E-17	1	Gapdh
Rps27	2.3721557743964E-20	-0.538296874004709	0.984	0.99	7.36625532623313E-16	1	Rps27
Hmgb1	7.5834208795323E-20	0.696452323022391	0.935	0.805	2.35487968572117E-15	1	Hmgb1
Ybx1	1.43698687875737E-19	0.587052762794741	0.908	0.656	4.46227535460526E-15	1	Ybx1
C1qb	2.1130376789021E-19	-0.317571579786213	1	0.999	6.56161590429468E-15	1	C1qb
Ctss	3.87896330866326E-19	-0.371111585194315	1	0.999	1.2045344762392E-14	1	Ctss
Rbm3	5.02442857182374E-19	0.720059055393812	0.822	0.583	1.56023580440842E-14	1	Rbm3
Hspa8	8.46099287966658E-19	0.533963930241726	0.973	0.887	2.62739211892286E-14	1	Hspa8
Tyrobp	4.32360751945819E-17	-0.386412663083304	1	0.999	1.34260984301735E-12	1	Tyrobp
Hnrnpd	4.97460993026326E-17	0.510467402474567	0.778	0.43	1.54476562164465E-12	1	Hnrnpd
Cd300c2	5.59711452660734E-17	-0.578958189118655	0.822	0.902	1.73807197394738E-12	1	Cd300c2
Selenop	1.04478660247113E-15	-0.534049653650265	0.973	0.984	3.24437583665359E-11	1	Selenop
Trem2	2.98433161948128E-15	-0.348133915407529	0.995	0.997	9.26724497797523E-11	1	Trem2
Hint1	3.40336260533027E-15	0.56227473209876	0.811	0.575	1.05684618983321E-10	1	Hint1
Itm2b	5.42970254893917E-15	-0.302825472442435	1	1	1.68608553252208E-10	1	Itm2b
Cst3	8.34803314181557E-15	-0.273078787394303	1	1	2.59231473152799E-10	1	Cst3
Set	6.87585763141454E-14	0.521393732728281	0.805	0.54	2.13516007028316E-09	1	Set
Sumo2	4.24089041328231E-13	0.478605323350229	0.849	0.669	1.31692370003655E-08	1	Sumo2
Hnrnpf	4.98591132037963E-13	0.50611696743529	0.914	0.755	1.54827504231749E-08	1	Hnrnpf
Srsf3	1.17389744598453E-12	0.465040084255532	0.914	0.73	3.64530373901577E-08	1	Srsf3
Tra2b	2.73248436302316E-12	0.464800630833684	0.854	0.571	8.48518369249582E-08	1	Tra2b
Fkbp2	2.82828767615021E-12	0.472862391580013	0.811	0.583	8.78268172074924E-08	1	Fkbp2
Fau	3.80617373744277E-12	-0.318549156826642	1	0.999	1.1819311306881E-07	1	Fau
Hmgn1	4.65068976610108E-12	0.530992653386055	0.746	0.495	1.44417869306737E-07	1	Hmgn1
Mafb	4.66549584194598E-12	-0.49449101126898	0.951	0.969	1.44877642379949E-07	1	Mafb
Ctsl	9.42729264986922E-12	-0.348261968358648	0.989	0.985	2.92745718656389E-07	1	Ctsl
Srsf2	1.02575931740359E-11	0.438969505739476	0.881	0.684	3.18529040833336E-07	1	Srsf2
Rpl10	1.43163108807182E-11	-0.361700259002224	0.984	0.986	4.44564401778943E-07	1	Rpl10
Fcrls	2.90994564327388E-11	0.311076370276798	0.984	0.981	9.03625420605838E-07	1	Fcrls
Rps21	4.26841268914367E-11	-0.339062273869301	0.978	0.993	1.32547019235978E-06	1	Rps21
Tnfaip8l2	5.36380944232295E-11	-0.53814686726608	0.703	0.782	1.66562374612454E-06	1	Tnfaip8l2
Fcer1g	6.37945635802906E-11	-0.263936659146291	1	0.998	1.98101258285877E-06	1	Fcer1g
Tmed3	1.0754260347785E-10	0.466938395193858	0.822	0.586	3.33952046579768E-06	1	Tmed3

(*Continued*)

Table 1. (Continued)

	p_val	avg_log2FC	pct.1	pct.2	p_val_adj	cluster	gene
Psma1	1.66119232220977E-10	0.446075860887791	0.795	0.559	5.158500518158E-06	1	Psma1
Arpc5l	1.75191797056051E-10	0.39732277338557	0.719	0.447	5.44023087398157E-06	1	Arpc5l
Rdx	2.13276878714269E-10	0.437170143436664	0.735	0.471	6.62288691471421E-06	1	Rdx
Rpl34	2.37232782293395E-10	-0.363219690411769	0.962	0.98	7.36678958855679E-06	1	Rpl34
Rpl18a	3.06354794751935E-10	-0.34323886858764	1	0.99	9.51323544143184E-06	1	Rpl18a
Hpgds	3.36135732673178E-10	-0.438932432518431	0.854	0.894	1.04380229067002E-05	1	Hpgds
Rgs10	4.47597935361456E-10	-0.307172198260009	0.995	0.991	1.38992586867793E-05	1	Rgs10
Snrpb	4.67843328377099E-10	0.413190868562448	0.784	0.532	1.4527938876094E-05	1	Snrpb
Arhgap45	4.70613034812082E-10	-0.452800221852119	0.827	0.863	1.46139465700196E-05	1	Arhgap45
Rhob	5.52858229337787E-10	-0.400284166352431	0.968	0.985	1.71679065956263E-05	1	Rhob
Mat2a	6.26598559094021E-10	0.530173555260338	0.773	0.539	1.94577650555466E-05	1	Mat2a
Cd14	7.67210172997373E-10	-0.511463111549875	0.697	0.766	2.38241775020874E-05	1	Cd14
Ubc	7.69507150300919E-10	-0.326626404355029	0.978	0.982	2.38955055382944E-05	1	Ubc
Atp5j	1.75650670044555E-09	0.417626525618481	0.816	0.589	5.45448025689356E-05	1	Atp5j
Rps28	1.76539118301755E-09	-0.360637976228019	0.935	0.96	5.48206924062439E-05	1	Rps28
Cyth4	2.10874307651391E-09	-0.351714215247656	0.951	0.952	6.54827987549865E-05	1	Cyth4
Arpp19	2.38518165511063E-09	0.38091381431864	0.741	0.488	7.40670459361504E-05	1	Arpp19
Serbp1	2.55101978251909E-09	0.38784972715402	0.838	0.641	7.92168173065652E-05	1	Serbp1
Fus	2.66784790070403E-09	0.390071870812651	0.914	0.771	8.28446808605624E-05	1	Fus
Rpl27a	2.70291125013243E-09	-0.280378564108046	1	0.994	8.39335030503622E-05	1	Rpl27a
Rps9	2.80398096428665E-09	-0.299546709086227	0.989	0.992	8.70720208839932E-05	1	Rps9
Unc93b1	5.48196964472685E-09	-0.326759267704769	0.984	0.971	0.000170231603377703	1	Unc93b1
Hsp90ab1	5.48759669595159E-09	0.379697208168531	0.962	0.842	0.000170406340199385	1	Hsp90ab1
Sat1	7.00238163299055E-09	-0.466706580894777	0.816	0.825	0.000217444956849256	1	Sat1
Sdf2l1	7.71873440094701E-09	0.428214183100575	0.751	0.529	0.000239689859352608	1	Sdf2l1
Ncl	1.02643612176332E-08	0.408798932373841	0.757	0.539	0.000318739208891163	1	Ncl
Ctsh	1.3463319994624E-08	-0.365810852573241	0.957	0.959	0.000418076475793058	1	Ctsh
Luc7l3	1.63859177020499E-08	0.374340806920861	0.735	0.509	0.000508831902401754	1	Luc7l3
Gpr34	1.75013116124881E-08	-0.309543649893288	0.995	0.994	0.000543468229502592	1	Gpr34
Hnrnpu	1.86697190265684E-08	0.444684316604392	0.773	0.575	0.000579750784932027	1	Hnrnpu
Npm1	1.93181103203264E-08	0.357196757849688	0.859	0.676	0.000599885279777096	1	Npm1
Siglech	2.02177609332656E-08	-0.314329101316197	0.984	0.985	0.000627822130260696	1	Siglech
Ly6e	2.13663690455209E-08	0.321078844882404	1	0.95	0.000663489857970561	1	Ly6e
Rpl37	3.12019157428408E-08	-0.297504305854286	0.995	0.99	0.000968913089562434	1	Rpl37
Rps11	3.35645910112025E-08	-0.287174007621304	0.995	0.991	0.00104228124467087	1	Rps11
Krtcap2	3.42358140248358E-08	0.356697568476341	0.773	0.559	0.00106312473291322	1	Krtcap2
Vsir	3.5670013407074E-08	-0.292221943492612	0.995	0.974	0.00110766092632987	1	Vsir
Rps14	4.88294740494431E-08	-0.330743683722173	0.973	0.972	0.00151630165765736	1	Rps14
Atp5g2	5.19240667853224E-08	0.342104746319781	0.865	0.715	0.00161239804588462	1	Atp5g2
Tmem86a	5.93103286608248E-08	-0.438237955943034	0.751	0.802	0.00184176363590459	1	Tmem86a
Hnrnpa3	8.03083969054611E-08	0.35880449845111	0.811	0.61	0.00249381664910528	1	Hnrnpa3
Rpl30	8.92590016704123E-08	-0.277157973870885	0.995	0.993	0.00277175977887131	1	Rpl30
Ddx39b	1.094308618947E-07	0.312806546724517	0.724	0.472	0.00339815655441611	1	Ddx39b
Ucp2	1.558370009489E-07	-0.478146626722825	0.676	0.715	0.0048392063904662	1	Ucp2
Eef1a1	1.86689142780994E-07	-0.255407835345328	1	0.999	0.0057972579507782	1	Eef1a1
Npc2	2.03204908357552E-07	-0.347704687966907	0.886	0.907	0.00631012201922706	1	Npc2
Oxct1	2.26751989989881E-07	0.339510758811187	0.719	0.488	0.00704132954515576	1	Oxct1

(*Continued*)

Table 1. (Continued)

	p_val	avg_log2FC	pct.1	pct.2	p_val_adj	cluster	gene
Asah1	2.72265402997823E-07	-0.332856862920483	0.881	0.872	0.0084546575592914	1	Asah1
Tmco1	2.82169670483339E-07	0.3623435952691	0.827	0.679	0.00876221477751911	1	Tmco1
Manf	3.49670468087565E-07	0.311832302426752	0.881	0.694	0.0108583170455231	1	Manf
Rsrp1	5.00440099833167E-07	-0.306751601607958	0.984	0.967	0.0155401664201193	1	Rsrp1
Rtn3	5.01172309036219E-07	0.356832850856833	0.843	0.64	0.0155629037125017	1	Rtn3
Pnn	5.21385357248612E-07	0.370181361947366	0.8	0.612	0.0161905794986412	1	Pnn
Ctsb	6.1023082567593E-07	-0.359563025071504	0.984	0.981	0.0189494978297147	1	Ctsb
Arl6ip1	7.01630549834455E-07	0.750850023988365	0.935	0.846	0.0217877334640093	1	Arl6ip1
H3f3a	8.38953437624406E-07	0.295467828959084	0.957	0.908	0.0260520210985507	1	H3f3a
Tecr	8.42991360865655E-07	0.303451132843531	0.784	0.572	0.0261774107289612	1	Tecr
Rps4x	1.103021160002E-06	-0.287811032418148	1	0.984	0.034252116081542	1	Rps4x
Gnas	1.30870944451629E-06	0.315752460718663	0.93	0.803	0.0406393543805645	1	Gnas
Pf4	0	4.37853701752422	0.732	0.004	0	2	Pf4
Mrc1	0	3.5577447697175	0.798	0.013	0	2	Mrc1
Ms4a7	0	3.40638520934347	0.789	0.001	0	2	Ms4a7
Ifi27l2a	0	3.24285935674792	0.781	0.066	0	2	Ifi27l2a
Ifitm3	0	3.23400977150058	0.772	0.038	0	2	Ifitm3
Dab2	0	3.00672179121753	0.789	0.065	0	2	Dab2
Ifitm2	0	2.49528029256268	0.789	0.008	0	2	Ifitm2
Cybb	0	2.30254592729466	0.75	0.005	0	2	Cybb
Tgfbi	4.47252324827468E-265	1.77732641493551	0.741	0.084	1.38885264428673E-260	2	Tgfbi
Clec2d	7.46815160856889E-159	1.58661840196453	0.719	0.126	2.3190851190089E-154	2	Clec2d
Lyz2	6.02324004023014E-158	4.77109415482144	0.939	0.363	1.87039672969267E-153	2	Lyz2
Ms4a6c	9.68378544392257E-146	2.22060451823559	0.89	0.278	3.00710589390128E-141	2	Ms4a6c
Hexb	3.2821132815041E-137	-2.14183056509067	0.908	1	1.01919463730547E-132	2	Hexb
Cst3.1	1.44533002050378E-126	-1.79844146468655	1	1	4.4881833126704E-122	2	Cst3
Cd81	1.38644013247434E-119	-1.76461710714318	0.763	1	4.30531254337256E-115	2	Cd81
Selplg	7.73281113121192E-119	-2.10983603366066	0.711	0.999	2.40126984057524E-114	2	Selplg
Ctsd	1.35285054753601E-115	-1.84984214818543	0.917	1	4.20100680526356E-111	2	Ctsd
Slfn2	2.30893285361598E-112	1.53688870812899	0.768	0.191	7.1699291903337E-108	2	Slfn2
Apoe	4.25915344390955E-109	5.30931722027963	0.912	0.536	1.32259491893723E-104	2	Apoe
Tmem119	1.08702043580267E-108	-2.05633221631248	0.504	0.995	3.37552455929804E-104	2	Tmem119
Sparc	1.10731990003302E-108	-2.18920919186698	0.395	0.999	3.43856048557254E-104	2	Sparc
Gpr34.1	1.17601731559925E-108	-1.9206505045212	0.697	0.997	3.65188657013036E-104	2	Gpr34
P2ry12	5.99649932345756E-107	-2.05673790980279	0.592	0.998	1.86209293491328E-102	2	P2ry12
Emp3	3.58773656012687E-104	1.44030125325655	0.741	0.184	1.1140998340162E-99	2	Emp3
Lgmn	1.18029779044412E-103	-1.27122497369596	0.899	1	3.66517872866611E-99	2	Lgmn
Basp1	1.49916241944672E-97	-1.56657531259554	0.711	0.992	4.6553490611079E-93	2	Basp1
Lpcat2	1.56060019007985E-97	-1.58297183978522	0.702	0.984	4.84613177025495E-93	2	Lpcat2
Cd9	2.81122177457997E-97	-1.95986925080908	0.5	0.977	8.72968697660318E-93	2	Cd9
Siglech.1	6.9924039237018E-96	-1.75210623490392	0.539	0.991	2.17135119042712E-91	2	Siglech
Trem2.1	3.64304257704326E-94	-1.38189806163724	0.833	0.999	1.13127401144924E-89	2	Trem2
Fth1	5.98699638709904E-92	1.38644395257302	1	0.996	1.85914198808586E-87	2	Fth1
Olfml3	6.06554782323319E-91	-1.88338859679	0.539	0.983	1.8835345655486E-86	2	Olfml3
H2-D1	2.91813651021523E-90	1.98566369064107	0.982	0.73	9.06168930517134E-86	2	H2-D1
Ftl1	2.37952852709334E-85	1.42217462241371	0.996	0.991	7.38914993518295E-81	2	Ftl1
P2ry13	8.4235960171982E-82	-1.58759443807461	0.553	0.948	2.61577927122056E-77	2	P2ry13

(*Continued*)

Table 1. (Continued)

	p_val	avg_log2FC	pct.1	pct.2	p_val_adj	cluster	gene
Rps29	1.64269073202869E-81	0.89813665302241	1	1	5.10104753016868E-77	2	Rps29
Rpl38	9.60280179882922E-81	1.30848779604445	1	0.948	2.98195804259044E-76	2	Rpl38
Bst2	3.48009518058583E-80	1.93397290584532	0.89	0.454	1.08067395642732E-75	2	Bst2
Tgfbr1	5.40223262672918E-80	-1.44059083748452	0.68	0.983	1.67755529757821E-75	2	Tgfbr1
Ecscr	7.18100739610371E-80	-1.80915350358947	0.294	0.872	2.22991822671208E-75	2	Ecscr
F11r	9.60117541097144E-80	-1.48570202289293	0.601	0.952	2.98145300036896E-75	2	F11r
Vsir.1	5.57946969933843E-77	-1.34683059790175	0.702	0.978	1.73259272573556E-72	2	Vsir
Tpt1	2.74581544793537E-76	1.02463312939067	1	0.999	8.5265807104737E-72	2	Tpt1
Rps28.1	3.53577718174795E-74	1.16956321559522	1	0.96	1.09796488824819E-69	2	Rps28
H2-K1	6.17140763481889E-74	1.92678722793731	0.965	0.721	1.91640721284031E-69	2	H2-K1
Plxdc2	2.80633430416144E-73	-1.51331744882972	0.439	0.932	8.71450991471253E-69	2	Plxdc2
Rhob.1	2.93193482936845E-72	-1.28479026105139	0.724	0.988	9.10453722563784E-68	2	Rhob
Ptgs1	7.2002608414574E-72	-1.51227437491087	0.474	0.918	2.23589699909777E-67	2	Ptgs1
Rpl23.1	3.23109700045626E-71	1.08637702647503	1	0.987	1.00335255155168E-66	2	Rpl23
Ldhb	9.05798562013014E-71	-1.63829853914837	0.338	0.868	2.81277627461901E-66	2	Ldhb
Rpl37a	1.43310945448441E-70	1.01422226398218	1	0.99	4.45023478901044E-66	2	Rpl37a
Arhgap5	6.60636293556999E-70	-1.6067265971305	0.425	0.9	2.05147388238255E-65	2	Arhgap5
Rpl36	1.19721664514944E-69	1.14988474740412	0.991	0.94	3.71771684818255E-65	2	Rpl36
Anxa3	1.81590409647394E-69	-1.34705219627591	0.64	0.925	5.63892699078053E-65	2	Anxa3
Ctsl.1	2.01461651198014E-69	-1.2536159141747	0.737	0.988	6.25598865465194E-65	2	Ctsl
Itgb5	4.74246415531213E-68	-1.18989921233838	0.741	0.973	1.47267739414908E-63	2	Itgb5
Rpl35a	1.01960511083218E-67	0.878857222054372	1	0.996	3.16617975066717E-63	2	Rpl35a
Cx3cr1	1.62671077483876E-67	-1.17100557971701	0.807	0.997	5.05142496910679E-63	2	Cx3cr1
Serpine2	1.58976242454601E-66	-1.6481148706064	0.272	0.81	4.93668925694274E-62	2	Serpine2
Golm1	2.82521076190506E-66	-1.52798439541282	0.386	0.87	8.77312697894377E-62	2	Golm1
Bin1	2.90672846628869E-66	-1.20513616006694	0.746	0.958	9.02626390636626E-62	2	Bin1
Marcks	6.03288513195467E-66	-1.01387761035684	0.895	0.998	1.87339182002588E-61	2	Marcks
Mafb.1	3.57243353116995E-65	-1.32719830606566	0.645	0.973	1.1093477844342E-60	2	Mafb
Rps14.1	5.04552057570057E-64	1.04504392772565	1	0.972	1.5667855043723E-59	2	Rps14
Csf1r	1.39554589011637E-63	-0.842085678092108	0.947	0.999	4.33358865257837E-59	2	Csf1r
Fau.1	5.96253375808519E-63	0.908726323565812	1	0.998	1.85154560789819E-58	2	Fau
Epb41l2	1.13055315978884E-62	-1.39707650837606	0.561	0.92	3.51070672709228E-58	2	Epb41l2
Blvrb	1.13472513015967E-62	1.21667315947308	0.724	0.272	3.52366194668482E-58	2	Blvrb
Ctss.1	2.4625640409105E-62	-0.807902515258847	0.974	0.999	7.64700011623938E-58	2	Ctss
Rpl41	3.25881180885314E-62	0.958201245201018	1	0.99	1.01195883100317E-57	2	Rpl41
Frmd4a	4.00387893533487E-61	-1.34974482658083	0.509	0.895	1.24332452578954E-56	2	Frmd4a
Rps24	8.77557802691455E-61	1.05993848607014	1	0.994	2.72508024469777E-56	2	Rps24
Syngr1	2.61156370496386E-60	-1.49672836820486	0.311	0.817	8.10968877302427E-56	2	Syngr1
Rps16	9.88784117838514E-58	1.06824195585608	1	0.976	3.07047132112394E-53	2	Rps16
Slc2a5	1.04127416006617E-57	-1.59635854274501	0.276	0.751	3.23346864925347E-53	2	Slc2a5
Rgs10.1	4.68493353484417E-57	-0.894680861429364	0.908	0.992	1.45481241057516E-52	2	Rgs10
Adgrg1	6.60135897920662E-57	-1.50416282898137	0.25	0.764	2.04992000381303E-52	2	Adgrg1
Apbb1ip	1.26901082167329E-56	-1.20756930256106	0.667	0.913	3.94065930454206E-52	2	Apbb1ip
Sgk1	1.61830969338922E-56	-1.6611609749098	0.399	0.823	5.02533709088155E-52	2	Sgk1
Laptm5	1.04408337195052E-55	-0.755142974938095	1	0.998	3.24219209491795E-51	2	Laptm5
mt-Co1	1.21565705128143E-55	0.861842071564895	1	0.995	3.77497984134423E-51	2	mt-Co1
Qk	2.16292981198365E-55	-1.15060464424042	0.732	0.95	6.71654594515284E-51	2	Qk

(*Continued*)

Table 1. (Continued)

	p_val	avg_log2FC	pct.1	pct.2	p_val_adj	cluster	gene
Lair1	5.87645385493111E-55	-1.12265963056934	0.654	0.949	1.82481521557176E-50	2	Lair1
Rpl34.1	7.51178606524087E-55	0.851997036602266	1	0.98	2.33263492683925E-50	2	Rpl34
Ly86	7.96859894336671E-54	-0.8430398632039	0.939	0.998	2.47448902988366E-49	2	Ly86
Ctsc	9.62976248405467E-54	1.31457238506344	0.93	0.793	2.9903301441735E-49	2	Ctsc
Rps20	5.13338900201088E-53	0.935431181690971	0.996	0.975	1.59407128679444E-48	2	Rps20
Scoc	2.23458401200199E-52	-1.23605155298513	0.522	0.879	6.93905373246979E-48	2	Scoc
Mtdh	3.82516583174803E-52	-1.02669205808061	0.803	0.951	1.18782874573271E-47	2	Mtdh
Rpl32	5.24332040362482E-52	1.07124573322813	0.996	0.976	1.62820828493762E-47	2	Rpl32
Cd37.1	6.94897702491066E-52	-1.15320572072195	0.61	0.912	2.15786583554551E-47	2	Cd37
Abi3	1.40466419235075E-50	-1.28755434239719	0.487	0.813	4.36190371650678E-46	2	Abi3
Rpsa.1	1.61464824119565E-50	1.29934946888645	0.996	0.927	5.01396718338487E-46	2	Rpsa
Rps27.1	2.69830768249901E-49	0.918246575738408	1	0.99	8.37905484646417E-45	2	Rps27
Ywhah	6.04398170133699E-49	-1.10395660944086	0.645	0.891	1.87683763771618E-44	2	Ywhah
Rps5	8.32478323478892E-49	1.17874358688984	0.982	0.935	2.585094937899E-44	2	Rps5
Rps21.1	1.33097135745923E-48	0.780835835863661	1	0.993	4.13306535631816E-44	2	Rps21
Smap2.1	3.31030089662752E-48	-1.11136371948752	0.596	0.885	1.02794773742974E-43	2	Smap2
Sirpa	2.78083792154E-47	-0.962211967519336	0.803	0.953	8.63533599775816E-43	2	Sirpa
Tspo	5.72334987447643E-47	1.10649210379914	0.702	0.285	1.77727183652117E-42	2	Tspo
Abhd12	6.52282304221931E-47	-0.94860583957851	0.811	0.956	2.02553223930036E-42	2	Abhd12
Rps8	9.6621982205978E-47	0.818544937418142	1	0.988	3.00040241344223E-42	2	Rps8
Rps11.1	1.7077466735659E-46	0.943239073532013	1	0.991	5.30306574542417E-42	2	Rps11
Srgap2	4.05268128991621E-46	-1.07099346742274	0.645	0.892	1.25847912095768E-41	2	Srgap2
Ckb	6.89654116612596E-46	-0.998274422757237	0.741	0.947	2.14158292831709E-41	2	Ckb
Rps18	1.31827227921182E-45	0.997279685321421	0.996	0.947	4.09363090863646E-41	2	Rps18
Ms4a6b	9.16833993975502E-45	1.27792244054769	0.846	0.531	2.84704460149213E-40	2	Ms4a6b
Crybb1.1	2.08730665091023E-44	-1.47503900453205	0.346	0.751	6.48171334307153E-40	2	Crybb1
Rpl9	3.19767960741829E-44	0.818950457928426	0.991	0.971	9.92975448491602E-40	2	Rpl9
Rps19	1.42626373898353E-43	1.0256620630084	0.996	0.955	4.42897678866557E-39	2	Rps19
Cmtm6.1	5.2967192036309E-43	-1.06640093420613	0.57	0.846	1.6447902143035E-38	2	Cmtm6
Rpl35	9.36879505784493E-43	0.888952922927077	0.987	0.879	2.90929192931259E-38	2	Rpl35
Rpl19	1.05040006003692E-42	0.878038009827109	1	0.979	3.26180730643264E-38	2	Rpl19
Susd3	3.00815492263626E-42	-1.14012521134304	0.469	0.793	9.34122348126239E-38	2	Susd3
Ifngr1	3.48575387480282E-42	-0.765868368922916	0.877	0.986	1.08243115074252E-37	2	Ifngr1
Rplp2	1.1310891111252E-41	0.782773604849853	1	0.97	3.51237101677709E-37	2	Rplp2
Lst1	4.63101893743306E-41	1.1576677823991	0.86	0.524	1.43807031064109E-36	2	Lst1
Bin2	5.72091079395355E-41	-1.11533586630113	0.5	0.789	1.7765144288464E-36	2	Bin2
Rps2	9.37280871500094E-41	0.950537762372105	0.987	0.93	2.91053829026924E-36	2	Rps2
Rpl26	1.00539157764906E-40	0.795670949450634	1	0.978	3.12204246607362E-36	2	Rpl26
Rpl37.1	1.19094531662208E-40	0.780985551079742	0.996	0.99	3.69824249170654E-36	2	Rpl37
Rps13	1.73666732047638E-40	0.924497538292701	1	0.973	5.39287303027529E-36	2	Rps13
Itgam	2.74450358186367E-40	-1.11131849358202	0.509	0.799	8.52250697276126E-36	2	Itgam
Rpl28	5.60285208941422E-40	0.857128531911679	0.996	0.962	1.7398536593258E-35	2	Rpl28
mt-Co2	6.47857775620827E-40	0.670142604630995	1	0.996	2.01179275063535E-35	2	mt-Co2
Ivns1abp	7.67752062451974E-40	-1.06242646981053	0.548	0.829	2.38410047953212E-35	2	Ivns1abp
Rps15a	1.94187121079116E-39	0.941272043627357	1	0.98	6.03009267086979E-35	2	Rps15a
mt-Atp6	2.24104034651716E-39	0.69265004247674	1	0.998	6.95910258803974E-35	2	mt-Atp6
Pycard	3.65055581578758E-39	-0.950699305390988	0.702	0.859	1.13360709747652E-34	2	Pycard

(*Continued*)

Table 1. (Continued)

	p_val	avg_log2FC	pct.1	pct.2	p_val_adj	cluster	gene
Pmepa1	2.07730008367523E-38	-0.983359951596355	0.697	0.945	6.45063994983671E-34	2	Pmepa1
Rps3	2.75588349361709E-38	0.728452549014768	1	0.978	8.55784501272914E-34	2	Rps3
Cd53	4.49045896493436E-38	-0.759006897984039	0.899	0.955	1.39442222238107E-33	2	Cd53
Rpl13	6.10702094950391E-38	0.819593896024524	1	0.995	1.89641321544945E-33	2	Rpl13
Rpl22	1.59647247931969E-37	0.790790226705827	0.987	0.901	4.95752599003143E-33	2	Rpl22
Tsc22d3	1.75280341918441E-37	1.0081073961963	0.75	0.374	5.44298045759336E-33	2	Tsc22d3
Rpl39	4.49669520593599E-37	0.861742369483312	1	0.989	1.3963587622993E-32	2	Rpl39
Csnk1e	4.54898314242523E-37	-1.09265166129746	0.504	0.757	1.41259573521731E-32	2	Csnk1e
Zfhx3	6.13786298668869E-37	-0.934197836332535	0.689	0.913	1.90599059325644E-32	2	Zfhx3
Tanc2	7.87999510824324E-37	-1.05982725448567	0.43	0.779	2.44697488096277E-32	2	Tanc2
Ltc4s	1.41946911233159E-36	-0.924676039563155	0.684	0.945	4.40787743452328E-32	2	Ltc4s
Rps3a1	1.57345645959343E-36	0.729620660822639	1	0.987	4.88605434397548E-32	2	Rps3a1
Rpl27a.1	3.7615177916447E-36	0.733875411989987	1	0.994	1.16806411983943E-31	2	Rpl27a
Rpl8	1.19032041802324E-35	0.801573760709803	0.991	0.95	3.69630199408756E-31	2	Rpl8
Ccr5.1	1.39313133410864E-35	-1.02873563003041	0.61	0.827	4.32609073180757E-31	2	Ccr5
Cyth4.1	1.61792099199388E-35	-0.745483595441052	0.886	0.953	5.02413005643861E-31	2	Cyth4
Cd48	2.90081136043008E-35	0.761626993725923	0.794	0.371	9.00788951754353E-31	2	Cd48
Saraf	3.24056360820088E-35	-0.950425840993859	0.57	0.801	1.00629221725462E-30	2	Saraf
mt-Co3	3.5772538527277E-35	0.625568359835822	1	0.997	1.11084463888753E-30	2	mt-Co3
C1qc	3.75117077978036E-35	-0.529470818122499	0.917	0.999	1.16485106224519E-30	2	C1qc
Mertk	5.63814159319826E-35	-1.02146196342641	0.447	0.8	1.75081210893586E-30	2	Mertk
Serinc3	6.44188403335451E-35	-0.601390773295421	0.974	0.999	2.00039824887758E-30	2	Serinc3
Fcgrt	6.54353484334029E-35	1.04901210452634	0.763	0.384	2.03196387490246E-30	2	Fcgrt
Fam105a	1.00338882832065E-34	-0.832422395588597	0.754	0.891	3.11582332858412E-30	2	Fam105a
Rps10	2.07572719222703E-34	0.686997136282966	1	0.987	6.44575565002258E-30	2	Rps10
Nrip1	2.11674730336753E-34	-0.975113945672293	0.618	0.85	6.57313540114719E-30	2	Nrip1
Rps12	2.57156588815914E-34	0.668437002689803	1	0.991	7.98548355250059E-30	2	Rps12
Rps27a	2.89960243850952E-34	0.748616172118519	0.996	0.991	9.00413545230361E-30	2	Rps27a
Rps7	3.56506367281024E-34	0.847120536430435	0.991	0.962	1.10705922231776E-29	2	Rps7
Rpl10.1	8.387418159678E-34	0.699711580428214	0.996	0.986	2.60454496112481E-29	2	Rpl10
Rpl17	9.563550845489E-34	0.87383180455266	0.996	0.964	2.9697694440497E-29	2	Rpl17
Sh3bgrl3	9.76158924357623E-34	0.795986411196578	0.952	0.857	3.03126630780773E-29	2	Sh3bgrl3
Sft2d1	9.85822330190378E-34	-0.88554150170981	0.689	0.859	3.06127408194018E-29	2	Sft2d1
Pag1	1.86811546576051E-33	-1.06360172440379	0.439	0.735	5.80105895582611E-29	2	Pag1
Ybx1.1	1.96528295466773E-33	0.741968184007215	0.943	0.655	6.10279315912969E-29	2	Ybx1
Tmem173	2.14931437160311E-33	-1.00883233801719	0.535	0.778	6.67426591813912E-29	2	Tmem173
Rps23	2.99005499986355E-33	0.682515133189967	0.991	0.986	9.28501779107628E-29	2	Rps23
Capza2	3.09653814842897E-33	-0.704135964682668	0.868	0.956	9.61567991231647E-29	2	Capza2
Rgs2.1	1.40863055805506E-32	-0.903480834111316	0.627	0.859	4.37422047192838E-28	2	Rgs2
Stab1	1.56342977170071E-32	1.85187288313102	0.776	0.601	4.85491847006221E-28	2	Stab1
Slco2b1	1.66100400695275E-32	-0.848262399588577	0.645	0.892	5.15791574279036E-28	2	Slco2b1
Rrbp1	2.72969020582539E-32	-0.694365179796032	0.912	0.977	8.4765069961496E-28	2	Rrbp1
Rpl7.1	2.79852752833827E-32	0.740244390373251	0.987	0.945	8.69026753374885E-28	2	Rpl7
Sem1	2.85631882126126E-32	0.760395327591849	0.873	0.575	8.8697268356626E-28	2	Sem1
Rpl30.1	3.65671927697142E-32	0.663597450528015	0.996	0.993	1.13552103707793E-27	2	Rpl30
H2afj	7.25277323500704E-32	0.711669514668641	0.759	0.36	2.25220367266674E-27	2	H2afj
Calm1.1	1.17470735463791E-31	0.776829449931705	0.952	0.734	3.64781874835709E-27	2	Calm1

(*Continued*)

Table 1. (Continued)

	p_val	avg_log2FC	pct.1	pct.2	p_val_adj	cluster	gene
Itm2c.1	1.29778111744128E-31	-0.783257557834447	0.776	0.885	4.02999970399041E-27	2	Itm2c
Cd52.1	1.55573908049899E-31	1.84343415323955	0.785	0.575	4.83103656667353E-27	2	Cd52
Rpl18	1.66767624865276E-31	0.790669945685992	0.996	0.955	5.17863505494141E-27	2	Rpl18
Rnase4.1	4.5759743818341E-31	-0.781528453072231	0.746	0.955	1.42097732479094E-26	2	Rnase4
Cyfip1	8.17903003125012E-31	-0.808421153189823	0.728	0.884	2.5398341956041E-26	2	Cyfip1
Rps15	1.11461615447363E-30	0.76834726437119	0.965	0.856	3.46121754448695E-26	2	Rps15
Rps4x.1	3.29110068340267E-30	0.778118990663748	0.996	0.984	1.02198549521703E-25	2	Rps4x
Rpl24	3.5565992195344E-30	0.781497756878446	0.987	0.912	1.10443075564202E-25	2	Rpl24
Elmo1	6.62421466554566E-30	-0.976764742893299	0.526	0.76	2.05701738009189E-25	2	Elmo1
Gmfg	1.01118716645815E-29	0.73616623240517	0.772	0.396	3.14003950800251E-25	2	Gmfg
Fam102b	1.08754203658136E-29	-1.04028643720283	0.425	0.71	3.37714428619609E-25	2	Fam102b
Rps9.1	1.09511560293501E-29	0.704884356242325	1	0.992	3.4006624817941E-25	2	Rps9
Prdx1.1	1.51334436846022E-29	0.841059755905203	0.882	0.562	4.69938826737951E-25	2	Prdx1
Arsb	2.34653092631895E-29	-0.858093440530267	0.575	0.812	7.28668248549822E-25	2	Arsb
St3gal6	2.47913778446241E-29	-0.831997443141878	0.575	0.81	7.69846656209111E-25	2	St3gal6
Ubc.1	4.72295742003184E-29	-0.596793288073421	0.961	0.982	1.46661996764249E-24	2	Ubc
Scamp2	1.7992441589114E-28	-0.699814393833229	0.816	0.923	5.58719288666757E-24	2	Scamp2
Hpgds.1	1.88230663134722E-28	-0.782773761312334	0.684	0.896	5.84512678232252E-24	2	Hpgds
Rps17	5.19530330078899E-28	0.670345331197419	0.956	0.737	1.61329753399401E-23	2	Rps17
Rpl18a.1	7.76043637396675E-28	0.793812803597784	0.991	0.99	2.40984830720789E-23	2	Rpl18a
Bsg	8.15809532181704E-28	-0.704895218165514	0.838	0.908	2.53333334028384E-23	2	Bsg
Fcrls.1	1.10454665367038E-27	-0.698843764515964	0.807	0.984	3.42994872364262E-23	2	Fcrls
Fcgr2b	1.30796736690552E-27	0.923588939518299	0.833	0.534	4.06163106445171E-23	2	Fcgr2b
Rpl6	1.3304284799526E-27	0.629321133923917	0.996	0.977	4.13137955879682E-23	2	Rpl6
Rps25.1	1.75439516044992E-27	0.675317724024114	0.987	0.915	5.44792329174513E-23	2	Rps25
Mef2c	1.8442992871488E-27	-0.625578907102627	0.925	0.982	5.72710257638315E-23	2	Mef2c
Rpl29	2.43402483342969E-27	0.712549025409821	0.978	0.897	7.55837731524921E-23	2	Rpl29
Rpl10a	3.02778906567368E-27	0.815767368598848	0.978	0.901	9.40219338563647E-23	2	Rpl10a
Comt	3.06714731521305E-27	-0.799587225546452	0.632	0.804	9.5244125579311E-23	2	Comt
Rpl11	3.40973355260908E-27	0.680598526419851	1	0.974	1.0588245600917E-22	2	Rpl11
B2m	3.44383123112973E-27	0.579322228662936	0.991	0.964	1.06941291220271E-22	2	B2m
Tmem256	6.1781720998658E-27	0.677440811848066	0.719	0.35	1.91850778217133E-22	2	Tmem256
Glul.1	1.21799877868603E-26	-0.76840490613593	0.711	0.9	3.78225160745373E-22	2	Glul
Tpst2	1.50011468190259E-26	-0.852008747731548	0.588	0.747	4.65830612171211E-22	2	Tpst2
Mef2a	1.61073037904817E-26	-0.771936677762354	0.728	0.886	5.00180104605828E-22	2	Mef2a
Cox8a	3.46709588545212E-26	0.639076388156213	0.978	0.773	1.07663728530945E-21	2	Cox8a
Fam49b	5.58292474366426E-26	-0.672354580710964	0.789	0.885	1.73366562065006E-21	2	Fam49b
Rhoh.1	6.13284524338528E-26	-0.879333826138547	0.496	0.71	1.90443243342843E-21	2	Rhoh
Camk1	1.48727846897817E-25	-0.710522147433676	0.732	0.862	4.6184458297179E-21	2	Camk1
Commd8	1.65174766647102E-25	-0.852890850953875	0.579	0.741	5.12917202869247E-21	2	Commd8
Ctsz	1.83029403078458E-25	-0.603759026638196	0.969	0.992	5.68361205379535E-21	2	Ctsz
Rack1	1.93941295589834E-25	0.863300856820349	0.956	0.874	6.02245905195112E-21	2	Rack1
C1qb.1	2.01183469974534E-25	-0.46318479879185	0.921	1	6.24735029311922E-21	2	C1qb
Lyn	2.28953271321653E-25	-0.702786006518549	0.741	0.889	7.10968593435129E-21	2	Lyn
Calm2	3.65052984655318E-25	-0.614166804344637	0.895	0.955	1.13359903325016E-20	2	Calm2
Hint1.1	3.985705354814E-25	0.654508830560937	0.899	0.573	1.23768108383039E-20	2	Hint1
Rpl12	6.43598945712959E-25	0.756182890797111	0.969	0.93	1.99856780612245E-20	2	Rpl12

(*Continued*)

Table 1. (Continued)

	p_val	avg_log2FC	pct.1	pct.2	p_val_adj	cluster	gene
Psmb8	7.75352707732209E-25	0.735953070738275	0.868	0.582	2.40770276332083E-20	2	Psmb8
Rps26	7.80870237134121E-25	0.834676440921305	0.991	0.894	2.42483634737259E-20	2	Rps26
Inpp5d	1.14097929978285E-24	-0.723984430038733	0.715	0.862	3.54308301961567E-20	2	Inpp5d
Aes	2.48151757874713E-24	0.583932304064419	0.746	0.366	7.70585653728345E-20	2	Aes
Myl6	2.81157060156106E-24	0.68334685805671	0.908	0.668	8.73077018902755E-20	2	Myl6
Tmsb4x	5.96640437559762E-24	0.351196725090372	1	1	1.85274755075433E-19	2	Tmsb4x
Lrp1	6.03510512267145E-24	-0.830068501201574	0.539	0.719	1.87408119374317E-19	2	Lrp1
Kctd12	9.14781295030041E-24	-0.76111521251526	0.693	0.866	2.84067035545679E-19	2	Kctd12
Retreg1	1.93719930313547E-23	-0.832257718252235	0.526	0.706	6.01558499602658E-19	2	Retreg1
Arhgap45.1	2.14521954624873E-23	-0.71780158952278	0.746	0.864	6.66155025696619E-19	2	Arhgap45
Cttnbp2nl	3.33725450876171E-23	-0.827507243556233	0.553	0.74	1.03631764260578E-18	2	Cttnbp2nl
Rpl14	3.94460636808284E-23	0.684022418979118	0.965	0.848	1.22491861548076E-18	2	Rpl14
Ucp2.1	4.45340374812402E-23	0.755344589434527	0.917	0.712	1.38291546590495E-18	2	Ucp2
Pmp22	5.63640904019733E-23	-0.847044435448738	0.548	0.77	1.75027409925248E-18	2	Pmp22
Tmem59	6.00716115893676E-23	-0.575754757571115	0.868	0.92	1.86540375468463E-18	2	Tmem59
Rpl27	1.15482406206726E-22	0.740210454514907	0.925	0.717	3.58607515993747E-18	2	Rpl27
Rpl23a	1.50294500510015E-22	0.707093700402501	0.925	0.742	4.6670951243375E-18	2	Rpl23a
Daglb	3.66474970894117E-22	-0.773376118406158	0.509	0.7	1.1380147271175E-17	2	Daglb
Mpc1	5.21675078696293E-22	-0.774423292019402	0.588	0.731	1.6199576218756E-17	2	Mpc1
Tmem176a	5.3530396448917E-22	0.972885278837874	0.842	0.665	1.66227940092822E-17	2	Tmem176a
Tomm7	6.46684834253959E-22	0.580152159964919	0.825	0.474	2.00815041580882E-17	2	Tomm7
Pfdn5	7.24795528442122E-22	0.568547018024899	0.956	0.762	2.25070755447132E-17	2	Pfdn5
Ctsb.1	9.70653139672359E-22	0.669640432860307	0.969	0.981	3.01416919462458E-17	2	Ctsb
Actr3	1.08420298615427E-21	0.687592131968084	0.851	0.605	3.36677553290485E-17	2	Actr3
Rpl3	1.16736165147781E-21	0.674643660646569	0.987	0.95	3.62500813633405E-17	2	Rpl3
Tmem86a.	1.86614112622408E-21	-0.692928953459548	0.667	0.803	5.79492803926364E-17	2	Tmem86a
Rpl7a	3.90595359722725E-21	0.589709881901216	0.974	0.862	1.21291577054698E-16	2	Rpl7a
Bmp2k	3.91901003201135E-21	-0.769547939336852	0.526	0.703	1.21697018524048E-16	2	Bmp2k
Pid1	4.28378399015217E-21	0.840207692327847	0.763	0.494	1.33024344246195E-16	2	Pid1
Entpd1.1	5.23967263322189E-21	-0.739274124008819	0.596	0.776	1.62707554279439E-16	2	Entpd1
Naca	5.84668580030608E-21	0.561787133525499	0.974	0.837	1.81557134156905E-16	2	Naca
Sec61g	7.94864504561606E-21	0.607931814588986	0.873	0.59	2.46829274601516E-16	2	Sec61g
Tmed5	1.61241682790358E-20	-0.764937442767754	0.522	0.702	5.00703797568898E-16	2	Tmed5
Snx3	1.62629907124698E-20	0.614404847258087	0.754	0.447	5.05014650594323E-16	2	Snx3
Ppfia4	2.22624146172467E-20	-0.774532140291307	0.57	0.721	6.91314761109361E-16	2	Ppfia4
H2-T23	2.53369663680952E-20	0.674358150249728	0.763	0.466	7.8678881662846E-16	2	H2-T23
Son.1	2.60482431248504E-20	-0.535917096816427	0.89	0.951	8.08876093755979E-16	2	Son
Ehd4	3.11003457430786E-20	0.6897944233036	0.781	0.471	9.65759036359819E-16	2	Ehd4
Mt1	3.47650849655269E-20	0.680895418997291	0.728	0.399	1.07956018343451E-15	2	Mt1
Rpl36a	3.62895326120945E-20	0.650968035845183	0.952	0.841	1.12689885620337E-15	2	Rpl36a
Rps27l	6.43260459701728E-20	0.5421500450493	0.768	0.437	1.99751670551178E-15	2	Rps27l
Spcs2	6.86775129445452E-20	-0.643852255285866	0.737	0.825	2.13264280946696E-15	2	Spcs2
Tmem176b	7.85020462903516E-20	0.773257735340698	0.904	0.836	2.43772404345429E-15	2	Tmem176b
Cox6c	8.57056456935238E-20	0.605245459499571	0.846	0.581	2.661417415721E-15	2	Cox6c
Cd63	1.27519916407629E-19	0.691534146975824	0.789	0.64	3.9598759642061E-15	2	Cd63
Tcn2	1.4602976459746E-19	-0.744801159901859	0.57	0.712	4.53466228004493E-15	2	Tcn2
Atp5l	1.89838258220387E-19	0.567280719247145	0.882	0.591	5.89504743251766E-15	2	Atp5l

(*Continued*)

Table 1. (Continued)

	p_val	avg_log2FC	pct.1	pct.2	p_val_adj	cluster	gene
Rpl15	3.07097086627031E-19	0.557641703050111	0.987	0.942	9.53628583102918E-15	2	Rpl15
Rnf13	3.87666192829017E-19	-0.688859824809731	0.649	0.753	1.20381982859195E-14	2	Rnf13
Cox7c	4.52920782720762E-19	0.555958155038005	0.904	0.719	1.40645490658278E-14	2	Cox7c
Rplp1	5.91682305275823E-19	0.359073311600416	1	1	1.83735106257301E-14	2	Rplp1
Rpl31	7.77773702822651E-19	0.623893897532578	0.904	0.631	2.41522067937518E-14	2	Rpl31
C1qa	7.81610007737381E-19	-0.409850072089153	0.925	1	2.42713355702689E-14	2	C1qa
Ptpn18	1.14761038011707E-18	0.516656744246749	0.934	0.806	3.56367451337755E-14	2	Ptpn18
Eef1a1.1	3.57994467976022E-18	0.568783481346547	1	0.999	1.11168022140594E-13	2	Eef1a1
Rps6	4.04092882049739E-18	0.643250621339852	0.982	0.886	1.25482962662905E-13	2	Rps6
H3f3a.1	4.40439225179128E-18	0.524539791686793	0.982	0.908	1.36769592594875E-13	2	H3f3a
Eif3f	7.11532154483854E-18	0.638658177445678	0.825	0.562	2.20952079931871E-13	2	Eif3f
Eef1b2	7.75419073253225E-18	0.577171799788871	0.961	0.821	2.40790884817044E-13	2	Eef1b2
Arpc3	1.04315733764028E-17	0.483922068005486	0.974	0.786	3.23931648057436E-13	2	Arpc3
Arglu1	2.02097951461616E-17	-0.682988503365991	0.662	0.751	6.27574768673757E-13	2	Arglu1
Eif3h	3.41739574262987E-17	0.562016403816608	0.789	0.504	1.06120389995885E-12	2	Eif3h
Prdx5	3.87550996381471E-17	0.739891645843199	0.846	0.588	1.20346210906338E-12	2	Prdx5
Pnp	4.90305156600558E-17	-0.494625803065984	0.816	0.872	1.52254460279171E-12	2	Pnp
Tgfb1	6.88233198928374E-17	-0.586690661816359	0.772	0.834	2.13717055263228E-12	2	Tgfb1
Foxn3	7.3705271395484E-17	-0.667641328948523	0.61	0.746	2.28876979264396E-12	2	Foxn3
Ms4a6d	8.60366474539993E-17	0.61154469289023	0.724	0.447	2.67169601338904E-12	2	Ms4a6d
Rplp0	1.09056191663698E-16	0.702211541507748	0.987	0.971	3.38652191973281E-12	2	Rplp0
Hspa8.1	1.56197945904361E-16	0.470378971744203	0.965	0.887	4.85041481416811E-12	2	Hspa8
Atp5e	2.42588741559493E-16	0.585325510235871	0.904	0.701	7.53310819164692E-12	2	Atp5e
Rpl21	3.13796727693619E-16	0.422360188942156	1	0.992	9.74432978506994E-12	2	Rpl21
Tnfaip8l2.1	3.64328222922003E-16	-0.604274789119811	0.68	0.783	1.1313484306397E-11	2	Tnfaip8l2
Ptma.1	3.81800635973008E-16	0.537655722787899	0.974	0.898	1.18560551488698E-11	2	Ptma
Irf8.1	5.12200357781794E-16	-0.352892873093243	0.75	0.883	1.59053577101981E-11	2	Irf8
Sec11c	5.63946739952162E-16	-0.612254554062919	0.632	0.732	1.75122381157345E-11	2	Sec11c
Serp1	9.88418587553427E-16	0.541444407721974	0.715	0.416	3.06933623992966E-11	2	Serp1
Clec4a2	1.53916622018373E-15	0.590675749404319	0.737	0.447	4.77957286353653E-11	2	Clec4a2
Serf2	1.63799845503095E-15	0.453107248407598	0.939	0.845	5.0864766024076E-11	2	Serf2
Cd164.1	1.71026950314588E-15	-0.584039146591802	0.588	0.786	5.31089988811891E-11	2	Cd164
2010107E0	2.22991439473136E-15	0.450199688477386	0.746	0.431	6.92455316995929E-11	2	2010107E0
Smdt1	2.74099793053947E-15	0.49467478923778	0.715	0.43	8.51162087370421E-11	2	Smdt1
Rpl22l1	4.23611667368067E-15	0.522468784729402	0.754	0.479	1.31544131067806E-10	2	Rpl22l1
Cd33	4.29042563578647E-15	-0.636769274627958	0.632	0.742	1.33230587268077E-10	2	Cd33
Evi2a	5.66013255909521E-15	-0.639937308576002	0.693	0.758	1.75764096357583E-10	2	Evi2a
Selenos.1	6.53286622059542E-15	-0.596870120933453	0.689	0.766	2.0286509474815E-10	2	Selenos
Adap2.1	8.59651579534985E-15	-0.60070179142482	0.614	0.75	2.66947604992999E-10	2	Adap2
Atp2b1	9.88937082897032E-15	0.563152562728331	0.785	0.544	3.07094632352015E-10	2	Atp2b1
Itm2b.1	1.56483621131164E-14	-0.34207768307802	0.996	1	4.85928588698605E-10	2	Itm2b
Cox4i1	1.73829051328893E-14	0.465310919735593	0.943	0.787	5.39791353091612E-10	2	Cox4i1
Fam46a	3.47214424122003E-14	0.476616892301095	0.746	0.485	1.07820495122605E-09	2	Fam46a
Hsp90b1.1	6.18215951978017E-14	-0.484638532373759	0.886	0.926	1.91974599567733E-09	2	Hsp90b1
Orai1.1	6.71121736687443E-14	-0.619303901072518	0.627	0.703	2.08403432893552E-09	2	Orai1
Adgre1	6.99987429333859E-14	0.597590887376601	0.789	0.596	2.17367096431043E-09	2	Adgre1
Arpc1b	7.63029712041265E-14	0.440521332744438	0.974	0.874	2.36943616480174E-09	2	Arpc1b

(*Continued*)

Table 1. (Continued)

	p_val	avg_log2FC	pct.1	pct.2	p_val_adj	cluster	gene
Rab14	9.80977666089721E-14	-0.464272454452693	0.855	0.884	3.04622994650841E-09	2	Rab14
Unc93b1.1	1.08174346111864E-13	-0.430922987828662	0.939	0.972	3.3591379698117E-09	2	Unc93b1
Cebpb	1.08548840940362E-13	0.809938093235967	0.829	0.666	3.37076715772105E-09	2	Cebpb
Calr	1.27446320696064E-13	-0.49503901974792	0.877	0.918	3.95759059657486E-09	2	Calr
Pdia3	1.39633655237055E-13	-0.515791708181206	0.746	0.838	4.33604389607626E-09	2	Pdia3
mt-Nd5	1.68909338778915E-13	0.57037688786207	0.789	0.564	5.24514169710163E-09	2	mt-Nd5
Ncf1	1.83549288950651E-13	-0.593821472983735	0.645	0.718	5.69975606978457E-09	2	Ncf1
Hk2	1.94290967488945E-13	-0.615854643090809	0.605	0.725	6.03331741343421E-09	2	Hk2
Akr1a1	1.95008687975717E-13	0.472807958731164	0.882	0.609	6.05560478770994E-09	2	Akr1a1
Atox1	2.14680821129842E-13	0.459402577988173	0.86	0.642	6.66648353854499E-09	2	Atox1
Tmcc3.1	2.85500668047395E-13	-0.572372442918023	0.64	0.778	8.86565224487575E-09	2	Tmcc3
Cox6b1	2.91510308413542E-13	0.432586906239381	0.825	0.566	9.05226960716572E-09	2	Cox6b1
Tmed9	4.1261014248474E-13	-0.446285221443814	0.833	0.836	1.28127827545786E-08	2	Tmed9
Wasf2	5.80925546477217E-13	-0.539868907824566	0.715	0.768	1.8039480994757E-08	2	Wasf2
Pou2f2	6.07475280846745E-13	-0.523732848806352	0.759	0.855	1.8863929896134E-08	2	Pou2f2
Eif3k	6.32109411786736E-13	0.46403757658889	0.706	0.433	1.96288935642135E-08	2	Eif3k
Atp5j2.1	6.48674554089823E-13	0.400823430424063	0.868	0.613	2.01432909281513E-08	2	Atp5j2
Vapa	7.76325531603396E-13	-0.527717274224154	0.689	0.725	2.41072367328803E-08	2	Vapa
Atp5h	7.92275180019517E-13	0.435181751620122	0.829	0.597	2.46025211651461E-08	2	Atp5h
Nsa2	1.07668680358859E-12	0.495672231672429	0.724	0.492	3.34343553118363E-08	2	Nsa2
Picalm.1	1.15093543288937E-12	-0.551282814916409	0.75	0.801	3.57399979975136E-08	2	Picalm
Tmbim6	1.18646866729683E-12	-0.409831108048267	0.908	0.928	3.68434115255686E-08	2	Tmbim6
Arpc5	1.35497631737332E-12	0.441132733784555	0.785	0.523	4.20760795833937E-08	2	Arpc5
Rpl13a	1.6774315897726E-12	0.465434219821935	0.759	0.48	5.20892831572086E-08	2	Rpl13a
Cox7a2.1	1.87555283437666E-12	0.391213564657996	0.785	0.5	5.82415421658985E-08	2	Cox7a2
Ndufa6	3.24436685093557E-12	0.452574139901997	0.728	0.467	1.00747323822102E-07	2	Ndufa6
Snrnp70	4.13613670415112E-12	-0.495022876687839	0.759	0.801	1.28439453074005E-07	2	Snrnp70
Scand1	4.68957594510304E-12	0.433166918575086	0.724	0.449	1.45625401823285E-07	2	Scand1
Npc2.1	5.60309454406054E-12	0.380155710831326	0.961	0.906	1.73992894876712E-07	2	Npc2
Cox5b	5.69592409992186E-12	0.412029800084562	0.728	0.477	1.76875531074874E-07	2	Cox5b
Arl6ip1.1	5.83813307652816E-12	-0.458777819236145	0.785	0.848	1.81291546425429E-07	2	Arl6ip1
Eef1g	6.47500465450656E-12	0.428483441042687	0.706	0.455	2.01068319536392E-07	2	Eef1g
Gabarap.1	1.01582746029182E-11	0.390442387362671	0.952	0.826	3.15444901244419E-07	2	Gabarap
Nfkbia	1.15086054013787E-11	0.482027663203991	0.719	0.447	3.57376723529014E-07	2	Nfkbia
Erp29	1.21534700611123E-11	-0.39655207901034	0.912	0.94	3.77401705807719E-07	2	Erp29
Fcgr3.1	1.2902289123316E-11	-0.375803714089854	0.904	0.977	4.00654784146332E-07	2	Fcgr3
Git2	1.29284053524272E-11	-0.55988854371515	0.627	0.725	4.01465771408923E-07	2	Git2
Tsc22d4	1.48716300925404E-11	-0.494477224250263	0.737	0.817	4.61808729263658E-07	2	Tsc22d4
Cmtm7	1.92498356468171E-11	-0.510427757890673	0.772	0.814	5.97765146340613E-07	2	Cmtm7
Gng5	2.05514432429599E-11	0.413648900219296	0.943	0.791	6.38183967023634E-07	2	Gng5
Man2b1	2.62346445839065E-11	-0.415589677224585	0.895	0.924	8.14664418264049E-07	2	Man2b1
Uqcrh	2.81757942265659E-11	0.475159873244601	0.846	0.615	8.74942938117551E-07	2	Uqcrh
Atp6v0b	4.61401899983726E-11	-0.343793062997714	0.952	0.974	1.43279132001947E-06	2	Atp6v0b
Rsrp1.1	6.43177903556122E-11	-0.370787565919689	0.956	0.967	1.99726034391283E-06	2	Rsrp1
Jpt1	8.62927444891784E-11	0.341009440074251	0.75	0.489	2.67964859462246E-06	2	Jpt1
Fcer1g.1	1.08958511112352E-10	0.272297431879171	0.987	0.998	3.38348864557187E-06	2	Fcer1g
Creg1	1.41038051668578E-10	-0.475781888805909	0.724	0.78	4.37965461846435E-06	2	Creg1

(*Continued*)

Table 1. (Continued)

	p_val	avg_log2FC	pct.1	pct.2	p_val_adj	cluster	gene
Psme1	1.47323393780053E-10	0.422671529364266	0.816	0.55	4.57483334705199E-06	2	Psme1
Ubl5	1.47450856708473E-10	0.392864945793996	0.803	0.543	4.57879145336821E-06	2	Ubl5
Rpl5	1.99864697414574E-10	0.476468163493443	0.978	0.884	6.20639844881477E-06	2	Rpl5
Pld4	2.30090399846905E-10	-0.408974129671601	0.886	0.931	7.14499718644595E-06	2	Pld4
Vdac2	3.919204262526E-10	-0.442481150148007	0.728	0.78	1.2170304996422E-05	2	Vdac2
Tmem55b	4.56930863337687E-10	-0.467993373728767	0.654	0.708	1.41890740992252E-05	2	Tmem55b
Mpeg1.1	4.71286620147909E-10	-0.508901748180138	0.68	0.77	1.4634863415453E-05	2	Mpeg1
Ost4	6.35857589584537E-10	0.353310442518575	0.719	0.453	1.97452857293686E-05	2	Ost4
Gpr183	7.32353795986329E-10	-0.499465593977062	0.654	0.732	2.27417824267635E-05	2	Gpr183
Cltc	7.47922259956494E-10	0.473139696164029	0.825	0.645	2.3225229938429E-05	2	Cltc
Zfp36l1	8.51516131995623E-10	0.537085332735128	0.807	0.648	2.64421304468601E-05	2	Zfp36l1
Cd84	8.65355225546132E-10	-0.522710669275974	0.658	0.72	2.6871875818884E-05	2	Cd84
Tmed2	8.90348849238215E-10	-0.427134474025206	0.746	0.752	2.76480028153943E-05	2	Tmed2
Elob	1.29786719630003E-09	0.385235777012019	0.803	0.596	4.03026700467049E-05	2	Elob
Srsf9	1.4331232907252E-09	-0.460266446373846	0.711	0.714	4.45027775468897E-05	2	Srsf9
Aif1	1.60268597213407E-09	-0.33429851865648	0.89	0.947	4.97682074926794E-05	2	Aif1
Pdia6	1.94660805115674E-09	-0.400423903771478	0.781	0.811	6.04480198125702E-05	2	Pdia6
Chchd2	1.97686579783406E-09	0.317890286717916	0.921	0.758	6.13876136201412E-05	2	Chchd2
Gpx1.1	2.93448564451033E-09	0.636187030617774	0.842	0.688	9.11245827189793E-05	2	Gpx1
Tnfaip8	3.0552979798693E-09	0.35818091509245	0.776	0.5	9.48761681688815E-05	2	Tnfaip8
Syngr2	3.3173348646555E-09	-0.47593829723017	0.697	0.74	0.000103013199552147	2	Syngr2
Ier5	6.21051944992603E-09	-0.493171392040171	0.658	0.701	0.000192855260478553	2	Ier5
Celf2	7.21452141717146E-09	-0.442634223025389	0.719	0.784	0.000224032533567425	2	Celf2
Sec62	7.48421264989531E-09	-0.431900661025612	0.772	0.779	0.000232407255417199	2	Sec62
Ndufb8	8.13975524301523E-09	0.305804498089606	0.702	0.448	0.000252763819561352	2	Ndufb8
Srrm2	1.03075971495809E-08	-0.413640317673794	0.838	0.836	0.000320081814285935	2	Srrm2
Hsp90ab1.	1.07825571632432E-08	0.35167219462207	0.947	0.842	0.000334830747590192	2	Hsp90ab1
Ndufa7	1.75951932985345E-08	0.276316399359865	0.759	0.492	0.000546383537499391	2	Ndufa7
Hnrnpk	1.93996633697784E-08	-0.417497792561588	0.763	0.78	0.000602417746621728	2	Hnrnpk
Lrrc25	3.70835540880664E-08	0.267227337642733	0.702	0.441	0.00115155560509673	2	Lrrc25
Rpl36al	3.93891109134153E-08	0.370586462376766	0.759	0.561	0.00122315006119429	2	Rpl36al
Cd300c2.1	5.65715851736389E-08	-0.32719075565138	0.842	0.902	0.00175671743439701	2	Cd300c2
Bri3	6.46423008951682E-08	0.377938167940918	0.899	0.74	0.00200733736969766	2	Bri3
Rpl4	6.9124941094832E-08	0.426069966657198	0.904	0.767	0.00214653679581782	2	Rpl4
Atpif1	7.22844032746643E-08	0.303405735826749	0.842	0.629	0.00224464757488815	2	Atpif1
Ssr4	7.25749685482032E-08	-0.391343642451748	0.776	0.829	0.00225367049832735	2	Ssr4
Luc7l2	1.29567945512172E-07	-0.406661315044541	0.715	0.763	0.00402347341198948	2	Luc7l2
Plekho1	1.52226021603442E-07	-0.38843882657898	0.754	0.793	0.00472707464885167	2	Plekho1
Sec61b	1.71237666370415E-07	0.378977311169671	0.737	0.518	0.0053174432538005	2	Sec61b
Npm1.1	1.71443561553923E-07	0.367223103794778	0.846	0.676	0.00532383691693398	2	Npm1
mt-Nd1	2.46361188125729E-07	0.268297311325853	0.996	0.976	0.00765025397486825	2	mt-Nd1
Grn	2.93040379222069E-07	-0.320905218024805	0.912	0.967	0.0090997828959829	2	Grn
Slc3a2	3.3370673524831E-07	-0.348898592772481	0.737	0.783	0.0103625952496658	2	Slc3a2
Eef1d	3.55973951207723E-07	0.269002142533624	0.811	0.58	0.0110540591068534	2	Eef1d
Canx	4.41443875948037E-07	-0.372167163753741	0.706	0.756	0.0137081566798144	2	Canx
Uqcrb	5.85956651206878E-07	0.298075406343959	0.719	0.49	0.0181957118899272	2	Uqcrb
Timp2.1	6.22958875926944E-07	-0.309246663169858	0.754	0.829	0.0193447419741594	2	Timp2

(*Continued*)

Table 1. (Continued)

	p_val	avg_log2FC	pct.1	pct.2	p_val_adj	cluster	gene
Ppia.1	6.78980834658084E-07	0.253461947964809	1	0.978	0.0210843918586375	2	Ppia
Cd68	6.89605518846881E-07	-0.318176816151383	0.912	0.924	0.0214143201767522	2	Cd68
Pnisr	7.93169266411563E-07	-0.362165507531715	0.768	0.764	0.0246302852298783	2	Pnisr
AC149090.	9.49503992252892E-07	-0.29735851658342	0.816	0.89	0.0294849474714291	2	AC149090.
Tmem50a	1.14847766254682E-06	-0.309422963631777	0.86	0.867	0.0356636768550665	2	Tmem50a
Rbm3.1	1.18434860854952E-06	0.397520068361228	0.772	0.583	0.0367775773412884	2	Rbm3
Bst2.1	2.01646289492601E-74	1.38439663150328	0.75	0.452	6.26172222761374E-70	3	Bst2
Ly6e.2	1.92434322389912E-67	0.739293231124573	0.987	0.95	5.97566301317395E-63	3	Ly6e
H2-K1.1	4.96994621078869E-59	1.27752330969304	0.857	0.721	1.54331739683621E-54	3	H2-K1
H2-D1.1	4.65728297656834E-54	1.30019558248527	0.86	0.73	1.44622608271377E-49	3	H2-D1
B2m.1	3.28005039221323E-45	0.689996466519465	0.987	0.964	1.01855404829398E-40	3	B2m
Fcgr1	9.07626885562554E-33	0.605810030608563	0.943	0.848	2.8184537677374E-28	3	Fcgr1
Ctss.2	4.9740995639246E-31	0.312989083056316	1	0.999	1.5446071375855E-26	3	Ctss
Cd52.2	1.8577059954905E-18	0.690089060723365	0.708	0.575	5.76873442779664E-14	3	Cd52
P2ry12.1	3.3125041389265E-17	-0.270613801836562	0.996	0.993	1.02863191026085E-12	3	P2ry12
Fth1.1	6.59341646245358E-14	0.279168891302981	0.998	0.996	2.04745361408571E-09	3	Fth1
Fcrls.2	1.98059140044036E-13	-0.287053091425957	0.958	0.982	6.15033047578744E-09	3	Fcrls
Pmp22.1	1.82547290265218E-11	-0.353956253292346	0.662	0.77	5.6686410046058E-07	3	Pmp22
Ctsc.1	1.16760387624373E-10	0.256879870591931	0.86	0.793	3.62576031689965E-06	3	Ctsc
Ltc4s.1	2.00381776458447E-09	-0.27512615461476	0.91	0.942	6.22245530436416E-05	3	Ltc4s
Scoc.1	5.03017141696932E-09	-0.275312760761899	0.809	0.876	0.000156201913011148	3	Scoc
Ecscr.1	1.71398903752471E-08	-0.26091754977706	0.792	0.867	0.000532245015822548	3	Ecscr
mt-Co1.1	4.89170012285646E-50	0.911573447295116	1	0.995	1.51901963915062E-45	4	mt-Co1
mt-Atp6.1	4.88980916070267E-44	0.879017763203261	1	0.998	1.518432438673E-39	4	mt-Atp6
mt-Co2.1	3.06810772268287E-36	0.796225032041781	0.996	0.996	9.52739491124712E-32	4	mt-Co2
mt-Nd4.1	3.7542266892755E-34	0.754760456201156	0.996	0.985	1.16580001382072E-29	4	mt-Nd4
mt-Co3.1	8.47897809981095E-33	0.767706717834705	1	0.997	2.63297706933429E-28	4	mt-Co3
mt-Cytb	1.17225110026362E-29	0.7108238306546	1	0.995	3.64019134164862E-25	4	mt-Cytb
mt-Nd2	1.68140822162614E-26	0.75607274901141	0.996	0.984	5.22127695061567E-22	4	mt-Nd2
mt-Nd5.1	1.79530917608E-25	0.912413599377397	0.787	0.564	5.57497358448124E-21	4	mt-Nd5
mt-Nd1.1	2.63088450330986E-22	0.613005696500472	0.989	0.976	8.16968564812812E-18	4	mt-Nd1
Cox8a.1	3.29069008015369E-16	0.706411586331548	0.886	0.773	1.02185799059013E-11	4	Cox8a
mt-Nd3	2.99026928224297E-12	0.502502909497057	0.924	0.877	9.28568320214909E-08	4	mt-Nd3
Cox6c.1	2.5258890333218E-11	0.715996887894111	0.707	0.583	7.84364321517419E-07	4	Cox6c
Ly86.1	2.08763416869304E-10	-0.274517307712901	0.973	0.997	6.48273038404251E-06	4	Ly86
Rplp0.1	2.19739072057878E-10	-0.31178168522705	0.966	0.971	6.82355740461328E-06	4	Rplp0
Rps4x.2	3.39074375974169E-08	-0.264979678898781	0.989	0.984	0.00105292765971259	4	Rps4x
Rps3.1	1.67955234009716E-07	-0.259162542879798	0.97	0.978	0.0052155138817037	4	Rps3
Ctsh.1	1.97605186356664E-07	-0.260443089324299	0.932	0.959	0.00613623385193348	4	Ctsh
Calm1.2	5.22910084451952E-07	0.324001925143003	0.833	0.735	0.0162379268524865	4	Calm1
Cd68.1	1.05331549467576E-06	-0.291650987813162	0.882	0.925	0.0327086060561664	4	Cd68
Ndufa4.2	1.10795031705453E-06	0.534336615943904	0.749	0.639	0.0344051811954944	4	Ndufa4
Cox7c.1	1.13620517299142E-06	0.383436152828528	0.764	0.721	0.0352825792369025	4	Cox7c
Rpl12.1	1.31378473666861E-06	-0.272205465122428	0.928	0.931	0.0407969574277704	4	Rpl12
Ccr1	0	3.07531506005891	1	0.022	0	5	Ccr1
Ccr5.2	5.14078518699322E-24	-0.753167180196993	0.608	0.828	1.596368024117E-19	5	Ccr5
Olfml3.1	9.78357254864611E-07	0.276063226593715	0.981	0.977	0.0303809278353108	5	Olfml3

(*Continued*)

Table 1. (Continued)

	p_val	avg_log2FC	pct.1	pct.2	p_val_adj	cluster	gene
Cdkn1a	0	3.43376426832513	0.972	0.05	0	6	Cdkn1a
Bax	1.78413315147855E-50	1.12222946231033	0.76	0.421	5.54026867528634E-46	6	Bax
Rps19.1	4.02821470596027E-16	0.407865038514133	0.984	0.955	1.25088151264184E-11	6	Rps19
Rpl39.1	1.98736775387821E-12	-0.350866959010792	0.972	0.989	6.171373086118E-08	6	Rpl39
Ier5.1	5.62964216852923E-12	0.443912759843309	0.823	0.698	1.74817278259338E-07	6	Ier5
Rps21.2	8.52504182983921E-12	-0.316852473757971	0.98	0.993	2.64728123941997E-07	6	Rps21
P2ry6	1.18390267393689E-11	0.388269615427526	0.894	0.824	3.67637297337621E-07	6	P2ry6
Rps27.2	3.8523551423191E-10	-0.295547680851792	0.984	0.99	1.19627184234435E-05	6	Rps27
Rpl27a.2	4.56205919601485E-09	-0.267107089592812	0.98	0.994	0.000141665624213849	6	Rpl27a
Rpl37.2	7.16647630177139E-09	-0.273654908740777	0.976	0.99	0.000222540588598907	6	Rpl37
Spi1	1.9974177378623E-08	0.307728327827713	0.906	0.834	0.000620258130138381	6	Spi1
Rpl34.2	5.86662206674482E-08	-0.27461414839775	0.953	0.98	0.00182176215038627	6	Rpl34
Rpl35.1	5.9931739241275E-08	-0.351479459708379	0.85	0.881	0.00186106029865931	6	Rpl35
Serpine2.1	7.44329446370467E-08	0.360029125698304	0.843	0.802	0.00231136622981421	6	Serpine2
Rps13.1	4.38472064916861E-07	-0.27805651534537	0.957	0.973	0.0136158730318633	6	Rps13
Rps28.2	1.18174271621467E-06	-0.283720314635626	0.925	0.961	0.0366966565666141	6	Rps28
Exosc2	0	2.62781902812805	0.802	0.174	0	7	Exosc2
AC160336.	1.21301659981191E-66	1.26554518644694	0.724	0.549	3.76678044739591E-62	7	AC160336.
Ctsb.2	4.9558050594268E-10	-0.263144543594134	0.976	0.981	1.53892614510381E-05	7	Ctsb
H2-D1.3	2.87271958679412E-07	-0.308652586201546	0.674	0.736	0.00892065613287179	7	H2-D1
Cd63.1	0	2.29804463066512	0.982	0.625	0	8	Cd63
Cd9.2	0	1.54516801762404	1	0.969	0	8	Cd9
Ctsb.3	0	1.4831233398661	1	0.98	0	8	Ctsb
Ctsz.1	0	1.17071096447867	1	0.992	0	8	Ctsz
Ftl1.1	5.65089639532407E-294	1.16671616962344	1	0.99	1.75477285763998E-289	8	Ftl1
Ctsd.1	1.79024356661208E-292	0.869949891126517	1	0.999	5.5592433474005E-288	8	Ctsd
Cd83	2.36809750628E-288	1.77625205682349	0.739	0.242	7.35365318625127E-284	8	Cd83
Selplg.1	4.50056348535248E-217	-0.844289085888205	0.991	0.995	1.3975599791065E-212	8	Selplg
P2ry12.2	9.29318214429668E-209	-0.88717634919471	0.985	0.993	2.88581185126845E-204	8	P2ry12
Cd68.2	1.49821242901075E-161	0.872830488647879	0.992	0.921	4.65239905580709E-157	8	Cd68
C3ar1	3.61601153140924E-158	1.17628780865338	0.806	0.434	1.12288006084851E-153	8	C3ar1
Tmem119.	7.96821126874067E-151	-0.764803249988697	0.954	0.99	2.47436864528204E-146	8	Tmem119
Cadm1	2.3262945185331E-149	1.12785916619523	0.72	0.347	7.22384236840084E-145	8	Cadm1
Mt1.1	1.02058751643929E-129	1.00238842930129	0.753	0.386	3.16923041479893E-125	8	Mt1
Serinc3.1	1.04518546520817E-126	-0.524012008424553	0.996	0.999	3.24561442511093E-122	8	Serinc3
Cyba	3.82448354443321E-123	0.616547774323673	0.996	0.984	1.18761687505285E-118	8	Cyba
Siglech.2	2.65875617706483E-100	-0.586574062026276	0.96	0.986	8.25623555663941E-96	8	Siglech
Ctsa.1	9.18401407056005E-93	0.621153848629843	0.981	0.896	2.85191188933101E-88	8	Ctsa
Hsp90ab1.	2.90712968092798E-89	0.726831439873448	0.937	0.839	9.02750979818565E-85	8	Hsp90ab1
Eif4a1.1	1.64176735410592E-88	0.850410645825236	0.916	0.758	5.09818016470511E-84	8	Eif4a1
Calr.1	4.96261680677063E-87	0.638624914782328	0.982	0.914	1.54104139700648E-82	8	Calr
Pnp.1	5.13930432087951E-87	-0.721953086032058	0.744	0.877	1.59590817076271E-82	8	Pnp
Slc2a5.1	3.11323812318665E-84	-0.834339218013318	0.529	0.756	9.66753834393152E-80	8	Slc2a5
Grn.1	4.51604419356786E-81	0.524743282064129	0.991	0.965	1.40236720342863E-76	8	Grn
Fth1.2	4.37030643933904E-80	0.582813678919012	1	0.996	1.35711125860795E-75	8	Fth1
Aldoa	2.82589552574676E-79	0.755421841772364	0.799	0.538	8.77525337610142E-75	8	Aldoa
Rhob.2	2.8780395990474E-79	-0.544094079948244	0.964	0.986	8.93717636692191E-75	8	Rhob

(*Continued*)

Table 1. (Continued)

	p_val	avg_log2FC	pct.1	pct.2	p_val_adj	cluster	gene
Prdx1.2	7.61299861361345E-78	0.701066346725705	0.802	0.555	2.36406445948539E-73	8	Prdx1
Zfhx3.1	1.19082320953699E-76	-0.655635845403785	0.801	0.916	3.69786331257521E-72	8	Zfhx3
Sdf2l1.1	2.79868653556119E-76	0.899185252664238	0.765	0.52	8.69076129887817E-72	8	Sdf2l1
Dnase2a	5.24110074378046E-75	0.725973414614582	0.745	0.469	1.62751901396615E-70	8	Dnase2a
Hspa5.1	9.69014544666345E-75	0.717897713426487	0.947	0.845	3.0090808655524E-70	8	Hspa5
Npc2.2	1.14135772665376E-74	0.505345295003798	0.973	0.904	3.54425814857792E-70	8	Npc2
Ivns1abp.1	1.14067577595922E-73	-0.696114089343054	0.703	0.831	3.54214048708617E-69	8	Ivns1abp
Gapdh.1	2.09532399991922E-73	0.655580269017518	0.942	0.826	6.50660961694916E-69	8	Gapdh
Adrb2	2.37770893871912E-72	-0.776856535810651	0.476	0.707	7.38349956740447E-68	8	Adrb2
Trem2.2	8.4390685350099E-72	0.361999080628309	1	0.996	2.62058395217662E-67	8	Trem2
Creg1.1	5.53050457214583E-69	0.562616411197819	0.919	0.773	1.71738758478845E-64	8	Creg1
Slc25a5	9.17219396097847E-69	0.615716490058619	0.902	0.75	2.84824139070265E-64	8	Slc25a5
P2ry13.1	3.28378602971041E-68	-0.560659783020534	0.895	0.946	1.01971407580597E-63	8	P2ry13
Commd8.1	1.97143990728E-64	-0.689170976350403	0.567	0.747	6.12191234407659E-60	8	Commd8
Rps2.1	1.06072351372311E-63	0.463212915612133	0.975	0.929	3.29386472716438E-59	8	Rps2
Vsir.2	1.44019860510305E-63	-0.455538521385318	0.95	0.976	4.47224872842651E-59	8	Vsir
Lamp1	1.44048180581282E-63	0.432711845443972	0.989	0.968	4.47312815159054E-59	8	Lamp1
Susd3.1	2.49406935986811E-62	-0.643544215633243	0.644	0.796	7.74483358319846E-58	8	Susd3
Csf1r.1	5.68150480837528E-62	-0.302051251303159	1	0.999	1.76427768814478E-57	8	Csf1r
Ifngr1.1	1.39615877046287E-59	-0.423827282757582	0.968	0.985	4.33549182991836E-55	8	Ifngr1
Syngr1.1	1.40977942076103E-59	0.5333823855998	0.932	0.805	4.37778803528922E-55	8	Syngr1
Ltc4s.2	7.58691910422862E-59	-0.564182294135025	0.89	0.944	2.35596598943611E-54	8	Ltc4s
Txnip.2	8.85849601099603E-58	-0.59230117569223	0.759	0.863	2.7508287662946E-53	8	Txnip
Pdia6.1	7.79778103288753E-57	0.535705404261183	0.932	0.805	2.42144494414257E-52	8	Pdia6
Cx3cr1.1	9.25539750103571E-57	-0.38126083411941	0.994	0.995	2.87407858599662E-52	8	Cx3cr1
Ssh2.1	2.86369276444416E-56	-0.616931158263941	0.674	0.814	8.89262514142845E-52	8	Ssh2
Srgap2.1	4.01773302646846E-56	-0.547167987541366	0.796	0.894	1.24762663670925E-51	8	Srgap2
Lpcat2.1	8.25845776565788E-56	-0.415881376807884	0.967	0.981	2.56449888996974E-51	8	Lpcat2
Elmo1.1	1.58885845794808E-55	-0.655133992864196	0.62	0.764	4.93388216946619E-51	8	Elmo1
Cotl1	2.11411084462814E-55	0.531945879892493	0.897	0.752	6.56494840582377E-51	8	Cotl1
Ctsl.2	1.27263286238336E-54	0.42806463878946	0.998	0.985	3.95190682755905E-50	8	Ctsl
Asph	1.79790327758073E-54	0.579853438524778	0.83	0.662	5.58302904787143E-50	8	Asph
Ptgs1.1	3.69722153716382E-54	-0.502842936711786	0.84	0.916	1.14809820393548E-49	8	Ptgs1
Apoe.1	6.47282283145754E-53	0.554447251148479	0.754	0.53	2.01000567385251E-48	8	Apoe
Tyrobp.1	3.10159317614079E-52	0.305938905874624	1	0.998	9.63137728987E-48	8	Tyrobp
Cmtm7.1	1.5400700048622E-51	-0.548754393893354	0.691	0.819	4.78237938609859E-47	8	Cmtm7
Rgs10.2	1.66585897471301E-51	-0.358646616428772	0.981	0.991	5.17299187417631E-47	8	Rgs10
Maf.1	4.08340130401126E-51	-0.531198348565383	0.869	0.924	1.26801860693462E-46	8	Maf
Ssr4.1	7.79359985860166E-51	0.438635378351858	0.939	0.823	2.42014656409157E-46	8	Ssr4
Cmtm6.2	8.343662334429E-49	-0.516184684673656	0.753	0.847	2.59095746471024E-44	8	Cmtm6
Bcl2a1b	2.29711597099703E-48	0.661957595851463	0.785	0.601	7.13323422473708E-44	8	Bcl2a1b
Gusb	5.78942773791784E-48	0.535575860894955	0.836	0.636	1.79779099545563E-43	8	Gusb
Calm2.1	1.05031706839045E-47	-0.418555464175271	0.93	0.956	3.26154959247287E-43	8	Calm2
Nrip1.1	1.18069866325771E-47	-0.538909753398394	0.744	0.852	3.66642355901417E-43	8	Nrip1
mt-Nd1.2	1.9537330253942E-47	0.476994712017097	0.979	0.976	6.06692716375661E-43	8	mt-Nd1
Rnase4.2	1.36624359127097E-46	-0.445893747711319	0.904	0.954	4.24259622397375E-42	8	Rnase4
Frmd4a.1	1.45309391865056E-46	-0.484704054430051	0.827	0.893	4.51229254558557E-42	8	Frmd4a

(*Continued*)

Table 1. (Continued)

	p_val	avg_log2FC	pct.1	pct.2	p_val_adj	cluster	gene
Psap.1	1.65466999957967E-46	0.377436847358631	1	0.992	5.13824674969474E-42	8	Psap
Hsp90b1.2	3.34452027332648E-46	0.444385462872208	0.977	0.923	1.03857388047607E-41	8	Hsp90b1
Hspa8.2	4.64694407314333E-46	0.471526992668645	0.951	0.885	1.4430155430332E-41	8	Hspa8
Cd164.2	9.76234682818389E-46	-0.573393832812395	0.664	0.79	3.03150156055594E-41	8	Cd164
St3gal6.1	2.63526344708144E-45	-0.513259352936535	0.697	0.813	8.18328358222198E-41	8	St3gal6
Glul.2	3.10760019011743E-45	-0.486655830058533	0.855	0.9	9.65003087037166E-41	8	Glul
Manf.1	8.06641154769464E-45	0.562405815075004	0.867	0.688	2.50486277790562E-40	8	Manf
Arhgap5.1	8.26471238944432E-45	-0.496287053145072	0.827	0.897	2.56644113829414E-40	8	Arhgap5
Adgrg1.1	1.76814132654111E-44	-0.563366193930639	0.662	0.763	5.4906092613081E-40	8	Adgrg1
mt-Atp6.2	2.26461394958704E-44	0.379968099492182	0.998	0.998	7.03230569765264E-40	8	mt-Atp6
Ssr2.1	3.5620009979267E-43	0.480146262859831	0.72	0.489	1.10610816988618E-38	8	Ssr2
Hpgd.1	1.06149621335982E-42	-0.506817022093743	0.756	0.845	3.29626419134624E-38	8	Hpgd
Pmepa1.1	1.12993168925879E-42	-0.485243666497403	0.892	0.944	3.50877687465531E-38	8	Pmepa1
Timp2.2	2.91883780301469E-42	0.418838401706748	0.93	0.823	9.06386702970152E-38	8	Timp2
Eif5a.2	1.12471932250698E-41	0.506050269259257	0.814	0.627	3.49259091218094E-37	8	Eif5a
F11r.1	1.14244009534915E-40	-0.395677475901032	0.918	0.949	3.54761922808772E-36	8	F11r
Atp6ap2	1.12674631950163E-39	0.459997633941989	0.864	0.688	3.49888534594842E-35	8	Atp6ap2
Ctsc.2	8.92662014852459E-39	0.424248652824609	0.91	0.789	2.77198335472134E-34	8	Ctsc
Rpsa.2	1.07208100139989E-38	0.348408228978954	0.967	0.926	3.32913313364707E-34	8	Rpsa
Srgn.1	1.25531540440601E-38	0.544902528289219	0.737	0.55	3.89813092530198E-34	8	Srgn
Mbnl1	3.11958903347287E-38	-0.466372473172114	0.821	0.868	9.6872598256433E-34	8	Mbnl1
Ncl.1	5.39752535990159E-38	0.573025026718125	0.725	0.532	1.67609355001024E-33	8	Ncl
Arhgap45.2	2.11705059672011E-37	-0.436209353845278	0.779	0.867	6.57407721799497E-33	8	Arhgap45
Mef2a.1	1.92288220047842E-36	-0.427905366142296	0.795	0.888	5.97112609714565E-32	8	Mef2a
Alox5ap	2.15109418600895E-35	-0.46890723391594	0.715	0.808	6.67979277581361E-31	8	Alox5ap
Fam102b.1	3.03171785061314E-35	-0.520044804258609	0.584	0.713	9.41439344150899E-31	8	Fam102b
Tmem173.	2.26393552520826E-34	-0.459229994702944	0.68	0.78	7.0301989864292E-30	8	Tmem173
Ckb.1	3.04536386991144E-34	-0.389467832746993	0.924	0.945	9.45676842523599E-30	8	Ckb
Rsrp1.2	3.42027370654977E-34	-0.353632733601948	0.942	0.968	1.0620975940949E-29	8	Rsrp1
Serpine2.2	5.79996807417822E-34	0.410739977569245	0.916	0.797	1.80106408607456E-29	8	Serpine2
Pdia3.1	6.68232734120519E-34	0.395636647450952	0.938	0.831	2.07506310926445E-29	8	Pdia3
Glmp	1.1221728070886E-33	0.433231412248728	0.716	0.493	3.48468321785222E-29	8	Glmp
Ptma.2	1.34349120677872E-33	0.348988784339256	0.973	0.895	4.17194324440995E-29	8	Ptma
Crybb1.3	2.16678752994459E-33	-0.547399860214337	0.65	0.751	6.72852531673695E-29	8	Crybb1
mt-Co2.2	2.18792909249224E-33	0.323932311570829	0.996	0.996	6.79417621091615E-29	8	mt-Co2
Slc3a2.1	4.81550555062895E-33	0.472699984515899	0.894	0.777	1.49535893863681E-28	8	Slc3a2
mt-Co3.2	7.78332976398412E-33	0.330243744764552	0.995	0.997	2.41695739160999E-28	8	mt-Co3
Tmem176b	9.25337770620232E-33	-0.502776632558105	0.767	0.841	2.87345137910701E-28	8	Tmem176b
Slco2b1.1	4.07562227134426E-32	-0.390407821211703	0.854	0.891	1.26560298392053E-27	8	Slco2b1
mt-Nd2.1	5.54387532988732E-32	0.378265178004132	0.995	0.984	1.72153960618991E-27	8	mt-Nd2
Tnfaip8l2.2	6.43387657448121E-32	-0.42878838441006	0.689	0.786	1.99791169267365E-27	8	Tnfaip8l2
Ybx1.3	8.31649704517378E-32	0.412576831129288	0.828	0.651	2.58252182743781E-27	8	Ybx1
Tsc22d4.1	2.84679965680923E-31	-0.40979953878853	0.743	0.82	8.8401669742897E-27	8	Tsc22d4
Ccr5.3	4.79441639813565E-31	-0.475058709648057	0.758	0.828	1.48881012411306E-26	8	Ccr5
H2-K1.3	5.94604051329431E-31	0.352520375604056	0.881	0.716	1.84642396059328E-26	8	H2-K1
Cfl1	6.84169804627813E-31	0.316152382715626	0.964	0.928	2.12455249431075E-26	8	Cfl1
Fam49b.1	7.91358930980715E-31	-0.369350308421919	0.842	0.886	2.45740688837442E-26	8	Fam49b

(*Continued*)

Table 1. (Continued)

	p_val	avg_log2FC	pct.1	pct.2	p_val_adj	cluster	gene
Abhd12.1	1.44236057381535E-30	0.323710406196794	0.986	0.953	4.47896228986881E-26	8	Abhd12
Pmp22.2	1.46922281469256E-30	0.601295803227464	0.862	0.762	4.56237760646481E-26	8	Pmp22
Pld4.1	8.01365025949018E-30	-0.365263790811843	0.895	0.932	2.48847881507949E-25	8	Pld4
Zfp36l2.1	1.05118544658868E-29	-0.469341907918229	0.703	0.779	3.26424616729183E-25	8	Zfp36l2
Kctd12.1	1.06632303539353E-29	-0.411060117067163	0.807	0.867	3.31125292180752E-25	8	Kctd12
Spcs2.1	1.51718078376072E-29	0.353380627016068	0.91	0.82	4.71130148781217E-25	8	Spcs2
Gnai2	1.81604525501735E-29	-0.31294722920072	0.944	0.961	5.63936533040539E-25	8	Gnai2
Ppia.2	1.30843519307151E-28	0.255180529847415	0.987	0.978	4.06308380504497E-24	8	Ppia
Canx.1	1.82964959839069E-27	0.347911268266192	0.874	0.749	5.68161089788261E-23	8	Canx
Ppfia4.1	3.57358274003528E-27	-0.408605345701883	0.621	0.724	1.10970464826316E-22	8	Ppfia4
Tanc2.1	4.43293618389633E-27	-0.430787794690276	0.702	0.778	1.37655967318533E-22	8	Tanc2
Tmem86a.	8.03801106610128E-27	0.387263850643032	0.904	0.797	2.49604357635643E-22	8	Tmem86a
Ptpn18.1	1.23027426761042E-26	-0.387948804438304	0.736	0.811	3.82037068321065E-22	8	Ptpn18
Dad1	1.25051437701368E-26	0.335097544921475	0.853	0.675	3.88322229494057E-22	8	Dad1
Git2.1	2.29123654626136E-26	-0.437054881693923	0.643	0.728	7.11497684710542E-22	8	Git2
Ecscr.2	3.76014584164265E-26	-0.368424805985026	0.814	0.867	1.16763808820529E-21	8	Ecscr
B2m.2	4.18012132656751E-26	0.264894224934046	0.987	0.963	1.29805307553901E-21	8	B2m
Rpl10a.2	4.18717109364947E-26	0.267339486076959	0.972	0.898	1.30024223971097E-21	8	Rpl10a
Gnas.1	9.62506960416419E-26	0.336030750707358	0.906	0.8	2.98887286418111E-21	8	Gnas
Npm1.2	1.16624609343738E-25	0.424022212543326	0.807	0.671	3.6215439939511E-21	8	Npm1
Atox1.1	1.94017907467132E-25	0.35244207601904	0.802	0.636	6.02483808057685E-21	8	Atox1
Krtcap2.1	2.09207368012998E-25	0.376558207810135	0.716	0.553	6.49651639890764E-21	8	Krtcap2
Arpc2.1	2.89371402697861E-25	0.296343146782166	0.952	0.893	8.98585016797667E-21	8	Arpc2
Pag1.1	4.08295281051541E-25	-0.404001156752083	0.639	0.735	1.26787933624935E-20	8	Pag1
Bin2.1	1.15333965206071E-24	-0.363982603522883	0.715	0.789	3.58146562154413E-20	8	Bin2
Rps9.2	1.35530652184561E-24	-0.265819223946562	0.996	0.992	4.20863334228717E-20	8	Rps9
Rgs2.2	2.58628292793391E-24	-0.35919293434617	0.802	0.859	8.03118437611316E-20	8	Rgs2
Ophn1	6.06412348593023E-24	-0.417371770115936	0.621	0.7	1.88309226608591E-19	8	Ophn1
H2-D1.4	7.03474391698801E-24	0.293824863571368	0.869	0.727	2.18449902854229E-19	8	H2-D1
Erp29.1	1.34760315333823E-23	0.275774488579251	0.979	0.938	4.1847120720612E-19	8	Erp29
mt-Nd4.2	6.18280053492699E-23	0.279258098452354	0.986	0.986	1.91994505011088E-18	8	mt-Nd4
Tpp1	7.02469912920861E-23	0.33132805368182	0.798	0.638	2.18137982059315E-18	8	Tpp1
Fam105a.1	2.79713073247418E-22	-0.317825770228975	0.858	0.891	8.68593006355208E-18	8	Fam105a
Epb41l2.1	2.87129950716644E-22	-0.331600967731752	0.909	0.916	8.91624635960396E-18	8	Epb41l2
Cd84.1	1.17397648087063E-21	0.338634989142378	0.848	0.713	3.64554916604757E-17	8	Cd84
Tm6sf1	1.30846335940964E-21	-0.375294604858226	0.64	0.729	4.06317126997476E-17	8	Tm6sf1
Wasf2.1	1.97627089527403E-21	-0.352331321243301	0.71	0.77	6.13691401109445E-17	8	Wasf2
Fcgr1.1	2.0859944076169E-21	-0.335460342069659	0.804	0.852	6.47763843397275E-17	8	Fcgr1
Cd52.3	2.25198730560763E-21	0.405529453782898	0.719	0.571	6.99309618010336E-17	8	Cd52
Hexa	2.87557606155249E-21	0.280108253479925	0.979	0.94	8.92952634393895E-17	8	Hexa
Tmed9.1	3.41793826931766E-21	0.264575197438471	0.913	0.832	1.06137237077121E-16	8	Tmed9
Ywhah.1	5.06032945066087E-21	-0.310117375924705	0.861	0.889	1.57138410431372E-16	8	Ywhah
Gabarap.2	1.00777190280094E-20	0.269071795962169	0.925	0.823	3.12943408976777E-16	8	Gabarap
Tpst2.1	1.98143311789268E-20	-0.369364197870582	0.663	0.749	6.15294426099213E-16	8	Tpst2
Celf2.1	3.13963279358223E-20	-0.359427416034551	0.727	0.786	9.7495017139109E-16	8	Celf2
Ddost	3.53733616391243E-20	0.338065951325238	0.753	0.588	1.09844899897973E-15	8	Ddost
Rbm3.2	5.67522503067435E-20	0.319863230590694	0.725	0.579	1.7623276287753E-15	8	Rbm3

(*Continued*)

Table 1. (Continued)

	p_val	avg_log2FC	pct.1	pct.2	p_val_adj	cluster	gene
Bmp2k.1	5.67839050545066E-20	-0.378820543412697	0.639	0.704	1.76331060365759E-15	8	Bmp2k
Fkbp2.1	6.06425874900776E-20	0.341080581066399	0.733	0.578	1.88313426932938E-15	8	Fkbp2
Ppib	1.17990901279462E-19	0.276677381713492	0.933	0.86	3.66397145743113E-15	8	Ppib
mt-Nd3.1	1.80257283677481E-19	0.322989800375962	0.924	0.876	5.59752943003682E-15	8	mt-Nd3
Rps27.3	1.96179690767096E-19	-0.263129105572359	0.982	0.991	6.09196793739063E-15	8	Rps27
Qk.1	4.08618647358674E-19	-0.259427144592222	0.933	0.948	1.26888348564289E-14	8	Qk
Itgam.1	1.51726815832078E-18	-0.348368882884458	0.759	0.797	4.71157281203351E-14	8	Itgam
Atp6ap1	2.4505176011153E-18	0.294891853050671	0.711	0.546	7.60959230674334E-14	8	Atp6ap1
Picalm.2	2.76314953025217E-18	-0.337154400684982	0.767	0.802	8.58040823629207E-14	8	Picalm
Arsb.1	6.15550705637644E-18	-0.321435432479596	0.796	0.81	1.91146960621657E-13	8	Arsb
Tmed3.1	6.31768087674275E-18	0.309292476936743	0.723	0.581	1.96182944265492E-13	8	Tmed3
Actr3.1	9.48092766075481E-18	0.318496050711825	0.752	0.6	2.94411246649419E-13	8	Actr3
Akr1a1.1	1.58133735972227E-17	0.286654861403575	0.757	0.605	4.91052690314556E-13	8	Akr1a1
Foxn3.1	5.67970975850568E-17	-0.328812781350265	0.708	0.746	1.76372027130877E-12	8	Foxn3
Atp6v1g1	6.75467183434774E-17	0.291408843619294	0.828	0.716	2.09752824472E-12	8	Atp6v1g1
Ucp2.2	8.16577942177794E-17	0.280251886059107	0.829	0.708	2.5357194838447E-12	8	Ucp2
Inpp5d.1	1.32954737965335E-16	-0.281699562948805	0.828	0.862	4.12864347803755E-12	8	Inpp5d
Atp5b	1.5718254786845E-16	0.311681993281979	0.726	0.584	4.88098965895898E-12	8	Atp5b
Cd33.1	3.75338961888481E-16	-0.342354740625025	0.706	0.742	1.1655400783523E-11	8	Cd33
Adap2.2	8.18950162837603E-16	-0.332638521542607	0.706	0.75	2.54308594065961E-11	8	Adap2
Myl6.1	8.46500370570202E-16	0.254229029958553	0.8	0.664	2.62863760073165E-11	8	Myl6
Srsf2.1	1.10768934574481E-15	0.370438246052577	0.772	0.682	3.43970772534135E-11	8	Srsf2
Golm1.1	1.18716005101352E-15	-0.28314526747922	0.849	0.865	3.68648810641229E-11	8	Golm1
Lrp1.1	1.8336777954223E-15	0.271717828057505	0.818	0.711	5.69411965812486E-11	8	Lrp1
Evi2a.1	2.33175862562294E-15	0.316409582377507	0.849	0.752	7.24081006014691E-11	8	Evi2a
Tmem55b.	2.85165465558581E-15	-0.292515967519428	0.647	0.71	8.85524320199062E-11	8	Tmem55b
Cfh	3.04296031432077E-15	-0.28333795605719	0.788	0.813	9.44930466406028E-11	8	Cfh
Ncf1.1	3.19760750604483E-15	-0.314301919825442	0.66	0.72	9.92953058852102E-11	8	Ncf1
Srrm2.1	4.4528764536497E-15	-0.283997988818107	0.834	0.837	1.38275172515184E-10	8	Srrm2
Limd2.1	4.95659390611145E-15	-0.315276879649246	0.653	0.71	1.53917110566479E-10	8	Limd2
St13	9.73498773734598E-15	0.255243002437833	0.717	0.565	3.02300574207805E-10	8	St13
Pou2f2.1	2.79475461122531E-14	-0.275270019843823	0.821	0.855	8.67855149423796E-10	8	Pou2f2
Cd86	3.2962670110266E-14	0.296821624433216	0.767	0.64	1.02358979493409E-09	8	Cd86
Hnrnpf.1	8.94709697622951E-14	0.258923973138191	0.843	0.753	2.77834202402855E-09	8	Hnrnpf
Cttnbp2nl.	2.89459752897827E-13	-0.279656275882088	0.695	0.74	8.98859370673621E-09	8	Cttnbp2nl
Pnisr.1	7.34931013600605E-13	-0.278718936771654	0.726	0.765	2.28218127653396E-08	8	Pnisr
Bri3.1	1.81400256566867E-12	0.276134042849792	0.811	0.739	5.63302216717092E-08	8	Bri3
Orai1.2	2.78215538141171E-12	-0.257773458393519	0.664	0.704	8.63942710589779E-08	8	Orai1
Arglu1.1	5.38956476588582E-12	-0.262554894028675	0.738	0.751	1.67362154675052E-07	8	Arglu1
Abi3.1	1.07306713457451E-11	-0.259439288002924	0.792	0.81	3.33219537299423E-07	8	Abi3
Btg1.1	1.19074769254943E-11	-0.274321022050926	0.76	0.785	3.69762880967376E-07	8	Btg1
Nfe2l2	3.69370483128489E-09	0.266359149816771	0.701	0.595	0.00011470061612589	8	Nfe2l2
Ier5.2	2.42193698956475E-07	-0.252914084851068	0.662	0.702	0.00752084093369542	8	Ier5
Klf2	0	2.82025264998077	0.814	0.081	0	9	Klf2
Junb	1.16836760080433E-102	1.70248126058051	0.848	0.587	3.62813191077768E-98	9	Junb
Fcrls.3	2.57574494889736E-81	-0.790511735720266	0.878	0.985	7.99846078981096E-77	9	Fcrls
Jun	2.05156090179544E-80	1.89047764374518	0.759	0.509	6.37071206834537E-76	9	Jun

(*Continued*)

Table 1. (Continued)

	p_val	avg_log2FC	pct.1	pct.2	p_val_adj	cluster	gene
Btg2	8.09839845879443E-80	1.94089546005116	0.814	0.651	2.51479567340943E-75	9	Btg2
P2ry12.3	1.65252076314068E-43	-0.412757412373791	0.996	0.993	5.13157272578075E-39	9	P2ry12
Ctss.3	5.85387757393451E-42	0.390604059286042	1	0.999	1.81780460303388E-37	9	Ctss
Jund	1.34193207002807E-40	1.01394096915674	0.797	0.676	4.16710165705818E-36	9	Jund
Ier5.3	2.58222047894291E-29	0.803120437595928	0.784	0.698	8.01856925326143E-25	9	Ier5
Rhob.3	2.79178080868891E-26	0.415679219283436	0.992	0.985	8.66931694522169E-22	9	Rhob
Ly86.2	4.99302980331277E-25	0.328105505001004	1	0.997	1.55048554482271E-20	9	Ly86
Eef1a1.2	2.47929669701862E-24	0.29245482371578	1	0.999	7.69896003325193E-20	9	Eef1a1
Rps8.1	5.52648186936241E-23	0.297128075596735	0.992	0.989	1.71613841489311E-18	9	Rps8
Cd164.3	8.76905685619847E-23	-0.469565999765011	0.624	0.789	2.72305522555531E-18	9	Cd164
Rsrp1.3	3.18560931266469E-21	-0.355396896629338	0.932	0.968	9.89227259861767E-17	9	Rsrp1
Tmem176a	1.98439828077123E-20	0.539880018119519	0.776	0.664	6.16215198127891E-16	9	Tmem176a
Gpr34.2	2.12843218975933E-20	-0.277039921694065	0.992	0.994	6.60942047885964E-16	9	Gpr34
Fth1.3	2.19199760566805E-19	0.330507664778572	0.998	0.996	6.80681016488101E-15	9	Fth1
H3f3b.1	2.67146802107176E-19	0.585715297948255	0.976	0.98	8.29570964583413E-15	9	H3f3b
P2ry13.2	5.15700588928796E-19	-0.359955828571151	0.893	0.945	1.60140503880059E-14	9	P2ry13
Rps4x.3	1.98263069520838E-18	0.294791024882537	0.992	0.984	6.15666309783057E-14	9	Rps4x
Srsf5	2.15993702535101E-18	0.492190333489135	0.808	0.737	6.70725244482249E-14	9	Srsf5
Rpl10a.3	3.39450595974726E-18	0.320687445665616	0.938	0.901	1.05409593568032E-13	9	Rpl10a
Ecscr.3	6.10041658134621E-18	-0.377100273492835	0.767	0.868	1.89436236100544E-13	9	Ecscr
Mcl1	8.28685557133532E-18	0.456863050903963	0.771	0.665	2.57331726056676E-13	9	Mcl1
Rps11.2	1.06223182907011E-17	0.269803998487436	0.991	0.991	3.29854849881142E-13	9	Rps11
Gm42418	1.10865672015124E-17	-0.416569643884278	0.962	0.981	3.44271171308565E-13	9	Gm42418
Rps25.2	4.8011995384876E-17	0.317410567520731	0.945	0.915	1.49091649268655E-12	9	Rps25
Rpl39.2	8.09618189794176E-17	0.273674024793626	0.994	0.989	2.51410736476785E-12	9	Rpl39
Cebpb.1	1.09902198141848E-16	0.467272430937489	0.759	0.665	3.4127929588988E-12	9	Cebpb
Rpl23.2	2.51874634811659E-16	0.269322720454198	0.996	0.987	7.82146303480645E-12	9	Rpl23
H2-D1.5	3.46757952696842E-16	0.447767623551638	0.825	0.731	1.0767874705095E-11	9	H2-D1
Rpl32.1	1.24659169879033E-15	0.29385711386566	0.989	0.976	3.8710412022536E-11	9	Rpl32
Tmem176b	9.60171917033495E-15	0.365325780539131	0.895	0.836	2.98162185396411E-10	9	Tmem176b
Rps26.1	9.74070498327059E-15	0.313264172190597	0.932	0.895	3.02478111845502E-10	9	Rps26
Ddx5	2.84147964342529E-14	0.305351617075877	0.97	0.969	8.82364673672857E-10	9	Ddx5
Gpx1.2	5.32081330322768E-14	0.393179791738437	0.748	0.688	1.65227215505129E-09	9	Gpx1
Rpsa.3	9.0822634976825E-14	0.296969070154704	0.953	0.927	2.82031528393535E-09	9	Rpsa
Psap.2	9.66474024142945E-14	0.263543211954765	0.996	0.993	3.00119178717109E-09	9	Psap
Scoc.2	1.49716050811527E-13	-0.291990643074513	0.795	0.877	4.64913252585034E-09	9	Scoc
Ctsh.2	1.81797505212348E-13	0.262350594762351	0.981	0.958	5.64535792935906E-09	9	Ctsh
Crybb1.4	3.46794919477157E-13	-0.439946095341386	0.662	0.749	1.07690226345242E-08	9	Crybb1
Rps5.1	3.90683227039514E-13	0.267510985717204	0.957	0.935	1.2131886249258E-08	9	Rps5
Kctd12.2	2.36396580907382E-11	0.395449704186906	0.898	0.863	7.34082302691694E-07	9	Kctd12
Rack1.1	3.42340862099143E-11	0.292098147095996	0.908	0.874	1.06307107907647E-06	9	Rack1
Ctsc.3	3.78717790789658E-11	0.295448959591156	0.821	0.794	1.17603235573912E-06	9	Ctsc
Slc2a5.2	6.18298733346207E-11	-0.327957207138233	0.641	0.748	1.92000305665998E-06	9	Slc2a5
Rpl12.2	6.86227555623138E-11	0.250831212315769	0.953	0.93	2.13094242847653E-06	9	Rpl12
Maf.2	9.22665231438888E-11	-0.267527733792997	0.882	0.923	2.86515234318718E-06	9	Maf
Hnrnpa2b1	1.21897330120586E-10	0.393305228609403	0.784	0.735	3.78527779223455E-06	9	Hnrnpa2b1
Tmcc3.2	1.2934751937977E-10	0.270706395051237	0.831	0.774	4.01662851930001E-06	9	Tmcc3

(*Continued*)

Table 1. (Continued)

	p_val	avg_log2FC	pct.1	pct.2	p_val_adj	cluster	gene
Rhoa	2.80652806231772E-10	0.289825411182493	0.893	0.855	8.71511159191521E-06	9	Rhoa
Canx.2	1.84188104039672E-09	-0.279387458745	0.664	0.758	5.71959319474392E-05	9	Canx
Btg1.2	4.79174153976171E-09	0.457718074690793	0.81	0.783	0.000148797950034221	9	Btg1
Srsf2.2	4.25975194152108E-08	0.280104036585748	0.733	0.685	0.00132278077040054	9	Srsf2
Tgfb1.1	4.50515354617021E-08	-0.255774461657109	0.763	0.835	0.00139898533069224	9	Tgfb1
Pabpc1	2.96376028677717E-07	0.292098202929933	0.712	0.649	0.00920336481852915	9	Pabpc1
Tmem86a.	4.9540598341497E-07	-0.256723117227967	0.711	0.804	0.0153838420029851	9	Tmem86a
Apoe.2	0	2.44003497858863	1	0.505	0	10	Apoe
Lyz2.1	5.32864964531461E-213	0.901723909166408	0.707	0.343	1.65470557435955E-208	10	Lyz2
Fau.2	5.62092126642786E-137	0.436383701380954	1	0.998	1.74546468086384E-132	10	Fau
Ctss.4	3.41684295195587E-126	0.350108610489573	1	0.999	1.06103224187086E-121	10	Ctss
Rps12.1	1.1191163682531E-123	0.479481668759049	0.999	0.99	3.47519205833634E-119	10	Rps12
Rpl23.3	5.8071642958955E-120	0.480767623427662	0.999	0.986	1.80329872880443E-115	10	Rpl23
Eef1a1.3	2.29028694521351E-117	0.409590399680411	0.999	0.999	7.1120280509715E-113	10	Eef1a1
Rpl32.2	1.78386135837906E-114	0.493211893354908	0.99	0.975	5.5394246761745E-110	10	Rpl32
Rps24.1	5.32205197027601E-111	0.415744395776548	0.999	0.994	1.65265679832981E-106	10	Rps24
Rpl30.2	1.59887548287395E-109	0.409811170735646	1	0.992	4.96498803696846E-105	10	Rpl30
Cd63.2	7.0900321665476E-105	0.641150455113905	0.834	0.627	2.20166768867803E-100	10	Cd63
Rpl27a.3	3.30325138611377E-104	0.39845492132839	1	0.994	1.02575865292991E-99	10	Rpl27a
Rpl13.1	5.15265706995985E-100	0.394215696867408	0.999	0.994	1.60005459993463E-95	10	Rpl13
Rpl39.3	1.57861668635376E-97	0.434118140092837	0.995	0.988	4.90207839613432E-93	10	Rpl39
Rpl21.1	1.97898335458091E-96	0.404715348040053	0.998	0.991	6.1453370109801E-92	10	Rpl21
Rps21.3	4.72160902988962E-96	0.407707564080355	1	0.992	1.46620125205162E-91	10	Rps21
Rpl41.1	8.82870490594265E-95	0.407272687093557	0.997	0.989	2.74157773444237E-90	10	Rpl41
Rps29.1	1.05505067599865E-94	0.343252389904265	1	1	3.27624886417862E-90	10	Rps29
Rps9.3	2.75762275113222E-93	0.387808719111042	1	0.992	8.56324592909087E-89	10	Rps9
Rpl37a.1	9.73524209661492E-93	0.402148492265271	0.998	0.99	3.02308472826183E-88	10	Rpl37a
Rpl35a.1	2.13476017455015E-91	0.369946186473899	0.997	0.996	6.62907077003057E-87	10	Rpl35a
Rps27a.1	3.10538076507345E-89	0.400949509386775	0.998	0.99	9.64313888978257E-85	10	Rps27a
Rps15a.1	1.53736502862585E-88	0.40665532148171	0.995	0.979	4.77397962339184E-84	10	Rps15a
Rplp1.1	1.61616939041949E-88	0.31168045604988	1	1	5.01869080806963E-84	10	Rplp1
Rpl37.3	2.08255099489522E-88	0.389553544395368	1	0.989	6.46694560444811E-84	10	Rpl37
Rps10.1	2.97167881274376E-88	0.376619587342426	0.996	0.986	9.22795421721319E-84	10	Rps10
Rpl18a.2	4.92684236482868E-88	0.386705855339309	0.997	0.99	1.52993235955025E-83	10	Rpl18a
Rps27.4	5.46287559460672E-88	0.398201608108706	0.998	0.99	1.69638675839323E-83	10	Rps27
Rps16.1	2.75199196332616E-86	0.406622627856963	0.994	0.975	8.54576064371673E-82	10	Rps16
Rps19.2	1.72685937025609E-83	0.460442404822361	0.986	0.953	5.36241640245624E-79	10	Rps19
Rps11.3	1.97493949173616E-83	0.386684165914418	0.998	0.99	6.13277960368829E-79	10	Rps11
Rplp2.1	1.03107469587375E-81	0.400882682574048	0.992	0.969	3.20179625309676E-77	10	Rplp2
Rps4x.4	1.20514410998781E-81	0.392169912629153	0.998	0.983	3.74233400474514E-77	10	Rps4x
Rps5.2	1.36023725659512E-81	0.441972016353041	0.976	0.932	4.22394475290484E-77	10	Rps5
Rps7.1	2.74340030282821E-81	0.412372551929382	0.984	0.961	8.51908096037243E-77	10	Rps7
Rpl34.3	9.39477652591638E-81	0.386903788610049	0.993	0.979	2.91735995459282E-76	10	Rpl34
Rpl19.1	2.79663453448762E-80	0.372463630566697	0.993	0.979	8.68438921994441E-76	10	Rpl19
Rps23.1	1.91938750090788E-79	0.36023126763653	0.996	0.985	5.96027400656923E-75	10	Rps23
Rps28.3	1.94794449129769E-77	0.431116843282908	0.984	0.958	6.04895202882671E-73	10	Rps28
Rps18.1	2.42056743269659E-77	0.421331677491286	0.986	0.945	7.51658804875273E-73	10	Rps18

(*Continued*)

Table 1. (Continued)

	p_val	avg_log2FC	pct.1	pct.2	p_val_adj	cluster	gene
Rps14.2	2.77086009426189E-75	0.384581456823455	0.996	0.97	8.60435185071144E-71	10	Rps14
Rpl10a.4	7.4482631842686E-75	0.476135843439428	0.969	0.897	2.31290916661093E-70	10	Rpl10a
Rpl9.1	1.97032386124247E-74	0.384219739440568	0.992	0.97	6.11844668631625E-70	10	Rpl9
Rplp0.2	2.84660380197437E-74	0.388083167460363	0.987	0.97	8.83955878627102E-70	10	Rplp0
Rpl10.2	3.01341092943011E-73	0.344537608979151	0.993	0.985	9.35754495915933E-69	10	Rpl10
Tpt1.1	7.83724032078323E-73	0.320611437626757	1	0.999	2.43369823681282E-68	10	Tpt1
Rps20.1	1.24503165961084E-71	0.38551875844823	0.99	0.974	3.86619681258953E-67	10	Rps20
Fth1.4	2.30597221173909E-70	0.364652912601929	0.997	0.996	7.1607355091134E-66	10	Fth1
Rps13.2	5.36387795949655E-69	0.365783471422239	0.991	0.972	1.66564502276246E-64	10	Rps13
Rpsa.4	1.63487468179917E-68	0.410456724629459	0.97	0.924	5.07677634939098E-64	10	Rpsa
Rpl3.1	5.97723052301204E-68	0.387927199526091	0.981	0.948	1.85610939431093E-63	10	Rpl3
Rpl36.1	7.04870864668595E-68	0.404048425273195	0.982	0.937	2.18883549605539E-63	10	Rpl36
Rps8.2	1.16696488474549E-67	0.346950650496585	0.996	0.988	3.62377605660016E-63	10	Rps8
Rps3a1.1	1.93801590074705E-67	0.345791660404939	0.995	0.986	6.01812077658983E-63	10	Rps3a1
Rpl26.1	2.37993036253762E-67	0.359023090019497	0.996	0.976	7.39039775478806E-63	10	Rpl26
Rpl17.1	1.08608517346208E-65	0.379172928689477	0.983	0.963	3.37262028915178E-61	10	Rpl17
Rps25.3	4.25329726385286E-65	0.408598988381816	0.972	0.911	1.32077639934423E-60	10	Rps25
Ctsb.4	5.30318151315412E-65	0.384643994854843	0.993	0.98	1.64679695527975E-60	10	Ctsb
Rps3.2	1.95664128551142E-61	0.330556146332798	0.991	0.977	6.07595818389862E-57	10	Rps3
Rpl28.1	1.31963476522321E-60	0.358901980683292	0.982	0.96	4.09786183644764E-56	10	Rpl28
Rpl36a.2	2.62634783211756E-58	0.431164599701323	0.918	0.836	8.15559792307465E-54	10	Rpl36a
Rpl11.1	5.62240790628403E-58	0.328057923109089	0.993	0.973	1.74592632713838E-53	10	Rpl11
Rpl38.2	1.93951840703342E-57	0.36332541060221	0.972	0.947	6.02278650936088E-53	10	Rpl38
P2ry12.4	8.00248196633807E-57	-0.297726944702868	0.996	0.993	2.48501072500696E-52	10	P2ry12
Rpl12.3	6.78621413778579E-55	0.379181959201782	0.973	0.927	2.10732307620662E-50	10	Rpl12
Rpl6.1	1.8192087184904E-54	0.332113960434845	0.989	0.976	5.64918883352823E-50	10	Rpl6
Rps2.2	5.47282412061971E-54	0.369715494690236	0.965	0.928	1.69947607417604E-49	10	Rps2
Rps26.2	1.23494681583076E-53	0.405454598280664	0.949	0.891	3.83488034719926E-49	10	Rps26
Lag3	2.92486249964473E-51	0.509404109510691	0.78	0.626	9.08257552014678E-47	10	Lag3
Npc2.3	5.79152611367355E-51	0.346329895070549	0.957	0.903	1.79844260407905E-46	10	Npc2
Rack1.2	2.47586316279089E-50	0.369052063003554	0.936	0.87	7.68829787941454E-46	10	Rack1
Rpl22.1	5.71801362044721E-46	0.334626348160738	0.951	0.898	1.77561476955747E-41	10	Rpl22
Rpl35.2	2.01505787678937E-44	0.376770581519025	0.937	0.876	6.25735922479402E-40	10	Rpl35
Cd52.4	6.1872743017145E-44	0.448903136652846	0.721	0.567	1.9213342889114E-39	10	Cd52
Ctsl.3	2.72123491388623E-43	0.284190613683329	0.996	0.984	8.45025077809092E-39	10	Ctsl
Rpl18.1	2.29040308462909E-42	0.300520279548212	0.981	0.954	7.11238869869871E-38	10	Rpl18
Rpl7.2	5.14463693650129E-41	0.297961810999176	0.969	0.943	1.59756410789175E-36	10	Rpl7
Psap.3	1.56936840978199E-40	0.28378041916547	0.995	0.992	4.873359722896E-36	10	Psap
Tmem119.	2.16754322664113E-40	-0.260587757532319	0.992	0.988	6.73087198168871E-36	10	Tmem119
mt-Cytb.1	6.45678746505167E-40	0.272066084543308	0.999	0.995	2.0050262115225E-35	10	mt-Cytb
Rps6.1	1.04810303037004E-39	0.328657002876134	0.94	0.883	3.2546743402081E-35	10	Rps6
H2-D1.6	1.87515117571797E-38	0.394205833110366	0.836	0.725	5.82290694595701E-34	10	H2-D1
Rpl15.1	4.28089666817188E-37	0.293058911889982	0.98	0.939	1.32934684236741E-32	10	Rpl15
Timp2.3	6.34282886957515E-37	0.332791434751504	0.909	0.822	1.96963864886917E-32	10	Timp2
mt-Atp6.3	1.52300244145514E-36	0.252990905825849	0.997	0.998	4.72937948145064E-32	10	mt-Atp6
P2ry13.3	1.00301657116551E-35	-0.319634017473755	0.906	0.946	3.11466735844026E-31	10	P2ry13
Slc2a5.3	2.8646323532995E-35	-0.409248653600007	0.64	0.754	8.89554284670095E-31	10	Slc2a5

(*Continued*)

Table 1. (Continued)

	p_val	avg_log2FC	pct.1	pct.2	p_val_adj	cluster	gene
Eef1b2.1	4.85093439092742E-35	0.327637074869775	0.887	0.817	1.50636065641469E-30	10	Eef1b2
mt-Co3.3	2.55484774620138E-34	0.262370728644558	0.999	0.997	7.93356870627915E-30	10	mt-Co3
Rpl24.1	1.9421406607979E-33	0.289836884812964	0.955	0.909	6.03092939397572E-29	10	Rpl24
Rpl29.1	3.46201996148353E-33	0.310869566924759	0.942	0.894	1.07506105863948E-28	10	Rpl29
Rpl14.1	4.11065687970827E-33	0.297427868549755	0.906	0.845	1.27648228085581E-28	10	Rpl14
Rpl8.1	5.34324561215846E-33	0.265504269500336	0.977	0.949	1.65923805994357E-28	10	Rpl8
Rhob.4	9.18523876076832E-33	-0.262286673786257	0.975	0.986	2.85229219238139E-28	10	Rhob
Rpl7a.2	1.43093670649655E-32	0.305299785249621	0.928	0.858	4.44348775468373E-28	10	Rpl7a
Cd164.4	1.734308858873E-32	-0.372118114507751	0.701	0.79	5.38554929945832E-28	10	Cd164
Rpl5.1	2.70937165640831E-32	0.292399526422159	0.926	0.882	8.41341180464472E-28	10	Rpl5
Selenop.2	2.08396899359105E-31	0.259331014138179	0.996	0.983	6.47134891579827E-27	10	Selenop
Maf.3	3.0337486787823E-30	-0.309198484593745	0.894	0.924	9.42069977222267E-26	10	Maf
Rps15.1	1.13040603362523E-28	0.277606219890133	0.912	0.853	3.51024985621643E-24	10	Rps15
Fcrls.4	5.91734346350332E-28	-0.251735939660225	0.964	0.983	1.83751266572169E-23	10	Fcrls
Txnip.3	1.07404125338772E-27	-0.320025913854964	0.796	0.863	3.33522030414488E-23	10	Txnip
Hspa5.2	1.12762003732415E-26	-0.330468576798668	0.8	0.854	3.50159850190269E-22	10	Hspa5
Pnp.2	8.47659834155748E-26	-0.30822938493096	0.821	0.875	2.63223808300384E-21	10	Pnp
Qk.2	2.29737035424808E-25	-0.255632507695065	0.931	0.949	7.13402416104656E-21	10	Qk
Olfml3.2	4.51994681811757E-24	-0.269320234359044	0.977	0.977	1.40357908543005E-19	10	Olfml3
Ecscr.4	1.34264082090337E-21	-0.279329181152027	0.828	0.868	4.16930254115122E-17	10	Ecscr
Sgk1.1	1.44186267417416E-21	-0.350283048414311	0.769	0.821	4.47741616211303E-17	10	Sgk1
Rpl23a.2	4.86343099846509E-19	0.25512405688848	0.82	0.738	1.51024122795336E-14	10	Rpl23a
St3gal6.2	3.86338671578639E-18	-0.25832486025904	0.778	0.81	1.19969747685315E-13	10	St3gal6
Adrb2.1	8.65493769283677E-16	-0.268154918999491	0.633	0.701	2.6876178017566E-11	10	Adrb2
Tmem176a	6.7798943506942E-13	0.257733376709122	0.732	0.662	2.10536059272107E-08	10	Tmem176a
Fau.3	1.00914476477373E-232	0.381999423516817	1	0.998	3.13369723805188E-228	11	Fau
Rps29.2	9.43918258808252E-224	0.38214608646211	1	1	2.93114936907726E-219	11	Rps29
Tpt1.2	6.71159108957138E-214	0.354767200406928	1	0.999	2.0841503810446E-209	11	Tpt1
Rps24.2	2.09495723409771E-190	0.37257557177707	1	0.994	6.50547069904363E-186	11	Rps24
Rps27.5	3.28508428123223E-182	0.401307940626227	0.999	0.989	1.02011722185104E-177	11	Rps27
Rpl35a.2	6.53988713176546E-181	0.359563973889564	1	0.995	2.03083115102713E-176	11	Rpl35a
Rplp1.2	1.60244849602338E-178	0.303506987704643	1	0.999	4.97608331470139E-174	11	Rplp1
Rpl13.2	1.41602548197314E-171	0.352014520317668	0.998	0.994	4.39718392917118E-167	11	Rpl13
Rpl18a.3	3.12666419403505E-169	0.375090781319993	0.999	0.989	9.70923032173704E-165	11	Rpl18a
Rps21.4	4.65892503892541E-167	0.367580377191951	0.998	0.992	1.44673599233751E-162	11	Rps21
Eef1a1.4	2.36315207780235E-166	0.321560710358294	1	0.999	7.33829614719964E-162	11	Eef1a1
Rpl27a.4	9.94077990134489E-166	0.351562712985399	0.998	0.993	3.08691038276463E-161	11	Rpl27a
Rpl30.3	4.42758546847812E-164	0.360361593397331	0.999	0.992	1.37489811552651E-159	11	Rpl30
Rpl37.4	2.91162145312323E-160	0.381895592625492	0.998	0.988	9.04145809838356E-156	11	Rpl37
Rps4x.5	6.5612485964065E-160	0.383473565703717	0.996	0.983	2.03746452664211E-155	11	Rps4x
Rpl39.4	9.21922912384732E-158	0.373089627349552	0.996	0.988	2.86284721982831E-153	11	Rpl39
Rpl23.4	6.49515229467765E-157	0.361843681811832	0.998	0.986	2.01693964206625E-152	11	Rpl23
Rps11.4	9.08134146129344E-155	0.352002225092217	0.998	0.99	2.82002896397545E-150	11	Rps11
Rps12.2	4.08413651522183E-152	0.35773662754193	0.999	0.99	1.26824691207183E-147	11	Rps12
Rps3a1.2	2.5381184623679E-150	0.368090150208279	0.998	0.985	7.88161926119103E-146	11	Rps3a1
Rps14.3	4.56068389300495E-147	0.37416042567773	0.996	0.969	1.41622916929483E-142	11	Rps14
Rps23.2	1.18296497115089E-145	0.353254698094795	0.999	0.984	3.67346112491485E-141	11	Rps23

(*Continued*)

Table 1. (Continued)

	p_val	avg_log2FC	pct.1	pct.2	p_val_adj	cluster	gene
Rpl32.3	8.27201479142128E-145	0.363332215199131	0.993	0.974	2.56870875318005E-140	11	Rpl32
Rps9.4	3.63828761099171E-144	0.335241390641472	0.999	0.991	1.12979745184126E-139	11	Rps9
Rpl34.4	7.48676616892516E-142	0.364636271007404	0.995	0.978	2.32486549843633E-137	11	Rpl34
Rps10.2	1.55928194586442E-139	0.347071749677379	0.998	0.985	4.84203822649277E-135	11	Rps10
Rpl37a.2	5.53164883999499E-139	0.347883044725671	0.998	0.989	1.71774291428364E-134	11	Rpl37a
Rps28.4	3.09118346777759E-138	0.391989780553777	0.988	0.956	9.59905202248976E-134	11	Rps28
Rps27a.2	7.54793958262459E-134	0.32725449420847	0.998	0.989	2.34386167859241E-129	11	Rps27a
Rps15a.2	9.79798161519934E-133	0.345163038528053	0.995	0.978	3.04256723096785E-128	11	Rps15a
Rpl10.3	6.07551720648778E-132	0.338773052296286	0.996	0.984	1.88663035813065E-127	11	Rpl10
Rps3.3	2.6712323087565E-126	0.345375495809468	0.992	0.976	8.29497768838156E-122	11	Rps3
Rpl21.2	6.37364036898494E-126	0.322197493857587	0.998	0.991	1.97920654378089E-121	11	Rpl21
Rps16.2	6.59716723865906E-111	0.325465074810795	0.994	0.974	2.0486183426208E-106	11	Rps16
Rps7.2	2.19006157515073E-109	0.338042230691532	0.99	0.959	6.80079820931557E-105	11	Rps7
Rps8.3	8.64234547986014E-109	0.298039019433599	0.998	0.987	2.68370754186097E-104	11	Rps8
Rpl9.2	1.61761781340538E-108	0.325624632190307	0.986	0.969	5.02318859596774E-104	11	Rpl9
Rpl26.2	1.95725094165712E-108	0.312442268029107	0.993	0.976	6.07785134912785E-104	11	Rpl26
Rpl17.2	5.80985842206008E-107	0.33049098392024	0.99	0.961	1.80413533580232E-102	11	Rpl17
Rps20.2	4.73480693974359E-104	0.318091813664898	0.991	0.972	1.47029959899858E-99	11	Rps20
Rps13.3	1.21905880387685E-102	0.323812065551955	0.99	0.971	3.78554330367878E-98	11	Rps13
Rplp0.3	4.73238316161159E-101	0.305816802408739	0.993	0.968	1.46954694317525E-96	11	Rplp0
Rps5.3	6.38893685139109E-98	0.346412740033853	0.977	0.929	1.98395656046248E-93	11	Rps5
Rpl19.2	8.97050772983177E-96	0.289876055080998	0.997	0.977	2.78561176534466E-91	11	Rpl19
Rplp2.2	2.65154903912819E-94	0.309600479990419	0.992	0.967	8.23385523120477E-90	11	Rplp2
Rpl6.2	3.82755198171549E-94	0.299438453505658	0.993	0.975	1.18856971688211E-89	11	Rpl6
Rpl38.3	8.03963332160593E-94	0.310446880242178	0.984	0.943	2.49654733535829E-89	11	Rpl38
Rpl41.2	1.00792066986345E-91	0.264868248455206	0.998	0.989	3.12989605612699E-87	11	Rpl41
Rpl3.2	5.81365803873062E-91	0.329307412654396	0.983	0.946	1.80531523076702E-86	11	Rpl3
Rpl7.3	2.51383515046433E-89	0.319576218282623	0.974	0.941	7.80621229273688E-85	11	Rpl7
Rpl28.2	2.65000638549962E-84	0.304941248955486	0.983	0.959	8.22906482889196E-80	11	Rpl28
Rpl11.2	3.49864512547977E-84	0.279991023874725	0.988	0.972	1.08643427081523E-79	11	Rpl11
Rps19.3	9.84093819519042E-83	0.298265270404637	0.985	0.951	3.05590653775248E-78	11	Rps19
Rpl36.2	9.18438382503191E-81	0.305223102981423	0.971	0.936	2.85202670918716E-76	11	Rpl36
Rpl22.2	1.90522207659401E-80	0.330100650419271	0.964	0.893	5.91628611444738E-76	11	Rpl22
Rpl35.3	1.68473527225578E-76	0.350261700737557	0.932	0.873	5.23160844093587E-72	11	Rpl35
Rps25.4	1.24177001344861E-73	0.315818509530406	0.96	0.909	3.85606842276196E-69	11	Rps25
Rpsa.5	1.01807660796439E-70	0.291177408056235	0.971	0.921	3.16143329071183E-66	11	Rpsa
Rpl36a.3	1.06678674559224E-70	0.33583204067196	0.921	0.83	3.31269288108757E-66	11	Rpl36a
Rps18.2	3.32921781962459E-70	0.277240190734208	0.979	0.943	1.03382200952802E-65	11	Rps18
Rpl12.4	2.19353700289621E-69	0.290606781007832	0.969	0.925	6.81159045509361E-65	11	Rpl12
Rpl8.2	2.36471572132581E-66	0.275503203926762	0.98	0.946	7.34315172943303E-62	11	Rpl8
Rpl24.2	3.494280603238E-64	0.295092117044214	0.955	0.906	1.0850789557235E-59	11	Rpl24
Rack1.3	2.49565553948227E-61	0.304077322097207	0.939	0.865	7.7497591467543E-57	11	Rack1
Rps6.2	5.00150686649441E-61	0.298369380250195	0.938	0.88	1.55311792725251E-56	11	Rps6
Rps26.3	1.26966434268137E-60	0.297643234062698	0.94	0.889	3.94268868332845E-56	11	Rps26
Rpl29.2	3.16301339934733E-56	0.272722548359096	0.941	0.891	9.82210550899325E-52	11	Rpl29
Rpl5.2	1.36563026567911E-55	0.289839622000832	0.931	0.879	4.24069166401335E-51	11	Rpl5
Rps15.2	1.3639847310554E-50	0.280519633695111	0.919	0.848	4.23558178534633E-46	11	Rps15

(*Continued*)

Table 1. (Continued)

	p_val	avg_log2FC	pct.1	pct.2	p_val_adj	cluster	gene
Eef1b2.2	9.30812220480122E-43	0.274538812066377	0.89	0.812	2.89045118825692E-38	11	Eef1b2
Rpl23a.3	2.46982059543098E-36	0.262569513023566	0.823	0.732	7.66953389499183E-32	11	Rpl23a
Cox7a2l.1	5.54353874942074E-32	0.258018288196526	0.739	0.65	1.72143508785762E-27	11	Cox7a2l
Sgk1.2	5.23988650792421E-29	-0.30962880324034	0.767	0.825	1.6271419573057E-24	11	Sgk1
Hspa5.3	2.53981627427702E-26	-0.263058929255922	0.806	0.856	7.88689147651242E-22	11	Hspa5
Rps24.3	5.998497889333E-256	-0.394633682522278	0.992	0.996	1.86271354957458E-251	12	Rps24
Fau.4	9.76651237936016E-254	-0.363755424813346	0.998	0.999	3.03279508916271E-249	12	Fau
Rplp1.3	4.05274804226819E-252	-0.303853877590739	0.999	1	1.25849984956554E-247	12	Rplp1
Rps29.3	1.02783850290498E-244	-0.3478531891415	1	1	3.19174690307084E-240	12	Rps29
Rpl32.4	7.36146606438397E-244	-0.449145532814297	0.963	0.982	2.28595605697315E-239	12	Rpl32
Rpl13.3	4.72415500770956E-233	-0.369887383196817	0.992	0.996	1.46699185454405E-228	12	Rpl13
Eef1a1.5	6.86996179280032E-233	-0.336337302721933	0.998	0.999	2.13332923551828E-228	12	Eef1a1
Rpl30.4	6.35993481676531E-230	-0.36908453872846	0.987	0.995	1.97495055865013E-225	12	Rpl30
Tpt1.3	3.6035813545058E-227	-0.332500402993238	0.998	0.999	1.11902011801468E-222	12	Tpt1
Rpl23.5	1.93266493794577E-223	-0.40265984053389	0.98	0.991	6.00150443180301E-219	12	Rpl23
Rps12.3	1.89927131848971E-222	-0.384929209045021	0.987	0.993	5.89780722530608E-218	12	Rps12
Rpl27a.5	6.67858021661473E-207	-0.34821989057002	0.991	0.996	2.07389951466537E-202	12	Rpl27a
Rpl35a.3	7.08543577549241E-201	-0.335045257881166	0.995	0.996	2.20024037136366E-196	12	Rpl35a
Rps15a.3	7.95132309895143E-200	-0.379339545341713	0.971	0.984	2.46912436191739E-195	12	Rps15a
Rps4x.6	4.6211320100241E-193	-0.377586458260358	0.975	0.989	1.43500012307278E-188	12	Rps4x
Rps23.3	2.34472949716352E-189	-0.346853130664285	0.978	0.989	7.28108850754189E-185	12	Rps23
Rpl39.5	6.25394959624099E-189	-0.375730006217627	0.986	0.99	1.94203896812071E-184	12	Rpl39
Rps27a.3	1.29381882390593E-188	-0.342395023515312	0.987	0.992	4.01769559387507E-184	12	Rps27a
Rps5.4	1.57135258894067E-182	-0.434082927439527	0.904	0.95	4.87952119443746E-178	12	Rps5
Rps10.3	1.25335640909659E-181	-0.336601909385188	0.978	0.991	3.89204765716765E-177	12	Rps10
Rps21.5	4.94076568327923E-181	-0.337282923967583	0.989	0.994	1.5342559676287E-176	12	Rps21
Rps19.4	8.52476128990415E-181	-0.41525534389086	0.932	0.966	2.64719412335393E-176	12	Rps19
Rplp0.4	1.00783904092009E-176	-0.367291936966278	0.957	0.978	3.12964257376914E-172	12	Rplp0
Rps11.5	2.76412675132683E-176	-0.342949794204847	0.986	0.993	8.5834428008952E-172	12	Rps11
Fth1.5	5.21330909873393E-175	-0.397345754084254	0.994	0.997	1.61888887442985E-170	12	Fth1
Rps27.6	7.53801247519455E-175	-0.356280739673766	0.986	0.992	2.34077901392217E-170	12	Rps27
Rpl41.3	6.04889103227734E-174	-0.344843624686359	0.985	0.992	1.87836213225308E-169	12	Rpl41
Rpsa.6	1.05790406705618E-170	-0.432708526614709	0.895	0.943	3.28510949942956E-166	12	Rpsa
Rps14.4	1.80112590003184E-169	-0.368835901755145	0.957	0.979	5.59303625736888E-165	12	Rps14
Rps20.3	3.96431676055841E-169	-0.357999180417248	0.963	0.98	1.2310392836562E-164	12	Rps20
Rplp2.3	4.42229075933991E-168	-0.349224307008848	0.954	0.978	1.37325394949782E-163	12	Rplp2
Rpl21.3	2.81581138828779E-167	-0.315616129596249	0.987	0.994	8.74393910405007E-163	12	Rpl21
Rpl9.3	1.27075603753764E-166	-0.351294713038499	0.958	0.977	3.94607872336564E-162	12	Rpl9
Rps16.3	1.82837205686959E-166	-0.364080728464849	0.965	0.981	5.67764374819714E-162	12	Rps16
Rpl37a.3	3.69790109019501E-164	-0.336910181842119	0.986	0.992	1.14830922553826E-159	12	Rpl37a
Rps8.4	3.73433120826548E-164	-0.324564582726674	0.983	0.991	1.15962187010268E-159	12	Rps8
Rps9.5	6.15482563128004E-162	-0.315387430991811	0.987	0.995	1.91125800328139E-157	12	Rps9
Rps28.5	7.27605386219421E-162	-0.405258706831361	0.944	0.967	2.25943300582717E-157	12	Rps28
Rps18.3	1.67553575870695E-160	-0.38181297434791	0.922	0.96	5.20304119151269E-156	12	Rps18
Rpl18a.4	2.21614169561422E-159	-0.327274803948634	0.985	0.993	6.88178480739085E-155	12	Rpl18a
Rpl19.3	2.86365460716991E-159	-0.334999459091495	0.97	0.984	8.89250665164473E-155	12	Rpl19
Rpl37.5	1.14640363064214E-157	-0.330275149065809	0.985	0.992	3.55992719423302E-153	12	Rpl37

(*Continued*)

Table 1. (Continued)

	p_val	avg_log2FC	pct.1	pct.2	p_val_adj	cluster	gene
Rpl12.5	2.51687814090459E-157	-0.385278273948043	0.9	0.945	7.81566169095103E-153	12	Rpl12
Rps3a1.3	5.90360652282855E-157	-0.325667325739164	0.979	0.991	1.83324693353395E-152	12	Rps3a1
Rpl3.3	2.08190974563607E-152	-0.365191454118041	0.922	0.964	6.46495433312367E-148	12	Rpl3
Rpl34.5	1.62582426919469E-150	-0.32491207001262	0.971	0.984	5.04867210313026E-146	12	Rpl34
Rps7.3	1.76873748120025E-149	-0.355279365881805	0.942	0.972	5.49246050037114E-145	12	Rps7
Rps2.3	4.16723898776737E-142	-0.369740104528157	0.909	0.941	1.2940527228714E-137	12	Rps2
Rps13.4	1.44419860567106E-137	-0.325902154289488	0.963	0.978	4.48466993019035E-133	12	Rps13
Rpl38.4	4.11375574979499E-137	-0.364147579138721	0.929	0.958	1.27744457298384E-132	12	Rpl38
Rpl17.3	4.78141555868286E-137	-0.339193322166393	0.948	0.973	1.48477297343779E-132	12	Rpl17
Rpl26.3	7.36095779827572E-135	-0.309841088700522	0.97	0.982	2.28579822509856E-130	12	Rpl26
Rpl36.3	2.82739964761746E-134	-0.357061997447862	0.918	0.951	8.77992412574649E-130	12	Rpl36
Rpl11.3	1.15645617274359E-128	-0.299634189101647	0.962	0.98	3.59114335322068E-124	12	Rpl11
Rpl10a.5	9.35831399712361E-127	-0.372085188043589	0.868	0.918	2.90603724552679E-122	12	Rpl10a
Rpl10.4	1.94579027655934E-126	-0.285769900995899	0.981	0.988	6.04226254579973E-122	12	Rpl10
Rps25.5	2.04610605598998E-126	-0.353084534513678	0.881	0.932	6.35377313566568E-122	12	Rps25
Rpl6.3	1.4342376550081E-118	-0.291404873015504	0.966	0.982	4.45373819009667E-114	12	Rpl6
Rps26.4	1.0411885363562E-114	-0.364583591613055	0.858	0.913	3.23320276194691E-110	12	Rps26
Rps3.4	1.39913011300749E-114	-0.285066365736839	0.971	0.981	4.34471873992215E-110	12	Rps3
Rpl28.3	3.0926701472285E-112	-0.302314255755959	0.952	0.967	9.60366860818867E-108	12	Rpl28
Rpl22.3	4.33368878606153E-106	-0.321218565685524	0.866	0.919	1.34574037873569E-101	12	Rpl22
Rhob.5	2.21122722150697E-104	0.252182566302041	0.994	0.98	6.86652389094558E-100	12	Rhob
Rpl36a.4	2.70741622684613E-104	-0.358370601150229	0.788	0.867	8.40733960922529E-100	12	Rpl36a
Ftl1.2	6.84809776551012E-100	-0.342876047619353	0.987	0.992	2.12653979912386E-95	12	Ftl1
Rpl18.2	5.65203863603851E-99	-0.282870723419333	0.935	0.965	1.75512755764904E-94	12	Rpl18
Rack1.4	3.11856957286769E-98	-0.341617954725745	0.836	0.893	9.68409409462603E-94	12	Rack1
Rpl8.3	5.01189483862522E-98	-0.276297040404362	0.934	0.959	1.55634370423829E-93	12	Rpl8
Rpl24.3	7.71138595738696E-97	-0.310609875188744	0.886	0.925	2.39461668134737E-92	12	Rpl24
Rpl7.4	1.28182443222934E-94	-0.280498806413339	0.926	0.954	3.98044940940175E-90	12	Rpl7
Rpl35.4	1.51352432837602E-91	-0.343336833023415	0.846	0.897	4.69994709690606E-87	12	Rpl35
Rpl29.3	5.32935827018169E-83	-0.291393811270776	0.861	0.914	1.65492562363952E-78	12	Rpl29
Rpl15.2	3.58838345990969E-81	-0.256817914774629	0.923	0.951	1.11430071580575E-76	12	Rpl15
Maf.4	5.95651685372799E-81	0.254707396642929	0.944	0.911	1.84967717858815E-76	12	Maf
Rps6.3	7.52314826845287E-81	-0.286056724047544	0.853	0.903	2.33616323180267E-76	12	Rps6
Rpl5.3	1.48269489999568E-73	-0.279652101424222	0.849	0.902	4.60421247295657E-69	12	Rpl5
Rpl14.2	3.37756180943416E-67	-0.262588510408555	0.812	0.867	1.04883426868359E-62	12	Rpl14
Ctsb.5	6.61924338402115E-65	-0.346605447257156	0.976	0.983	2.05547364804009E-60	12	Ctsb
Cd164.5	5.17020258536369E-64	0.2647341953667	0.827	0.764	1.60550300883299E-59	12	Cd164
Rps15.3	1.43352638386833E-63	-0.263614745836866	0.821	0.874	4.45152947982634E-59	12	Rps15
Nrip1.2	8.24849263444341E-62	0.254328721625188	0.879	0.832	2.56140441777371E-57	12	Nrip1
Sgk1.3	4.6793254259069E-60	0.288705226928264	0.854	0.8	1.45307092450687E-55	12	Sgk1
Eef1b2.3	5.97330209763794E-57	-0.261423029127211	0.782	0.841	1.85488950037951E-52	12	Eef1b2
H2-D1.7	1.49715182429795E-48	-0.425000702810103	0.692	0.753	4.64910555999243E-44	12	H2-D1
H2-K1.4	9.36544322381961E-25	-0.27956804594711	0.685	0.742	2.9082510842927E-20	12	H2-K1
Xist	0	2.24173168755572	0.998	0.307	0	13	Xist
Hspa8.3	6.06325114543686E-80	-0.31450326549286	0.841	0.905	1.88282137819251E-75	13	Hspa8
Hsp90ab1.	5.25446982066137E-56	-0.296097155215301	0.797	0.861	1.63167051340997E-51	13	Hsp90ab1
H2-D1.8	1.15028084631823E-40	-0.388842643535434	0.68	0.753	3.571967112072E-36	13	H2-D1

https://doi.org/10.1371/journal.pone.0296280.t001

express microglia marker genes and no border macrophage genes such as *Mrc1*, *Ms4a7*, and *Pf4* were detected. Cluster 6 expresses high levels of *Cdkn1a* and *Bax* suggesting that these cells may be undergoing a4poptosis. Lastly, Cluster 7 shows enrichment of *Pmepa1* which has been identified in TGF-ß signaling [37]. Given that these clusters do not have many differentially expressed genes, they are unlikely to be distinct populations.

The remaining clusters express genes associated with either distinct functions or were characteristic of non-microglial populations. The presence of non-microglia macrophages has been reported in numerous studies [11, 12, 35, 38, 39]. Cluster 2 appears to be a non-microglia macrophage population, based on, expression of genes associated with antigen presentation including *H2-Aa*, *H2-Eb1*, and *Cd74* in over half of the cells. These genes have been shown by previous findings to define adult choroid plexus macrophages [14]. The remaining cells in cluster 2 appear to have the same transcription profile associated with border macrophages or CNS-associated macrophages marked with expression of marker genes such as *Mrc1*, *Pf4*, and *Ms4a7 [40]*. These two groups thus likely comprise non-microglia myeloid lineage cells in the hippocampus.

In the healthy brain, there is some degree of microglial turnover. Approximately one percent of cells in the total myeloid population in the hippocampus express genes undergoing cell cycle transition. These cells, enriched in Cluster 1, are expressing *Mki67*, *Top2a*, *H2afz*, known to be found in proliferating microglia [14]. Cluster 3 expresses genes known to be implicated in interferon response. Many of these genes, such as *Rtp4*, *Ifit3*, *Ifit2*, *Ifitm3*, *Oasl2*, have also been implicated in the aging transcriptome [15]. By contrast, cluster 9 comprises cells that exhibit an activation profile, potentially as an artifact of the isolation protocol, as evidenced by the upregulation of immediate early genes such as *Fos*, *Egr1*, and *Jun*; these genes have been shown to correlate specifically with activation due to homogenization and other isolation-associated experimental steps [14]. Cluster 10 exhibits increased expression of genes associated with encoding ribosomal protein subunits (genes with *Rps* and *Rpl* as their prefix) and also contains the highest *ApoE* expression. This group of cells undergoing high metabolic activity has been identified by other groups and may reflect cells with more metabolic needs which are typically enriched with genes associated with immune reactivity [41–43]. The expansion of cells falling in this cluster may be a sign of reactivity in certain contexts. Cluster 8 exhibits expression of genes associated with the Disease-associated microglial (DAM) phenotype, namely *Cd9*, *Cd63*, *Cst7 [8]* and more detailed analysis localizes this novel cluster to the dentate gyrus subgranular zone (Figs 3 and 4).

Myeloid Cd68 expression localizes to the subgranular zone of the dentate gyrus

In order to test whether microglia associated with the neurogenic niche are represented as a distinct transcriptomic cluster, we used our double reporter mice (S1 Fig) to visualize both neural progenitor cells and myeloid lineage cells. The neural progenitor pool clearly demarcates the SGZ from the rest of the dentate gyrus/hippocampus (Fig 2A). Somas from these cells line the interior (medial area) of the dentate gyrus. Processes of these cells protrude through the granule cell layer in the dentate gyrus to the molecular layer. Microglia in this region break the tile pattern they normally have in the adult cortex where processes of adjacent microglia seldomly coincide (Fig 2B and 2E). Such high density, or clustering, of microglia is often associated with increased microglial activity, particularly in clearing apoptotic cells [44, 45]. Additionally, neural stem cell processes are highly wrapped around microglial processes. Microglia are observed in very close apposition to neural progenitors in this region (Fig 2D). Cd68, (macrosialin) is found on the surface of lysosomes and increased Cd68 expression is detected

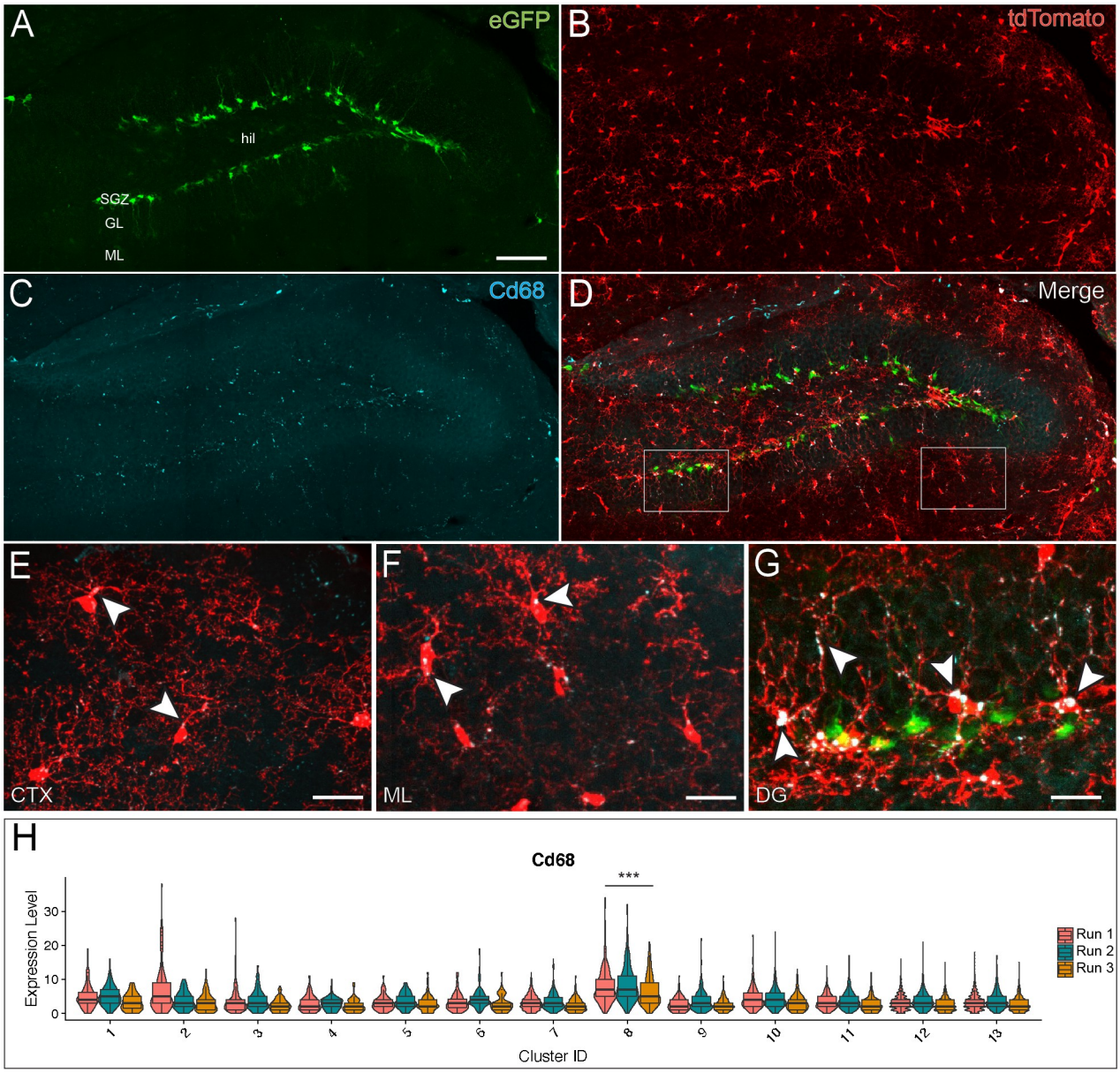

Fig 2. Increased Cd68 is localized to subgranular zone of the dentate gyrus and transcriptomic cluster 8. (A) Distribution of Nestin-eGFP expressing neural progenitors located in the SGZ. hil = hilus, GL = granule cell layer, ML = molecular layer. (B) Distribution of myeloid lineage cells expressing tdTomato in the dentate gyrus. (C) $CD68^{+}$ lysosomal content staining in the dentate gyrus. (D) Merge image at showing colocalization of Cd68+ lysosomes in myeloid cells in apposition to Nestin-GFP cells. $CD68^{+}$ lysosomal puncta in CTX (E) and ML (F) vs SGZ (G) with arrow heads to highlight CD68/tdTomato colocalization. Scale bars A&B = 40 μm; D-G: 100 μm; E = 25 μm F& G =: 20 μm. (H) Violin Plot with superimposed boxplots to show *Cd68* transcript counts and median values across clusters and runs.

https://doi.org/10.1371/journal.pone.0296280.g002

in regions with neuronal death such as the cerebellum and olfactory bulb [18, 45, 46]. Cd68 puncta show higher colocalization in cells within the SGZ as well as processes from these cells (Fig 2C, 2D and 2G) as compared to microglia in the cortex or elsewhere in the dentate gyrus (Fig 2E and 2F). We analyzed the hippocampal clusters to see whether any transcriptomic cluster expresses elevated levels of Cd68 and observe that cluster 8 has significantly higher expression of Cd68 when compared to all other clusters (log2FC = 0.87; p-val <0.001) (Fig 2H).

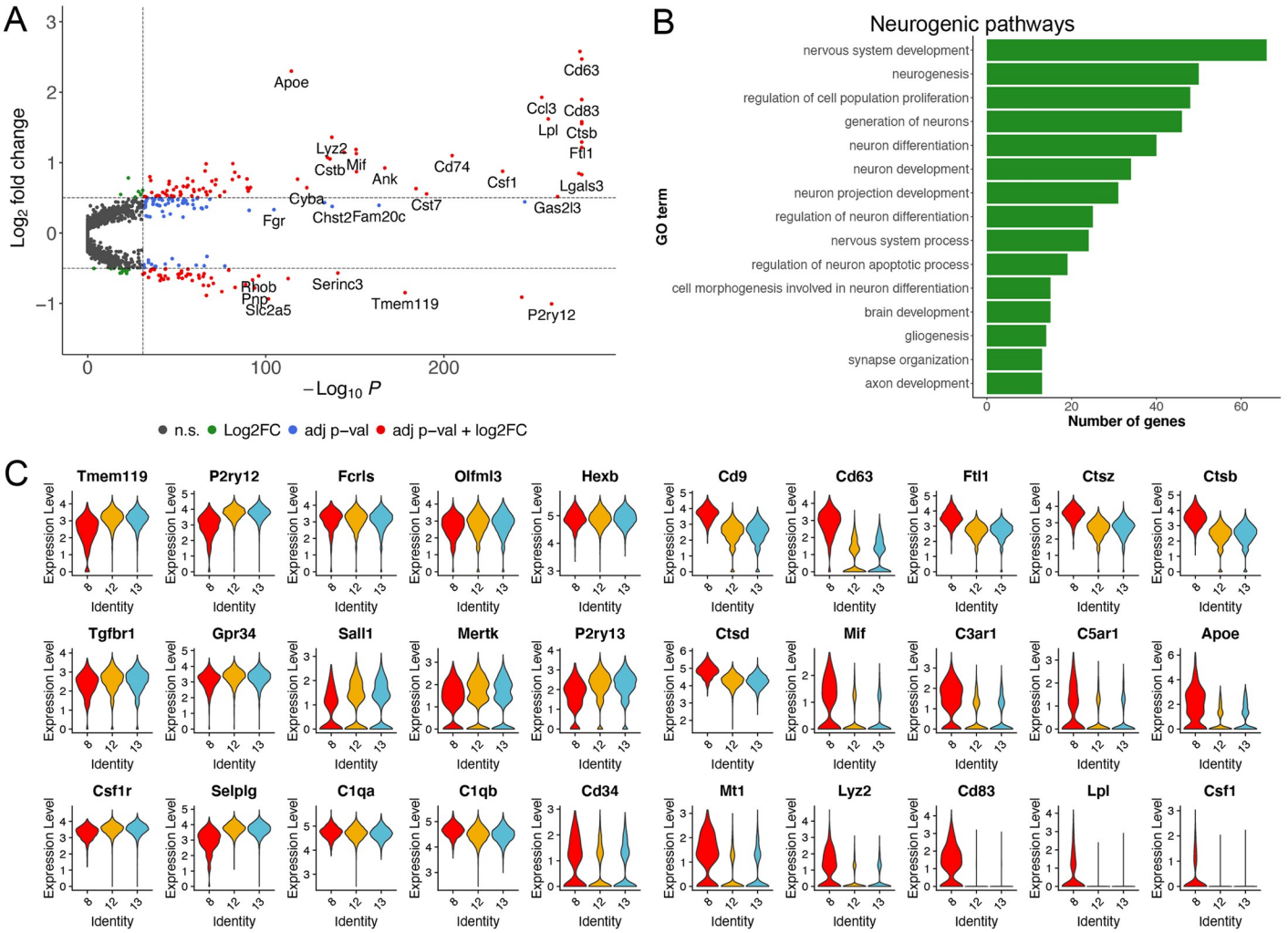

Fig 3. Transcriptomic profile of cluster 8. (A) Volcano plot showing differentially expressed genes in Cluster 8 microglia compared to other hippocampal microglia. Statistically significant genes (up or down- regulated) are represented by red dots (LFC > 0.25 and p-val < 10e-32). (B) Gene set enrichment analysis of upregulated genes in cluster 8 showing select ontology related to neurogenesis. (C) Violin Plots showing comparison of expression profiles of key genes in Cluster 8 vs homeostatic clusters (13 and 14).

https://doi.org/10.1371/journal.pone.0296280.g003

Transcriptomic analysis of the putative subgranular zone cluster demonstrates unique expression profile

After identifying Cluster 8 as the putative SGZ cluster, we tested for other genes differentially expressed by this cluster. We cross-referenced the Allen Institute *In Situ* Hybridization atlas to confirm spatial patterning of genes enriched or downregulated in this cluster (S6 Fig) [47]. Some previous studies have shown many microglia-specific marker genes to be downregulated in the context of immune activation [8]. Similarly, the SGZ microglia also exhibit decreased expression of microglia marker genes such as *Tmem119*, *P2ry12*, *Selplg*, and *Siglech* (Fig 3A).

Using the cluster-8 specific gene list, we next examined the gene set enrichment analysis applying the Kolmogorov-Smirnov test through the topGO package for annotation of terms. We set a stringent false discovery rate (adjusted p-value less than 0.05) and found several gene ontology (GO) terms related to nervous system development, which we have highlighted in

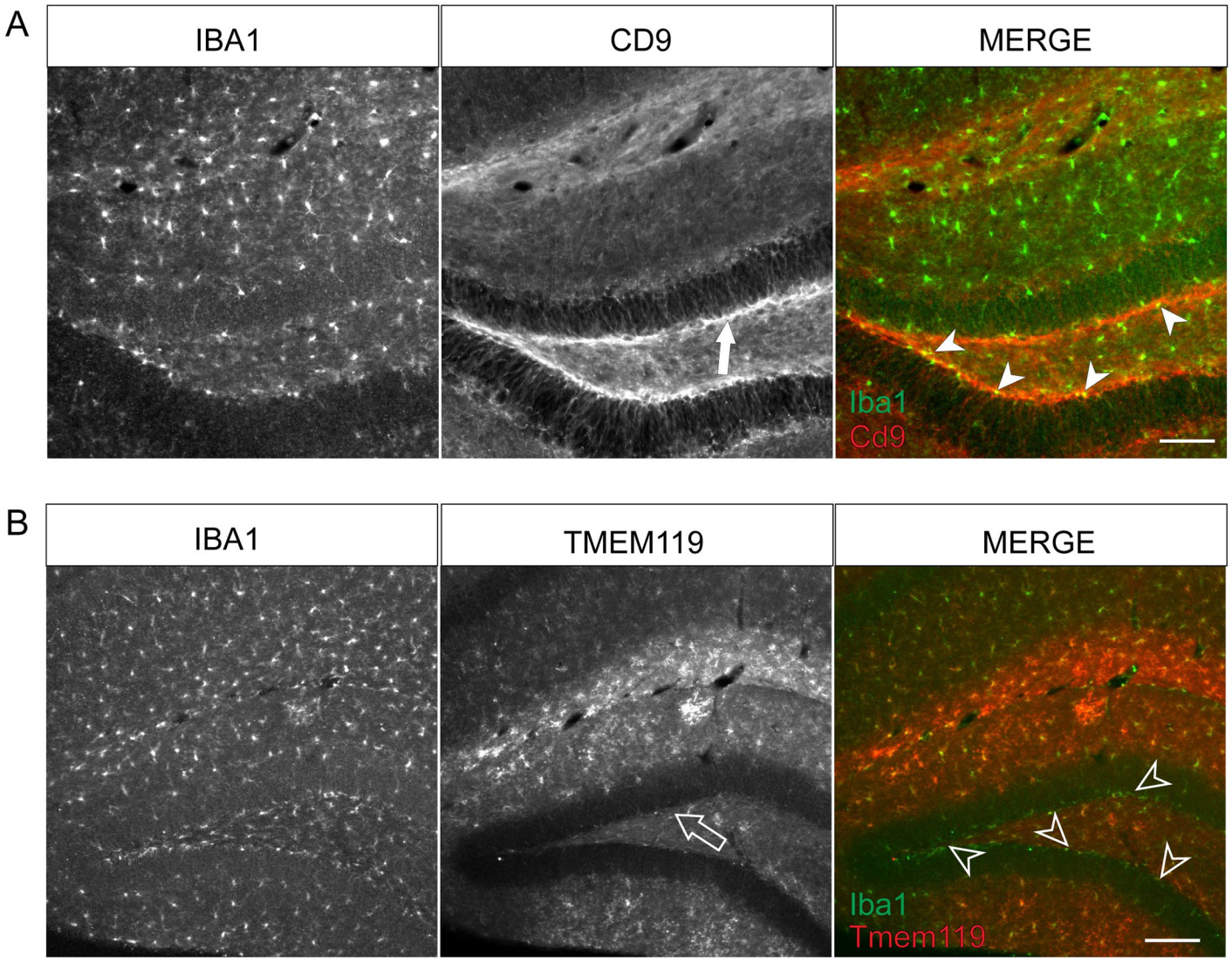

Fig 4. Immunoreactivity of marker genes for cluster 8 in the dentate gyrus. (A) Immunohistochemistry staining for Cd9 colocalized with Iba1 in the dentate gyrus. Decreased immunoreactivity to Cd9 as indicated with an arrow in molecular layer (middle) with increased Iba1 colocalization in SGZ as indicated by arrowheads (right panel). (B) Immunohistochemistry staining for Tmem119 colocalized with Iba1 in the dentate gyrus. Decreased Tmem119 immunoreactivity in SGZ (arrow in middle panel) and sparse colocalization with Iba1 in SGZ indicated by arrowheads (right panel). Scale for A and B = 80 μm.

https://doi.org/10.1371/journal.pone.0296280.g004

Fig 3B (see full list in S2 Table). This further suggests that this cluster of cells correlates to microglia spatially aligned to the neurogenic niche, the SGZ of the dentate gyrus in the hippocampus. Interestingly, other microglia-specific genes such as *Hexb*, *Fclrs*, *Olfml3* retain stable expression in this cluster (Fig 3C).

Cluster 8 shows an upregulation of genes associated with lysosomal function such as *Ctsz*, *Ctsb*, and *Ctsd* (Fig 3C). It is well established that complement receptors *C3ar1* and *C5ar1*, which are typically not found in resident microglia are expressed in the SGZ, and that complement cascade pathways are necessary for normal neuronal development and synaptic pruning [48–50]. Therefore, it is unsurprising that we see them upregulated in cluster 8.

Altered immunoreactivity in the SGZ correlates with cluster 8 gene expression

To validate whether the transcriptomic differences between cluster 8 and homeostatic clusters align with protein levels, we stained for candidate marker genes. We observed increased immunoreactivity to Cd9 in the SGZ (Fig 4A and S7 Fig). This is, however, not just localized to microglia and also expressed by neural progenitor/precursor cells [51]. Conversely, *Tmem119* immunoreactivity is decreased in the SGZ (Fig 4B). We also observed decreased immunoreactivity of Iba1+ cell processes in the granular layer of the dentate gyrus, similar to reports in the subventricular zone where this other brain neurogenic region also demonstrates lower Iba1 expression [18].

We next utilized confocal imaging to test whether neural stem/progenitor cells express Cd9 using our double reporter mice. We found little to no colocalization of GFP with Cd9 staining (S7 Fig). We note increased staining around vessels, suggesting that Cd9 is enriched in vascularized regions such as the neurogenic niche also often referred to as the neurovascular niche. Lastly, we referred to the Allen Brain Atlas in situ hybridization database to confirm spatial localization of genes for which we could not find suitable antibodies. We note high specificity of *Cd63* in the SGZ, further suggesting that this transcriptomic cluster might be specific to the neurogenic niche of the hippocampus (S6 Fig). These observations suggest that microglial cells deviating from conventionally defined homeostatic signatures may require alternative, combinatorial marker genes for identification and isolation of these cells.

SGZ microglia display morphology and gene expression profiles that deviate from a more homeostatic phenotype

Microglial morphology and distribution are well established methods to compare activation states of immune cells [18, 44, 45]. We first directly compared cells specifically in the sub granular zone with cells in the cortex. As the cortex is the largest region of the murine brain, microglia from this region represent the highest number of any one region. While the distribution of microglia in the resting brain is characterized as tiled with microglial branches from adjacent cells maintaining distinct, non-overlapping territories, some regions of the brain do not have this patterning, particularly in regions with high neuronal densities [44, 52]. We noted deviation in SGZ microglia from this tiled distribution compared to cortical microglia (Fig 5A and 5B) in the homeostatic brain. To characterize morphometric traits, we utilized Sholl analysis to compare ramification of myeloid cells derived from the cortex versus the sub granular zone of the hippocampus. We find that cells with their cell bodies located in the sub granular zone are less ramified than cells in the cortex (Fig 5C), which is consistent with a phagocytic phenotype [53, 54]. These results are in accordance with transcriptome analyses that suggest that subsets of microglia within the hippocampus display an alternative phenotype [28].

We next asked whether microglia in this population express genes correlating with immune reactivity and activation. We again filtered the list of gene ontology terms from S2 Table, but specifically for terms that show increased metabolic activity and immune processes (Fig 5D). These are typically associated with microglial reactivity. We closely examined whether genes upregulated in the cluster 8 overlapped with known activation profiles. We compared its transcriptome profile to that of Disease Associated Microglia (DAM) described by Keren-Shaul and others first by plotting genes shown to be differentially expressed in cells from diseased brains [8]. When plotting for these genes in our homeostatic clusters 12 and 13 along with our putative SGZ cluster 8, we find that these genes seem to follow a similar pattern of expression as DAM (S8A Fig). From the Keren-Shaul dataset, we integrated transcriptome data from microglia, excluding any potential non-microglial cells and clusters 8, 12, and 13 of our

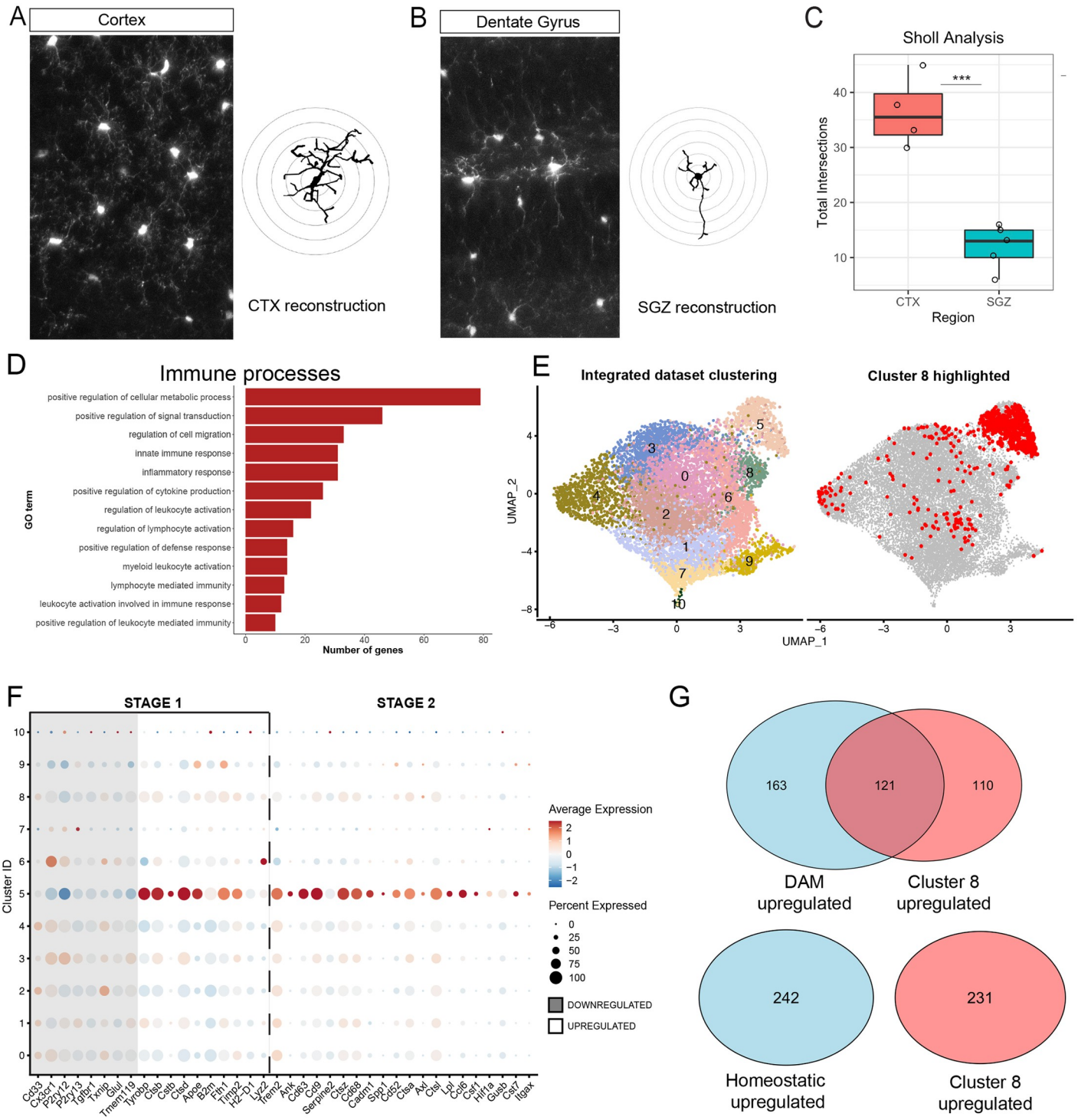

Fig 5. Subgranular zone (SGZ) microglia display a reactive phenotype. Representative projections of 3D z-stacked images of myeloid lineage cells labelled with tamoxifen induced tdTomato (*Cx3cr1*$^{CreErt2/+}$; *Rosa26*$^{loxp\text{-}tdTomato/+}$) in the cortex, CTX (A) and dentate gyrus (DG), with representative manual tracing of processes (right in A and B, respectively). (C) Sholl analysis to display morphometric differences between cell ramification of cells from cortex vs SGZ. p-val = 0.000227. (D) Gene set enrichment analysis of upregulated genes in cluster 4 showing select ontology related to immune activation. (E) UMAP plots showing integration of hippocampal myeloid dataset from this study (left) [8] with cells from cluster 8 in the hippocampal myeloid cells highlighted in red (right). (F) Dot Plot of key genes in integrated dataset (see E) known to be down regulated or upregulated in Stage-1 TREM2-independent activation versus Step-2 Trem2-dependent activation in DAM microglia. Shading corresponds to genes known to be downregulated in DAM profile (G) Venn diagram illustrating overlap of upregulated genes in Cluster 8 with Disease Associated Microglia (DAM) microglia (top) and overlap of upregulated genes in Cluster 8 with homeostatic microglia from [8] (bottom).

https://doi.org/10.1371/journal.pone.0296280.g005

dataset. Cells from cluster 8 predominantly fell in cluster 5 of this integrated dataset (Fig 5E and S8 Fig) [8]. While the cluster identities for individual cells from the Keren-Shaul dataset were not included in the publicly available dataframes, we identified cells showing the DAM state by plotting key genes previously identified in their study (Fig 5F). We found the pattern of downregulated homestatic genes and upregulated genes associated with reactive microglia in cluster 5 of the integrated dataset.

Additionally, we compared the list of all upregulated genes between cells labelled as DAM in the Keren-Shaul dataset compared to homeostatic cells in their dataset with the list of top upregulated genes by log fold change in cluster 8 relative to homeostatic clusters 12 and 13 (Table 2) in our study and found that over half the genes enriched in cluster 8 are also upregulated in DAM (Fig 5G). By contrast, we found no overlap between genes enriched in homeostatic cells from the Keren-Shaul dataset with those upregulated in cluster 8 (Fig 5G). As reactive microglia are not only found in disease, but also in development, we compared the whole list of upregulated genes in Table 2 with genes reported to be found in early postnatal microglia by Hammond and others (labeled cluster 3 in their dataset). We observed over a hundred genes enriched in both Cluster 8 and with many of these genes overlapping the DAM upregulated genes (S8 Fig) [15]. We investigated the expression patterns on the integrated dataset of genes overlapping in all three datasets and plotted three which were more specific to the reactive cluster 5 in the integrated dataset (S8 Fig). Therefore, cluster 8's gene expression profiles are consistent with other phenotypic states found in development and disease and appear to be distinct from most microglia in the adult brain which are typically not presented with a phagocytic challenge.

Discussion

As the involvement of immune cells in CNS development and health are examined in greater depth, the role of innate immune cells reveals diverse function depending on cell type and context [20, 39, 55]. Different cell types are tuned to recognize and respond to specific cues [11, 56, 57]. Some populations present in the brain express different sets of genes which may explain mechanisms involving aberrant immune activation and inflammation leading to neurodegenerative diseases coupled with cognitive decline [8, 58–60]. Immune cells are undoubtedly an important layer of defense for the central nervous system, while dysregulation of the neuroimmune axis can disrupt healthy neural and cognitive functions [61–64]. This makes characterizing the different players in the immune system key to uncovering pathological development and recovery in neurological diseases [21, 65, 66]. By sampling a large number of hippocampal cells, we provide evidence of heterogeneity in the adult hippocampus, which may help explain specialized roles for microglia in mitigating disease within discrete brain areas such as the hippocampal neurogenic niche.

We have uncovered a novel context in which immune cell heterogeneity potentially explains a specialized function. The subgranular zone of the hippocampus is a select site in the adult mammalian brain where neuronal development persists through adulthood. Thus, we have identified a subset of cells in the hippocampus with a distinct transcriptomic signature correlating to function within this niche. This population of cells comprises less than five percent of total immune cells in the hippocampus, highlighting why it may have been missed in studies that examine a smaller number of cells in the hippocampus.

Previous studies suggest that immune dynamics alter the neurogenic niche and immune input in this region appears highly specialized [16, 17, 28]. In the SGZ, cells labelled with tdTomato (resulting from fractalkine Cre recombinase reporter) show stark morphological differences when compared to cells from non-neurogenic regions. Similar to microglia in the adult

Table 2. List of upregulated genes.

	p_val	avg_log2FC	pct.1	pct.2	p_val_adj
Ctsz	0	1.21316411097896	1	0.991	0
Cd9	0	1.5543421129946	1	0.974	0
Ftl1	0	1.29233968681864	1	0.988	0
Cd63	0	2.4706052666907	0.982	0.585	0
Lgals3	0	0.829277774804711	0.154	0.001	0
Ctsb	0	1.58007383569573	1	0.977	0
Cd83	0	1.89489310308902	0.739	0.216	0
Ccl4	1.34568412142678E-281	2.57797468165877	0.264	0.02	4.17875290226658E-277
Ctsd	4.97895240219732E-281	0.845592630366848	1	1	1.54611408945433E-276
Gas2l3	4.54139318224689E-269	0.516476416191356	0.158	0.004	1.41023882488313E-264
P2ry12	1.10192603799569E-265	-1.00623764254092	0.985	1	3.42181092578801E-261
Lpl	7.76064173468084E-264	1.61971828850796	0.389	0.057	2.40991207787044E-259
Ccl3	3.65487488733058E-260	1.92695749766185	0.275	0.025	1.13494829876276E-255
Itgax	1.32483942819687E-250	0.442361492759136	0.149	0.004	4.11402387637974E-246
Selplg	6.06512079659385E-249	-0.911138664302458	0.991	1	1.88340196096629E-244
Csf1	3.2412266656412E-238	0.877158522936439	0.274	0.028	1.00649811648156E-233
Cd74	7.90449700843159E-210	1.0997831043934	0.31	0.043	2.45458345602826E-205
Cst7	1.68324179253974E-195	0.555691686979492	0.185	0.014	5.22697073837367E-191
Plaur	1.42548459170699E-189	0.630800536987574	0.214	0.021	4.42655730262773E-185
Tmem119	1.99055499282937E-183	-0.847447500045601	0.954	0.999	6.18127041923303E-179
Ank	4.76231172722668E-172	0.923590018242182	0.349	0.068	1.4788406606557E-167
Fam20c	9.09780361712421E-169	0.393238869351446	0.115	0.004	2.82514095722558E-164
Cd68	4.11575467235566E-156	0.871154160257722	0.992	0.918	1.2780652984066E-151
Mif	4.91689937546175E-156	1.12750523875927	0.653	0.268	1.52684476306214E-151
C3ar1	7.28773442939688E-156	1.18564814151043	0.806	0.422	2.26306017236061E-151
Cadm1	4.3280606929276E-149	1.14776033150113	0.72	0.336	1.34399268697481E-144
Serinc3	1.1313269549074E-145	-0.568979451404833	0.996	1	3.51310959307396E-141
Chst2	1.76392884399378E-142	0.377086774950856	0.103	0.005	5.47752823925388E-138
Lyz2	2.80210208313845E-142	1.35961382873573	0.654	0.279	8.70136759876981E-138
Cstb	3.07814858153347E-141	1.05254537321382	0.557	0.198	9.55857479023588E-137
Mt1	8.77481426751793E-140	1.07344863386028	0.753	0.365	2.72484307449234E-135
Nes	3.42213777542466E-138	0.431832942380394	0.11	0.006	1.06267644340262E-133
Cyba	3.06812357639266E-128	0.643865546819513	0.996	0.983	9.52744414177214E-124
Fth1	4.90300782311598E-123	0.764439179435085	1	0.994	1.52253101931221E-118
Apoe	1.30313503913993E-119	2.29920561902052	0.754	0.449	4.04662523704122E-115
Siglech	8.83413706086301E-118	-0.646255195550367	0.96	0.993	2.74326458150979E-113
Fgr	8.28797040183072E-110	0.332736968583023	0.115	0.01	2.57366344888049E-105
Slc2a5	9.40910967879824E-107	-0.93581431699063	0.529	0.791	2.92181082855722E-102
Rhob	3.39067862081181E-101	-0.608529496680619	0.964	0.992	1.05290743212069E-96
Pnp	5.68251320897039E-99	-0.78037994727031	0.744	0.884	1.76459082678157E-94
P2ry13	8.86445785140815E-98	-0.665371924270032	0.895	0.964	2.75268009659777E-93
Mfsd12	1.25107066793727E-96	0.647176621003028	0.297	0.079	3.88494974514561E-92
Sulf2	7.36585947817111E-96	0.322789125657732	0.149	0.021	2.28732034375648E-91
Rps2	1.65536181775218E-95	0.613476248060951	0.975	0.917	5.14039505266586E-91
Npc2	2.41479374849408E-95	0.595713731507814	0.973	0.891	7.49865902719867E-91
Ctsa	7.90944747065718E-95	0.642309559039543	0.981	0.892	2.45612072306318E-90
Hsp90ab1	1.10526330234185E-94	0.768389306887071	0.937	0.825	3.43217413276214E-90

(*Continued*)

Table 2. (Continued)

	p_val	avg_log2FC	pct.1	pct.2	p_val_adj
Zfhx3	6.90955450599031E-94	-0.730581763236332	0.801	0.929	2.14562396074517E-89
Pld3	4.25612980120331E-90	0.799466292950042	0.609	0.296	1.32165598716766E-85
Ivns1abp	5.42104342841098E-88	-0.77171959722175	0.703	0.846	1.68339661582446E-83
Eif4a1	8.31472515642672E-88	0.862075934098564	0.916	0.752	2.58197160282519E-83
Atf3	1.09177659056209E-86	0.985888098965569	0.225	0.053	3.39029384667244E-82
Prdx1	1.92081956743974E-86	0.759903519869938	0.802	0.53	5.96472100277062E-82
Vsir	2.18414905903913E-84	-0.527805954030406	0.95	0.983	6.78243807303421E-80
Cx3cr1	2.98478897474066E-82	-0.468087065801117	0.994	0.998	9.26866520326218E-78
Nab2	4.59372768530848E-82	0.586682880198139	0.278	0.078	1.42649025811884E-77
Adrb2	1.48935004990287E-80	-0.832061987359219	0.476	0.719	4.6248787099634E-76
Grn	2.09040166041137E-79	0.527480248748557	0.991	0.964	6.49132427607543E-75
Aldoa	2.78271375563998E-77	0.757008365792895	0.799	0.529	8.64116102538882E-73
Gapdh	6.30362869296444E-77	0.687114693582737	0.942	0.818	1.95746581802625E-72
Susd3	8.92059004040641E-76	-0.715643358436196	0.644	0.814	2.7701108252474E-71
Dnase2a	5.9995018301071E-75	0.736974353683346	0.745	0.46	1.86302530330316E-70
Ltc4s	1.38542069972164E-74	-0.638259235072411	0.89	0.955	4.30214689884561E-70
Calr	5.07915517047771E-74	0.592962075661038	0.982	0.92	1.57723005508844E-69
Lamp1	8.80046227934479E-74	0.479896362375576	0.989	0.965	2.73280755160494E-69
Commd8	4.74577308215989E-73	-0.746453712174256	0.567	0.757	1.47370491520311E-68
Rpsa	3.15030216262623E-72	0.542170257938339	0.967	0.906	9.78263330560322E-68
Csf1r	3.31940341793199E-72	-0.332214413260663	1	1	1.03077434337042E-67
Tyrobp	6.6543263906078E-72	0.36972771346155	1	0.999	2.06636797407544E-67
Cebpd	7.01898109246718E-72	-0.886805201414117	0.416	0.662	2.17960419864383E-67
C5ar1	9.83244862997868E-72	0.982565348891724	0.558	0.288	3.05327027306728E-67
Creg1	1.19134604088356E-71	0.585336993870734	0.919	0.763	3.69948686075571E-67
Sdf2l1	3.86056173202341E-71	0.881063114436453	0.765	0.522	1.19882023464523E-66
Ifngr1	1.20140591499939E-70	-0.465331691139475	0.968	0.986	3.7307257878476E-66
Ptgs1	1.41407948365729E-70	-0.577933036754695	0.84	0.933	4.391141020601E-66
Elmo1	3.56775241952291E-70	-0.742191907788343	0.62	0.782	1.10789415883445E-65
Slc25a5	4.23383739494567E-70	0.634582031922411	0.902	0.745	1.31473352625248E-65
Srgap2	4.34188939906534E-70	-0.616983535997769	0.796	0.906	1.34828691509176E-65
Fxyd5	1.2867385583887E-69	0.346519496333807	0.132	0.023	3.99570924536443E-65
Trem2	5.33445604855432E-69	0.355647681278468	1	0.999	1.65650863675757E-64
Hmox1	6.44133916650025E-68	0.614063258717888	0.302	0.102	2.00022905137332E-63
Txnip	6.95951761726012E-68	-0.638966702848192	0.759	0.872	2.16113900568778E-63
Maf	1.43241040877241E-67	-0.599860174585344	0.869	0.937	4.44806404236096E-63
Got1	4.88581578537014E-67	0.50288421121787	0.346	0.125	1.51719237583099E-62
S1pr1	1.11291697245524E-66	0.488531208232475	0.264	0.082	3.45594107456526E-62
Lpcat2	3.46520723112635E-66	-0.457011622282256	0.967	0.986	1.07605080148166E-61
Gpr65	4.92654181042412E-65	0.349856028660476	0.136	0.026	1.529839028391E-60
Apbb2	5.50700881264941E-65	0.58933610246463	0.387	0.156	1.71009144659202E-60
Nme1	1.03319222280149E-64	0.617959107016174	0.499	0.236	3.20837180946548E-60
Cacna1a	2.35393917026855E-64	0.466613332157352	0.204	0.054	7.30968730543494E-60
Glipr1	2.47564748560677E-64	0.402925315282	0.225	0.063	7.6876281370547E-60
Pkm	2.84282022129259E-64	0.737191820182225	0.691	0.429	8.82780963317989E-60
Cd164	6.58332821620466E-64	-0.674086540911718	0.664	0.816	2.04432091097803E-59
Sdc4	1.16134169168885E-63	0.527084310727749	0.209	0.058	3.6063143552014E-59

(*Continued*)

Table 2. (Continued)

	p_val	avg_log2FC	pct.1	pct.2	p_val_adj
Cmtm6	7.25774044112845E-63	-0.588213829776584	0.753	0.861	2.25374613918362E-58
Aplp2	1.54024166309499E-61	0.676463426508205	0.46	0.211	4.78291243640886E-57
Arhgap5	1.6330383964775E-61	-0.58341651663721	0.827	0.91	5.07107413258157E-57
Rnase4	1.7342655506065E-61	-0.512249790390645	0.904	0.963	5.38541481429837E-57
Pdgfa	2.93804991339461E-61	0.775302793475312	0.365	0.149	9.12352639606428E-57
Plin2	3.39733878887266E-61	0.413205438391448	0.251	0.078	1.05497561410863E-56
Hspa5	6.60104334289085E-61	0.65459591021307	0.947	0.858	2.0498219892679E-56
Nrip1	1.74792200519455E-60	-0.612028423098356	0.744	0.869	5.42782220273063E-56
Ctsl	2.10848833230955E-60	0.460529293443523	0.998	0.986	6.54748881832084E-56
Psap	5.29767740928728E-60	0.445380962728947	1	0.993	1.64508776590598E-55
Scd2	1.81891231399637E-59	0.482773140626862	0.336	0.127	5.64826840865291E-55
Nceh1	4.23303886520062E-59	0.424251858399195	0.181	0.047	1.31448555881075E-54
Tpi1	6.69427759448965E-59	0.663206734801895	0.487	0.239	2.07877402141687E-54
mt-Atp6	8.28514597497733E-59	0.460948833826779	0.998	0.998	2.57278637960971E-54
Dpp7	1.98350277475901E-58	0.424468311114338	0.229	0.07	6.15937116645916E-54
Ssh2	2.48741175253527E-58	-0.64276415770462	0.674	0.816	7.72415971514778E-54
Frmd4a	7.00243162399543E-58	-0.538165079495026	0.827	0.906	2.1744650921993E-53
Pmepa1	8.07063542729683E-58	-0.567143331483457	0.892	0.956	2.50617441923849E-53
Cotl1	1.40026649014461E-57	0.553502045934712	0.897	0.741	4.34824753184605E-53
Capg	3.01218792921459E-57	0.53396852890683	0.29	0.105	9.35374717659008E-53
Rhoc	3.31928202253687E-57	0.58494057735236	0.374	0.157	1.03073664645837E-52
St3gal6	9.06384537425771E-57	-0.581099272195043	0.697	0.827	2.81459590406825E-52
Calm2	1.98642331542267E-56	-0.457691301788096	0.93	0.96	6.16844032138201E-52
Adgrg1	2.54011540340229E-56	-0.631518305206502	0.662	0.782	7.88782036218513E-52
Anxa5	4.79872108327651E-56	0.389616253498145	0.201	0.058	1.49014685798986E-51
Cmtm7	4.98883593427602E-56	-0.586094685274199	0.691	0.822	1.54918322267073E-51
Uap1l1	7.24881444698784E-56	0.474409326235679	0.32	0.122	2.25097435022314E-51
Hif1a	5.03204379833433E-55	0.653191597752922	0.512	0.265	1.56260056069676E-50
mt-Nd1	1.27608557526488E-53	0.520390796544433	0.979	0.974	3.96262853687004E-49
Gnl3	1.82717015796429E-53	0.616290373611735	0.426	0.2	5.6739114915265E-49
Ssr4	7.53897622443318E-53	0.45670983091204	0.939	0.814	2.34107828697324E-48
Gaa	1.17172865138326E-52	0.481994161871853	0.427	0.19	3.63856898114044E-48
Rgs10	1.1744417795469E-52	-0.363248010659844	0.981	0.992	3.64699405802699E-48
Ctsc	3.14688415535714E-52	0.528662496677226	0.91	0.768	9.77201936763054E-48
Hspa8	3.80828837400191E-52	0.514928302750921	0.951	0.872	1.18258778877881E-47
Cox6a2	1.31166642786174E-51	0.270088241869821	0.116	0.023	4.07311775843906E-47
Syngr1	4.07815857552635E-51	0.495894306710773	0.932	0.819	1.2663905824582E-46
Id2	5.13004735203389E-51	0.73459631434953	0.273	0.105	1.59303360422708E-46
Bcl2a1b	7.34863786997375E-51	0.694498438592724	0.785	0.589	2.28197251776295E-46
Timp2	1.30496723397884E-50	0.474988225831741	0.93	0.811	4.0523147516745E-46
Rpl10a	1.69210900399288E-50	0.424073020099445	0.972	0.877	5.2545060900991E-46
Dock10	2.32679252778372E-50	-0.6479276023627	0.544	0.695	7.22538883652677E-46
Renbp	7.94640048410583E-50	0.532906728251976	0.454	0.223	2.46759574232938E-45
Cxcl16	9.43230042376968E-50	0.602180017993279	0.373	0.168	2.9290122505932E-45
Mef2a	5.20458524572297E-49	-0.508319662100362	0.795	0.9	1.61617985635435E-44
Slamf8	7.7520986511249E-49	0.401094433918377	0.186	0.056	2.40725919413382E-44
Glul	9.0328119522076E-49	-0.513087417236526	0.855	0.903	2.80495909551903E-44

(*Continued*)

Table 2. (Continued)

	p_val	avg_log2FC	pct.1	pct.2	p_val_adj
F11r	9.23182938042976E-49	-0.441225560157002	0.918	0.955	2.86675997750485E-44
Asph	9.56049840849747E-49	0.557115143524005	0.83	0.667	2.96882157079072E-44
Il10ra	9.8315954159412E-49	-0.611479440775794	0.529	0.699	3.05300532451222E-44
Nav3	7.56176135331455E-48	-0.659496669639548	0.516	0.687	2.34815375304477E-43
H2-D1	2.56348688205036E-47	0.578557305024221	0.869	0.687	7.96039581483099E-43
Adssl1	3.53597991589356E-47	0.306382037827989	0.179	0.053	1.09802784328243E-42
Il4i1	4.20175651273496E-47	0.466290645043656	0.192	0.061	1.30477144989959E-42
Pdia6	1.39516487264208E-46	0.489157209247046	0.932	0.813	4.33240547901544E-42
Lrba	1.41998096714974E-46	-0.639531221241718	0.48	0.652	4.4094668972901E-42
Fam102b	4.98193707083843E-46	-0.600723477825392	0.584	0.735	1.54704091860746E-41
Ms4a6b	6.74592017119362E-46	-0.675205168844468	0.353	0.556	2.09481059076076E-41
B2m	1.12607164109117E-45	0.387611579094594	0.987	0.957	3.49679026708041E-41
Gusb	2.20831554805777E-45	0.52775162670477	0.836	0.635	6.85748227138379E-41
Pgk1	2.60157539088621E-45	0.481031829728836	0.381	0.177	8.07867206131895E-41
Pde3b	3.35206535493397E-45	-0.600037422922937	0.599	0.721	1.04091685466764E-40
mt-Co2	1.24274205865524E-44	0.396079210932013	0.996	0.996	3.85908691474211E-40
Eif5a	2.4170403298965E-44	0.531295411154843	0.814	0.608	7.50563533642761E-40
mt-Co3	4.8481056297552E-44	0.403682409006687	0.995	0.997	1.50548224120788E-39
H2-K1	1.34360142659825E-43	0.521306515292163	0.881	0.691	4.17228551001555E-39
Ecscr	1.77748247088031E-43	-0.472796485355958	0.814	0.896	5.51961631682464E-39
Arhgap45	4.7752216343876E-43	-0.473616024242607	0.779	0.871	1.48284957412638E-38
Mbnl1	7.56394416450135E-43	-0.497500101930406	0.821	0.87	2.3488315814026E-38
Abcg1	7.92852332395055E-43	0.482203326305026	0.51	0.275	2.46204434778636E-38
Tmem173	1.15399896757026E-42	-0.519497631944832	0.68	0.793	3.58351299399594E-38
Scpep1	2.78590022785178E-42	0.456699152950326	0.368	0.172	8.65105597754812E-38
Dtnbp1	4.9079114166475E-42	0.446761420062665	0.415	0.203	1.52405373221155E-37
Plekhm2	6.58051470289304E-42	0.407477513791209	0.218	0.079	2.04344723068938E-37
Hpgd	8.47797549378708E-42	-0.508153796550951	0.756	0.843	2.6326657300857E-37
Il11ra1	1.52883061508586E-41	0.490177078291142	0.425	0.213	4.74747770902612E-37
Srgn	3.44371530112524E-41	0.575642140578165	0.737	0.534	1.06937691245842E-36
Slco2b1	4.34640691226016E-41	-0.444594167814038	0.854	0.902	1.34968973846415E-36
Sall1	1.18451927478039E-40	-0.526085879035089	0.592	0.714	3.67828770397553E-36
Slc15a3	1.22714213657559E-40	0.746930747140177	0.554	0.341	3.81064447670818E-36
Ccr5	2.13181090841299E-40	-0.54155723509141	0.758	0.841	6.61991241389486E-36
Ccl6	3.65725060136654E-40	0.798272506123976	0.637	0.434	1.13568602924235E-35
Rapgef5	2.07759564357415E-39	-0.62956656004199	0.34	0.526	6.45155775199082E-35
Ckb	2.42312692389765E-39	-0.417576140079039	0.924	0.95	7.52453603677936E-35
Rsrp1	2.42851834206525E-39	-0.384093406316538	0.942	0.97	7.54127800761523E-35
C1qbp	4.49682276672034E-39	0.496477885564906	0.517	0.296	1.39639837374967E-34
Ssr2	3.34190183013306E-38	0.454747008083742	0.72	0.49	1.03776077531122E-33
Selenow	4.34727701825501E-38	0.465379260277558	0.408	0.21	1.34995993247873E-33
Lipa	5.06489828428849E-38	0.511643152162503	0.602	0.373	1.5728028642201E-33
Atp5g1	8.32463194321884E-38	0.514547877550272	0.655	0.437	2.58504795732775E-33
Ptma	1.03202222180045E-37	0.385685821422643	0.973	0.889	3.20473860535695E-33
Arl11	1.1263253988904E-37	0.413895991508187	0.448	0.235	3.49757826117436E-33
Hsd17b12	1.15723930293936E-37	0.44315662785853	0.464	0.248	3.59357520741758E-33
Mettl1	1.27448087741679E-37	0.367524736031922	0.285	0.122	3.95764546864237E-33

(*Continued*)

Table 2. (Continued)

	p_val	avg_log2FC	pct.1	pct.2	p_val_adj
Tnfrsf12a	1.49404595039677E-37	0.391129481708753	0.106	0.026	4.63946088976708E-33
Manf	4.03636107863532E-37	0.51833924559785	0.867	0.697	1.25341120574863E-32
Alox5ap	4.56098489137684E-37	-0.489946018174042	0.715	0.808	1.41632263831925E-32
Crybb1	4.65994772545172E-37	-0.570595980047922	0.65	0.761	1.44705356718452E-32
Tsc22d4	7.61387646197082E-37	-0.449178642918815	0.743	0.827	2.3643370577358E-32
Cfl1	8.64782056780436E-37	0.357689979068086	0.964	0.92	2.68540772092029E-32
Rpl12	1.43027169743147E-36	0.360732032917497	0.972	0.911	4.44142270203393E-32
Nrp2	1.86121375230495E-36	0.381401397875395	0.305	0.137	5.77962706503256E-32
Fchsd2	2.94245025300602E-36	-0.585132766236506	0.55	0.671	9.13719077065958E-32
Cd52	4.10648684413692E-36	0.607683096004775	0.719	0.529	1.27518735970984E-31
Hsp90b1	5.21796424925618E-36	0.394919780147213	0.977	0.926	1.62033443832152E-31
Ybx1	1.10078801772538E-35	0.449645010630102	0.828	0.637	3.41827703144262E-31
Siglecf	1.85626910896376E-35	0.365474034182325	0.225	0.089	5.76427246406515E-31
Ppia	1.86196145422586E-35	0.298070488274917	0.987	0.975	5.78194890380757E-31
Tnfaip8l2	4.34056177515685E-35	-0.455328357507087	0.689	0.791	1.34787464803946E-30
Hsp90aa1	4.95683494488193E-35	0.542542963378589	0.665	0.465	1.53924595543419E-30
Ncl	5.34720815572171E-35	0.555769526277748	0.725	0.529	1.66046854859626E-30
mt-Nd2	6.37796598093349E-35	0.409317822483824	0.995	0.983	1.98054977605928E-30
Tanc2	1.20846051211416E-34	-0.491893007656888	0.702	0.793	3.75263242826812E-30
Kctd12	1.61289159875745E-34	-0.442687859566028	0.807	0.873	5.00851228162151E-30
Cpd	2.47259870435313E-34	0.361393105831768	0.239	0.099	7.67816075662778E-30
Gga2	2.53536388068479E-34	0.252459505003485	0.143	0.045	7.87306545869048E-30
Fam49b	3.19507640188712E-34	-0.396681310114844	0.842	0.887	9.92167075078009E-30
Npnt	3.55508175207553E-34	0.380220024707806	0.31	0.145	1.10395953647202E-29
Tpd52	3.57782112428065E-34	0.413351733171847	0.471	0.262	1.11102079372287E-29
Atp6ap2	4.45107453378929E-34	0.430346229411463	0.864	0.69	1.38219217497759E-29
Neat1	5.83218213790618E-34	0.418926472909667	0.265	0.118	1.81106751928401E-29
Qk	9.04642106126178E-34	-0.351134672140777	0.933	0.959	2.80918513215362E-29
Gpr34	9.70164297950284E-34	-0.295508692418895	0.994	0.999	3.01265119442502E-29
Ldha	1.09981846490267E-33	0.589677058542156	0.589	0.39	3.41526627906225E-29
Epb41l2	2.68551553006558E-33	-0.409889683349906	0.909	0.927	8.33933137551264E-29
Degs1	2.70083169875143E-33	0.362194420927888	0.42	0.219	8.38689267413281E-29
Tmem256	2.83506461863131E-33	0.433735219835239	0.539	0.327	8.80372616023581E-29
Ranbp1	3.71815025560179E-33	0.434065288948232	0.558	0.334	1.15459719887202E-28
Numb	4.09206681981799E-33	-0.492154464348105	0.535	0.674	1.27070950955808E-28
Glmp	4.76389604189922E-33	0.436446723942437	0.716	0.487	1.47933263789097E-28
Rpl41	7.20150170299407E-33	0.322278590479056	0.992	0.986	2.23628232383075E-28
Rplp0	1.80232812919758E-32	0.304482437819109	0.979	0.964	5.59676953959725E-28
Npm1	2.93613237905256E-32	0.482536597318115	0.807	0.648	9.11757187667191E-28
Plek	7.12401711659187E-32	0.509301833047534	0.614	0.401	2.21222103521527E-27
Pag1	2.00632874067246E-31	-0.457569141620418	0.639	0.749	6.23025263841018E-27
Pgam1	3.05771802647204E-31	0.445280801826828	0.591	0.378	9.49513178760362E-27
Sparc	3.16669775512935E-31	-0.270627876052526	0.999	1	9.83354653900318E-27
Ppa1	5.52914172778572E-31	0.259306316096504	0.164	0.059	1.7169643807293E-26
Zfp36l2	8.08830189219789E-31	-0.48735866589604	0.703	0.779	2.51166038658421E-26
Hspd1	8.54323149950983E-31	0.464596738031814	0.469	0.276	2.65292967754279E-26
Oxct1	9.65720787703265E-31	0.427226950903729	0.67	0.469	2.99885276205495E-26

(*Continued*)

Table 2. (Continued)

	p_val	avg_log2FC	pct.1	pct.2	p_val_adj
Speg	2.02576350776271E-30	0.284247564160621	0.185	0.072	6.29060342065555E-26
Git2	2.45457106397613E-30	-0.477957080409749	0.643	0.734	7.62217952496507E-26
Bin2	2.63336426847757E-30	-0.411471218127436	0.715	0.799	8.1773860629034E-26
mt-Co1	2.9815285100886E-30	0.314362725096399	0.998	0.995	9.25854048237814E-26
Tceal9	3.10988034443876E-30	0.315215003506278	0.243	0.107	9.65711143358569E-26
Atp6v1a	3.58475644284532E-30	0.383248952984662	0.288	0.139	1.11317441819676E-25
Rgs2	3.75744085442515E-30	-0.402337867752876	0.802	0.868	1.16679810852464E-25
Phgdh	3.77743806387575E-30	0.444600846374229	0.588	0.381	1.17300784197534E-25
Pld4	9.74867268662707E-30	-0.370617885375037	0.895	0.931	3.0272553293783E-25
Gnas	1.18071110411391E-29	0.377988569498271	0.906	0.787	3.66646219160493E-25
Wasf2	3.60333338977188E-29	-0.420581383513958	0.71	0.784	1.11894311752586E-24
Serpine2	6.66360639380897E-29	0.383617023599912	0.916	0.805	2.0692496934695E-24
Amdhd2	9.50418401866414E-29	0.283721022231996	0.24	0.106	2.95133426331578E-24
Cln5	1.25163031951808E-28	0.385480891055797	0.441	0.254	3.88668763119949E-24
Sco2	1.2688681370891E-28	0.323027067247246	0.264	0.123	3.94021622610277E-24
Ctc1	1.96077032129541E-28	-0.515265712329096	0.406	0.54	6.08878007871863E-24
Ankrd44	1.99210750792243E-28	-0.481944304536418	0.55	0.655	6.18609163958174E-24
mt-Nd4	2.12925484249E-28	0.324380571816951	0.986	0.985	6.6119750623842E-24
Dock4	2.41473238350482E-28	-0.491027036550414	0.577	0.673	7.49846847049752E-24
Ophn1	3.18027531495293E-28	-0.459503522424536	0.621	0.709	9.87570893552335E-24
Atox1	3.21306135826157E-28	0.382989950584401	0.802	0.626	9.97751943580966E-24
Bst2	3.90015542102088E-28	0.473950904762105	0.635	0.42	1.21111526288961E-23
Rps19	4.84974100350518E-28	0.303320235999598	0.978	0.94	1.50599007381846E-23
Ccl9	4.85264746596657E-28	0.781795381828554	0.646	0.49	1.5068926176066E-23
Itgam	4.86545775763175E-28	-0.425248716600044	0.759	0.817	1.51087059747739E-23
Snrpf	5.71359125903477E-28	0.38402897475651	0.509	0.313	1.77424149366807E-23
Dad1	6.59339415932594E-28	0.349207348922655	0.853	0.663	2.04744668829548E-23
Pdia3	1.70792539383179E-27	0.360406539745383	0.938	0.837	5.30362072546585E-23
Rpl14	1.86754165159592E-27	0.327840117468946	0.917	0.822	5.79927709070081E-23
Cyth4	2.39025681170063E-27	-0.314149804904163	0.94	0.959	7.42246447737397E-23
Plekha1	2.85601278093158E-27	0.396901309178602	0.391	0.218	8.86877648862684E-23
Tnfrsf13b	2.87678049562323E-27	-0.534342219557837	0.312	0.456	8.9332664730588E-23
Eef1g	3.34249016135725E-27	0.402534009396938	0.628	0.427	1.03794346980627E-22
Cysltr1	3.8713375903377E-27	-0.549305982203782	0.309	0.452	1.20216646192756E-22
Nav2	3.97079235172207E-27	-0.462955746775159	0.602	0.708	1.23305014898025E-22
Fam110a	4.23106492500756E-27	-0.573835045335538	0.207	0.368	1.3138725911626E-22
Abca1	4.26215470350909E-27	0.425279299180042	0.654	0.454	1.32352690008068E-22
Slc3a2	4.69825171128444E-27	0.435281850487179	0.894	0.785	1.45894810390516E-22
Rplp2	6.82383987623299E-27	0.259607179512908	0.988	0.96	2.11900699676663E-22
Ppfia4	6.94789351207204E-27	-0.414871911456713	0.621	0.72	2.15752937230373E-22
Bax	7.70025700162577E-27	0.402427060709431	0.618	0.402	2.39116080671485E-22
Golm1	9.87441790978386E-27	-0.36860114428039	0.849	0.883	3.06630299352518E-22
Tpst2	1.01725104788008E-26	-0.429870060579117	0.663	0.762	3.15886967898202E-22
mt-Cytb	1.03181450622033E-26	0.30454419833674	0.996	0.995	3.20409358616599E-22
Fam212a	1.13149238992867E-26	-0.495590373060695	0.416	0.554	3.51362331844549E-22
Fam105a	1.40097553025469E-26	-0.349219741897841	0.858	0.895	4.35044931409989E-22
Emp3	1.44511045424651E-26	0.392396547417138	0.295	0.15	4.48750149357168E-22

(*Continued*)

Table 2. (Continued)

	p_val	avg_log2FC	pct.1	pct.2	p_val_adj
Hspe1	1.78813839928288E-26	0.392766359842521	0.688	0.497	5.55270617129311E-22
Zfp710	2.44348399038032E-26	-0.539164156650091	0.373	0.503	7.58775083532802E-22
Bmp2k	2.62996673621556E-26	-0.443222658658454	0.639	0.718	8.16683570597017E-22
Gna15	2.72773098304417E-26	-0.416083889741095	0.587	0.685	8.47042302164705E-22
Gnai2	3.05770691698163E-26	-0.298679297813492	0.944	0.957	9.49509728930305E-22
Ypel3	3.4471788769902E-26	-0.437403754258679	0.537	0.654	1.07045245667177E-21
Cndp2	3.61671663232009E-26	0.35504280335393	0.481	0.288	1.12309901583436E-21
Krtcap2	7.4034101962161E-26	0.386307527376267	0.716	0.545	2.29898096823099E-21
Vegfb	1.04203975127724E-25	0.34051092407815	0.371	0.204	3.23584603964122E-21
Stmn1	1.19106567546169E-25	0.292210714096892	0.247	0.117	3.69861624201118E-21
Slc35f6	1.63740645745082E-25	0.374017824549108	0.354	0.195	5.08463827232204E-21
Ywhah	2.14595764889782E-25	-0.344055033282341	0.861	0.893	6.66384228712242E-21
Eif1a	2.82744485653522E-25	0.362899744606182	0.331	0.179	8.78006451299882E-21
Eya4	3.39899818163469E-25	0.297263128577378	0.255	0.124	1.05549090534302E-20
Cd48	4.18505561516487E-25	0.439721785823438	0.52	0.345	1.29958532017715E-20
Gabarap	4.56519320585279E-25	0.306175787038689	0.925	0.811	1.41762944621347E-20
Hnrnpa1	4.6228163739757E-25	0.384980462086857	0.586	0.395	1.43552316861067E-20
Eef2k	6.42429967611457E-25	-0.521510095504093	0.301	0.444	1.99493777842386E-20
Foxn3	6.86271308219647E-25	-0.40110624227457	0.708	0.763	2.13107829341447E-20
Abca9	8.18064836253267E-25	-0.517741276729229	0.329	0.461	2.54033673601727E-20
Plekho2	1.11946463496997E-24	0.301166850724053	0.153	0.061	3.47627353097224E-20
A830008E2	1.90463000073343E-24	-0.556834154765782	0.226	0.38	5.91444754127752E-20
Btg2	2.3474921785515E-24	-0.563013359238349	0.535	0.662	7.28966746205596E-20
Hexa	2.53828913455285E-24	0.306464484576321	0.979	0.936	7.88214924952697E-20
Arpc2	2.56276037140693E-24	0.295028510273021	0.952	0.888	7.95813978132994E-20
Picalm	2.83930104582616E-24	-0.391340020597646	0.767	0.811	8.81688153760398E-20
Csmd3	3.5594532771125E-24	-0.499633798501414	0.475	0.597	1.10531702614174E-19
Atp6v1c1	4.6926561120587E-24	0.351002030323345	0.475	0.288	1.45721050247759E-19
Spcs2	4.88697108308929E-24	0.319237328977595	0.91	0.824	1.51755113043172E-19
Tmem176b	7.17504520039447E-24	-0.426396027903934	0.767	0.826	2.22806678607849E-19
Tgfbr1	8.39155054450364E-24	-0.263542279712594	0.987	0.987	2.60582819058472E-19
Pmp22	9.11727216729362E-24	0.547298658890186	0.862	0.774	2.83118652610969E-19
Col27a1	1.03616588823734E-23	-0.497799037849485	0.368	0.497	3.21760593274341E-19
Pten	1.0643907370072E-23	-0.476323460985719	0.457	0.558	3.30525255562847E-19
Cox4i1	1.47827322268289E-23	0.2975999369363	0.882	0.756	4.59048183839717E-19
Tsc22d3	1.90309966487181E-23	-0.570077354715977	0.219	0.367	5.90969538932642E-19
Bmyc	2.18203247721525E-23	-0.412985900576483	0.535	0.633	6.77586545149652E-19
Chd9	2.22837449509304E-23	-0.479345180230731	0.448	0.556	6.91977131961243E-19
Rps26	2.96012696947443E-23	0.294476307294439	0.946	0.872	9.19208227830894E-19
Snn	3.76279383322177E-23	-0.486285080087485	0.37	0.486	1.16846036903036E-18
Prkca	3.99551096596017E-23	-0.50301747851366	0.2	0.344	1.24072602025961E-18
Mrps18b	4.54047365570421E-23	0.268032111545704	0.303	0.159	1.40995328430583E-18
Dip2b	7.16520090346016E-23	-0.457176208802776	0.43	0.547	2.22500983655148E-18
Cct3	7.18133986139772E-23	0.347759107295508	0.49	0.309	2.23002146715984E-18
Clk1	9.59466578713302E-23	-0.424915532010236	0.571	0.65	2.97943156687842E-18
Mef2c	1.19426506975782E-22	-0.264656789705501	0.968	0.986	3.70855132111897E-18
Celf2	1.22740575214403E-22	-0.386544231064657	0.727	0.788	3.81146308213287E-18

(*Continued*)

Table 2. (Continued)

	p_val	avg_log2FC	pct.1	pct.2	p_val_adj
Abhd12	1.25350096498218E-22	0.279705391607691	0.986	0.956	3.89249654655916E-18
Pebp1	1.28759235511961E-22	0.346322736777086	0.687	0.503	3.99836054035293E-18
Pkig	1.52134364274231E-22	-0.437935702103922	0.463	0.563	4.7242284138077E-18
mt-Nd3	1.52389567932705E-22	0.360814831157491	0.924	0.868	4.73215325301429E-18
Slc16a3	1.65809139698158E-22	0.361830850603775	0.316	0.176	5.14887121504691E-18
G3bp1	1.91696409836498E-22	0.380174457719334	0.612	0.424	5.95274861465277E-18
Tm6sf1	2.22506791082021E-22	-0.392208837137046	0.64	0.725	6.90950338346998E-18
Fcgr1	2.40226518345125E-22	-0.344414161211829	0.804	0.851	7.45975407417118E-18
Ptpn18	2.94117241161809E-22	-0.359820107776922	0.736	0.8	9.13322268979767E-18
mt-Nd4l	3.00643416440556E-22	0.437525676271991	0.689	0.534	9.33588001072857E-18
Hpf1	3.2908545829426E-22	0.325405936242127	0.454	0.278	1.02190907364117E-17
Lpar6	3.68266539289908E-22	-0.441485669117467	0.579	0.652	1.14357808445695E-17
Pea15a	3.76050014348994E-22	0.297686993077065	0.373	0.214	1.16774810955793E-17
Mrto4	4.00659697083673E-22	0.297995208709106	0.277	0.145	1.24416855735393E-17
Srrm2	4.22106077435486E-22	-0.348102490685013	0.834	0.847	1.31076600226041E-17
Ran	4.45176694180117E-22	0.368010010709252	0.661	0.474	1.38240718843752E-17
Tmem160	6.69363595911118E-22	0.331029688957387	0.473	0.297	2.07857477438279E-17
Acadl	7.84562625307841E-22	0.283939709052962	0.292	0.156	2.43630232036844E-17
Myl6	8.60720705007188E-22	0.324543917095488	0.8	0.643	2.67279600525882E-17
Ntpcr	1.27075013162379E-21	-0.377354672588958	0.575	0.659	3.94606038373135E-17
Slc35b1	1.28227950523366E-21	0.324301233020395	0.409	0.244	3.98186254760207E-17
Cd33	1.37174895458831E-21	-0.397263680216192	0.706	0.755	4.25969202868309E-17
Atp1b3	1.39030721546009E-21	0.36416752758522	0.639	0.447	4.31732099616823E-17
Mydgf	1.84362317078189E-21	0.35166869377745	0.629	0.447	5.72500303222902E-17
Tns1	1.94664366990437E-21	0.278223492035178	0.29	0.155	6.04491258815404E-17
Cct8	2.14096922120587E-21	0.322171857740395	0.572	0.377	6.64835172261059E-17
Erp29	2.2439166123147E-21	0.265004396150513	0.979	0.935	6.96803425622084E-17
Akr1a1	2.28774416967525E-21	0.327941413048129	0.757	0.585	7.10413197009256E-17
Dnajb11	2.84771560588368E-21	0.352570790141271	0.684	0.495	8.8430112709506E-17
Canx	2.98045704610599E-21	0.304679454238274	0.874	0.757	9.25521326527292E-17
Ddx5	3.07696546690176E-21	-0.262798198324156	0.967	0.973	9.55490086437002E-17
Hmgn2	3.68501113234346E-21	0.286467187348032	0.399	0.238	1.14430650692661E-16
Bola2	4.21623716577286E-21	0.31379305469731	0.432	0.263	1.30926812708745E-16
Arsb	4.39635672434192E-21	-0.355232794149626	0.796	0.815	1.3652006536099E-16
Slc6a6	4.52593770082542E-21	0.335763114024004	0.602	0.406	1.40543943423732E-16
Npl	5.08850186991542E-21	0.352882100817083	0.419	0.258	1.58013248566483E-16
Ogfrl1	5.17065398789115E-21	-0.455393350202006	0.475	0.567	1.60564318285984E-16
Cd34	5.79105523560748E-21	0.441877995625058	0.633	0.466	1.79829638231319E-16
Sft2d1	5.83530366903873E-21	-0.316307144515182	0.842	0.871	1.8120368483466E-16
Inpp5d	8.95122246639135E-21	-0.320474111370355	0.828	0.869	2.77962311248851E-16
Il6ra	9.21620560202215E-21	-0.394310742173464	0.637	0.699	2.86190832559594E-16
Tpm4	1.05342595620172E-20	0.271181645835348	0.204	0.098	3.27120362179321E-16
Rbm3	1.06529018324443E-20	0.335309695611084	0.725	0.572	3.30804560602894E-16
Tcf4	1.07209154748229E-20	-0.43010896893165	0.609	0.686	3.32916588239675E-16
Eng	1.07559986534675E-20	-0.474809410948009	0.196	0.328	3.34006026186126E-16
AU020206	1.11562881595433E-20	0.255641200769782	0.246	0.125	3.46436216218297E-16
Neu1	1.14480087762701E-20	0.313046714571744	0.377	0.222	3.55495016529515E-16

(*Continued*)

Table 2. (Continued)

	p_val	avg_log2FC	pct.1	pct.2	p_val_adj
Vps29	1.20794604224294E-20	0.343472020092991	0.506	0.33	3.751034844977E-16
Pld1	1.29195425587035E-20	-0.47277470803636	0.22	0.35	4.01190555075421E-16
Cttnbp2nl	1.30963284097332E-20	-0.357387214797646	0.695	0.758	4.06680286107447E-16
Itga6	1.62273809533733E-20	-0.422708778607816	0.563	0.651	5.039088607451E-16
Dnajb14	1.68113973048152E-20	0.336379748806099	0.439	0.277	5.22044320506425E-16
Clec4a2	1.68649949552416E-20	-0.460954076140435	0.344	0.456	5.23708688345117E-16
Rragc	1.79207168155747E-20	0.344496311440997	0.484	0.313	5.56492019274041E-16
Tpp1	2.05433713626289E-20	0.317589286024118	0.798	0.639	6.37933310923716E-16
Atp1a1	2.10163841726529E-20	0.342408747823385	0.519	0.342	6.52621777713392E-16
Adap2	2.12062053585025E-20	-0.378084340796438	0.706	0.759	6.58516294997577E-16
Kcnk12	2.20335453563795E-20	-0.440561300457441	0.119	0.252	6.84207683951653E-16
Rps18	2.49754121950701E-20	0.251631169651514	0.97	0.932	7.75561474893513E-16
Slc12a9	2.50575506470782E-20	-0.440747503217784	0.365	0.485	7.7811212024372E-16
Commd4	3.37034329662654E-20	0.281126624875675	0.367	0.217	1.04659270390144E-15
Mapkapk2	3.49853753855046E-20	0.26652535556196	0.338	0.189	1.08640086184607E-15
Mtus1	3.68722416066434E-20	-0.424309218665912	0.416	0.521	1.1449937186111E-15
Slc12a2	3.75485594725543E-20	0.332422140712737	0.468	0.302	1.16599541730123E-15
Uqcc2	4.31666990210354E-20	0.280946972087408	0.432	0.265	1.34045550470021E-15
Cd84	4.37521068579692E-20	0.333477594641535	0.848	0.713	1.35863417426052E-15
Lyl1	5.0726471734059E-20	-0.446324931864446	0.462	0.555	1.57520912675774E-15
Khdrbs3	5.88435176878513E-20	-0.49942136021998	0.173	0.302	1.82726775476085E-15
Atp6v0a2	6.83695758092147E-20	-0.4540460991717	0.273	0.398	2.12308043760355E-15
Bank1	8.72998276938563E-20	-0.463581420878649	0.185	0.314	2.71092154937732E-15
Grina	1.00314510712373E-19	0.319982884987649	0.598	0.414	3.11506650115132E-15
Ucp2	1.01744008111698E-19	0.317308618728166	0.829	0.694	3.15945668389257E-15
Mfsd11	1.04970316882176E-19	0.375373232182121	0.429	0.271	3.25964325014222E-15
Sgpl1	1.18012181943746E-19	0.326938686688929	0.444	0.28	3.66463228589914E-15
Tmem86a	1.22210473148769E-19	0.33259963190436	0.904	0.807	3.79500182268872E-15
Mfsd1	1.22972343918018E-19	0.279819868572921	0.345	0.201	3.81866019568621E-15
Yif1b	1.28729438539454E-19	0.317829682125488	0.545	0.363	3.99743525496567E-15
Cln8	1.69828330352658E-19	0.32443991266458	0.458	0.288	5.2736791424411E-15
Rps6ka1	1.73385019340581E-19	-0.429553091562141	0.47	0.553	5.38412500558305E-15
Rps27l	2.26903164414125E-19	0.335913800147433	0.587	0.411	7.04602396455182E-15
Tmem55b	2.36488507243722E-19	-0.344191530534683	0.647	0.719	7.34367761543929E-15
Klf7	2.8325196055687E-19	-0.495953343198119	0.256	0.379	8.79582313117247E-15
Cycs	3.9005245142487E-19	0.277145651818025	0.437	0.269	1.21122987740965E-14
Mtss1	4.21296766458036E-19	-0.442989148338404	0.154	0.283	1.30825284888214E-14
Sipa1	4.63539390497423E-19	-0.421767107683874	0.482	0.564	1.43942886931165E-14
Bcl2l1	5.59025175349705E-19	0.284054852072817	0.353	0.206	1.73594087701344E-14
Arglu1	8.11661808808381E-19	-0.329966313916827	0.738	0.768	2.52045341489267E-14
Ccng2	8.31122021168012E-19	-0.451676492248546	0.296	0.413	2.58088321233303E-14
Lgals3bp	8.79950920058822E-19	0.321461377148218	0.407	0.254	2.73251159205866E-14
Cox7a2l	8.87621598780657E-19	-0.379052985231203	0.582	0.636	2.75633135069357E-14
Rrp1	9.29740077857506E-19	0.293405835357007	0.478	0.311	2.88712186377091E-14
Atp6v1g1	9.44350247136255E-19	0.311739476909132	0.828	0.701	2.93249082243221E-14
Grap	9.77795686660405E-19	-0.464006627353637	0.281	0.398	3.03634894578655E-14
Atp5b	1.10492476068254E-18	0.33749467525466	0.726	0.572	3.43112285934748E-14

(*Continued*)

Table 2. (Continued)

	p_val	avg_log2FC	pct.1	pct.2	p_val_adj
Tkt	1.14127583794376E-18	0.297288021736379	0.518	0.344	3.54400385956677E-14
Cd47	1.17798198386232E-18	-0.373747055718565	0.623	0.682	3.65798745448765E-14
Wdr83os	1.20976344231692E-18	0.303102574968087	0.564	0.389	3.75667841742673E-14
Rcsd1	1.23815382135333E-18	-0.431168500218207	0.416	0.524	3.8448390614485E-14
Pnisr	1.48670064105816E-18	-0.338582899027254	0.726	0.779	4.61665150067789E-14
Ncf1	1.64229070392813E-18	-0.352372726457918	0.66	0.727	5.09980532290802E-14
Slc16a6	1.77838692411149E-18	-0.413486740549916	0.496	0.578	5.52242491544342E-14
Lat2	2.08306280396461E-18	0.350389003864938	0.549	0.383	6.46853492515129E-14
Plbd2	2.14664275958688E-18	0.285799369878017	0.468	0.302	6.66596976134514E-14
Gtf2h2	2.30374475078653E-18	-0.396965609894835	0.517	0.589	7.15381857461741E-14
Rbm39	2.33775999241838E-18	-0.261919826975625	0.929	0.926	7.25944610445679E-14
Upk1b	2.35006043009281E-18	-0.505774509767325	0.154	0.28	7.29764265356721E-14
Atp6v1b2	2.46514928877113E-18	0.285442312166701	0.378	0.23	7.655028086421E-14
Dusp7	2.70754994789811E-18	-0.424791809376384	0.359	0.466	8.407754853208E-14
Spg21	3.05252671370719E-18	0.29090779850723	0.363	0.221	9.47901120407495E-14
Pou2f2	3.24795451227099E-18	-0.316212820021629	0.821	0.863	1.00858731469551E-13
Hspa9	4.02544128885067E-18	0.259641227682286	0.352	0.209	1.2500202834268E-13
Creld2	4.5616502224761E-18	0.274122935939713	0.325	0.19	1.4165292435855E-13
Dapp1	4.92002507710908E-18	-0.425391449544058	0.333	0.443	1.52781538719468E-13
Sla	5.86274068312574E-18	-0.424364632129824	0.33	0.439	1.82055686433104E-13
Atp6ap1	6.05389879250639E-18	0.293302404392222	0.711	0.539	1.87991719203701E-13
Colgalt1	6.39124477930819E-18	0.308035376851334	0.508	0.342	1.98467324131857E-13
Scamp2	6.91689931949417E-18	-0.262392884928979	0.901	0.928	2.14790474568252E-13
Rsl1d1	7.35766121463398E-18	0.306352642651962	0.551	0.366	2.28477453698029E-13
Fkbp2	7.77905904855289E-18	0.325204521853408	0.733	0.578	2.41563120634713E-13
Wdr12	8.14270766388104E-18	0.254913645908266	0.253	0.138	2.52855501086498E-13
Ppib	8.41745387464041E-18	0.266468284640856	0.933	0.858	2.61387195169209E-13
Il6st	8.7027564716849E-18	-0.42636185457079	0.387	0.486	2.70246696715231E-13
Ndufa12	9.39030207484908E-18	0.253174833372587	0.43	0.268	2.91597050330289E-13
Phb	1.03525488065212E-17	0.254267723508659	0.304	0.174	3.21477698088901E-13
Tjp1	1.08297826060262E-17	-0.476632069318155	0.278	0.388	3.36297239264931E-13
Mgat1	1.29179754881149E-17	-0.432793495041039	0.416	0.511	4.01141892832433E-13
Cd37	1.40137257848825E-17	-0.278288085096139	0.904	0.916	4.35168226797957E-13
Ggt5	1.51270632008367E-17	-0.426077524703089	0.124	0.24	4.69740693575582E-13
Alas1	1.6623425615383E-17	0.274592162943472	0.358	0.215	5.16207235634487E-13
Il7r	1.81245134942228E-17	-0.469648368612809	0.209	0.328	5.62820517536102E-13
Abi3	1.95577304055468E-17	-0.316197954427222	0.792	0.824	6.07326202283444E-13
Sdhb	1.98657046045973E-17	0.269799655856111	0.505	0.331	6.16889725086559E-13
Cct2	2.05614424939656E-17	0.290584052373808	0.571	0.398	6.38494473765113E-13
Ddost	2.17632032943184E-17	0.316976146401421	0.753	0.59	6.7581275189847E-13
Dusp3	2.2018042889431E-17	0.257253282389059	0.284	0.162	6.83726285845502E-13
Tomm20	2.47177707857286E-17	0.351493561067022	0.696	0.552	7.6756093620923E-13
Ptpre	2.86465690103381E-17	-0.359509103708775	0.564	0.643	8.89561907478028E-13
Actr3	2.97296712302265E-17	0.321048632465373	0.752	0.593	9.23195480712224E-13
Pwwp2a	4.3929564092752E-17	-0.386760492013616	0.473	0.564	1.36414475377223E-12
Tnfaip8	4.49399400016815E-17	-0.420043677174188	0.419	0.509	1.39551995687222E-12
Eno1	5.00583791198731E-17	0.305968390382963	0.601	0.423	1.55446284680942E-12

(*Continued*)

Table 2. (Continued)

	p_val	avg_log2FC	pct.1	pct.2	p_val_adj
Prmt1	5.09174335238438E-17	0.276208284607023	0.414	0.263	1.58113906321592E-12
Gbp7	5.25700199766624E-17	-0.454576157339616	0.136	0.254	1.6324568303353E-12
Ang	5.41259363576779E-17	-0.378054544736609	0.564	0.622	1.68077270171497E-12
Ptp4a3	6.08362417358844E-17	-0.38464088088297	0.458	0.54	1.88914781462442E-12
Slamf9	6.8877059725291E-17	0.318172797931955	0.352	0.22	2.13883933564946E-12
Cox7b	6.93971162875382E-17	0.280689487662147	0.539	0.372	2.15498865207692E-12
Tnrc6b	8.26852170579065E-17	-0.394115289814842	0.432	0.519	2.56762404529917E-12
Cdkn1a	8.29339614202412E-17	0.289760707899465	0.105	0.042	2.57534830398275E-12
Tmem59	9.73302281885459E-17	-0.254573834050175	0.908	0.92	3.02239557593892E-12
Limd2	1.06040622241658E-16	-0.340310974759087	0.653	0.711	3.2928794424702E-12
Tmed3	1.06282554058161E-16	0.300893066937747	0.723	0.578	3.30039215116808E-12
Ddit4	1.18285230665959E-16	-0.489861585652333	0.215	0.34	3.67311126787003E-12
Mdh2	1.18585765217309E-16	0.261007102367462	0.446	0.288	3.68244376729309E-12
Slfn2	1.2509809273484E-16	0.268369261927096	0.284	0.166	3.88467107369499E-12
Ikzf1	1.31203969810136E-16	-0.348030404846223	0.564	0.635	4.07427687451416E-12
Gpr155	1.36916830808104E-16	-0.425079896635055	0.249	0.362	4.25167834708406E-12
Cct5	1.46571124427011E-16	0.262634154920281	0.494	0.331	4.55147312683197E-12
Gng5	1.59347456835924E-16	0.266547340884202	0.875	0.769	4.94821657712595E-12
Irf2	1.84647701387984E-16	-0.385496522741026	0.525	0.591	5.73386507120106E-12
Rbbp7	2.1900299100064E-16	0.261251212985066	0.344	0.21	6.80069987954286E-12
Nop56	2.26227028451707E-16	0.314039321004599	0.4	0.26	7.02502791451087E-12
Cfh	2.56692165599814E-16	-0.296556197481258	0.788	0.812	7.97106181837101E-12
Zfp36l1	4.45065883066545E-16	-0.397051626582696	0.577	0.65	1.38206308668654E-11
Map4k4	4.55184204184691E-16	-0.374420110721998	0.525	0.596	1.41348350925472E-11
Casp8	5.71473612734207E-16	-0.386243920167746	0.474	0.542	1.77459700962353E-11
Orai1	5.73103854736507E-16	-0.304532255045019	0.664	0.712	1.77965940011328E-11
Psmc5	6.27341260741128E-16	0.27134189169766	0.511	0.348	1.94808281697943E-11
Pdia4	6.76759851687717E-16	0.320574295099112	0.573	0.411	2.10154236744587E-11
Ogt	7.23541633333939E-16	-0.334368936474543	0.613	0.669	2.24681383399188E-11
Pip4k2a	7.42971727070723E-16	-0.391253442586827	0.434	0.513	2.30715010407271E-11
Rock2	8.27947521304489E-16	-0.388773605097724	0.471	0.547	2.57102543790683E-11
Snx18	8.80388343138845E-16	-0.343873013127123	0.614	0.668	2.73386992194905E-11
B4galt4	9.93181678801525E-16	-0.39356310119824	0.298	0.406	3.08412706718238E-11
Fgd2	1.00856634483731E-15	-0.311353869726041	0.628	0.687	3.13190107062331E-11
Whrn	1.3123436583685E-15	-0.409618387092258	0.207	0.32	4.0752207623317E-11
Pid1	1.33648074370879E-15	-0.388046487551891	0.407	0.497	4.15017365343891E-11
Sec61g	1.54658056248189E-15	0.30026104445314	0.724	0.566	4.80259662067502E-11
Klf3	1.96103615461628E-15	-0.338396161815291	0.546	0.614	6.08960557092993E-11
Fam46c	2.90453498475351E-15	0.290022214628318	0.382	0.246	9.01945248815508E-11
Morf4l2	3.36171005253021E-15	0.250687920314127	0.385	0.245	1.04391182261221E-10
9930111J2	3.41627266234598E-15	-0.378694567978912	0.519	0.581	1.0608551498383E-10
Sirt2	3.42492387105264E-15	0.251595821772263	0.465	0.307	1.06354160967798E-10
Ssr1	3.45844774266661E-15	0.293344707254471	0.635	0.481	1.07395177753026E-10
St13	3.47496970953192E-15	0.263534755232402	0.717	0.554	1.07908234390095E-10
Snrnp70	3.51852115485312E-15	-0.282435800880467	0.795	0.814	1.09260637421654E-10
Csk	3.61144217646443E-15	-0.379268699075924	0.45	0.52	1.1214611390575E-10
Zfp652	3.76640816468012E-15	-0.417103528605731	0.36	0.443	1.16958272737812E-10

(*Continued*)

Table 2. (Continued)

	p_val	avg_log2FC	pct.1	pct.2	p_val_adj
Ptms	3.84540517210156E-15	0.265344629410965	0.861	0.723	1.1941136680927E-10
Arrb2	3.92458471902766E-15	-0.329048071067822	0.572	0.628	1.21870129279966E-10
Bri3	4.36035451393967E-15	0.313088008367401	0.811	0.725	1.35402088721369E-10
Sec61b	4.73805636530629E-15	0.294593502863423	0.641	0.489	1.47130864311856E-10
Mycbp2	4.76926246483581E-15	-0.36555030851172	0.54	0.595	1.48099907320546E-10
Pnrc1	5.01864205033632E-15	-0.331902178871134	0.611	0.67	1.55843891589094E-10
Kdelr2	5.57713059386983E-15	0.298411420677201	0.553	0.396	1.7318663633144E-10
Ccni	6.87418285705523E-15	-0.35538547749027	0.48	0.544	2.13464000260136E-10
Dennd4a	7.04290606506537E-15	-0.353570907328834	0.539	0.616	2.18703362038475E-10
Stard3	7.78873700535385E-15	-0.360608336442906	0.436	0.523	2.41863650227253E-10
Fscn1	8.3098713983335E-15	-0.348168455031682	0.654	0.704	2.5804643653245E-10
Sigmar1	8.71901425163909E-15	0.256204682064242	0.349	0.217	2.70751549556149E-10
Gm26917	9.17217973786097E-15	0.353357847802252	0.31	0.194	2.84823697399797E-10
Slc11a1	9.68141793340423E-15	0.254679678964083	0.546	0.382	3.00637071086002E-10
Il16	1.00962597780429E-14	-0.398779919496901	0.281	0.377	3.13519154887567E-10
Scoc	1.08829198136043E-14	-0.270121450773693	0.871	0.888	3.37947308971855E-10
2010107E0	1.39661226384444E-14	0.266506234406527	0.563	0.404	4.33690006291615E-10
Ighm	1.44216628134759E-14	-0.347798026166093	0.552	0.632	4.47835895346868E-10
0610040J0	1.49847013934833E-14	-0.376701643247374	0.354	0.446	4.65319932371836E-10
Grk2	1.71727864009447E-14	-0.393591078538817	0.336	0.418	5.33266536108537E-10
Atp6v1d	1.77745472129953E-14	0.308335909507825	0.412	0.279	5.51953014605144E-10
Tubgcp5	2.12057341485409E-14	-0.378971940890316	0.428	0.506	6.58501662514642E-10
Olfml3	2.37307789960423E-14	-0.260508077012623	0.989	0.986	7.36911880164101E-10
Gpsm3	2.68428956663939E-14	-0.361411519079472	0.437	0.519	8.33552439128531E-10
Elovl1	3.13314908989516E-14	0.300216385321233	0.501	0.345	9.72936786885143E-10
Tmem206	3.20897139888298E-14	0.329988439763472	0.374	0.246	9.96481888495131E-10
Maml3	3.38781952630243E-14	-0.410146105599206	0.215	0.317	1.05201959750269E-09
Srsf2	3.68608948629561E-14	0.362475194084846	0.772	0.684	1.14464136817937E-09
Tra2a	4.14488149802628E-14	-0.319424393723889	0.632	0.675	1.2871100515821E-09
Tomm40	4.18849464803916E-14	0.253398728298092	0.395	0.258	1.3006532430556E-09
Sesn1	5.02027647396987E-14	-0.406158865338817	0.243	0.337	1.55894645346186E-09
Mycl	5.44136164760015E-14	-0.30138139032991	0.048	0.137	1.68970603242928E-09
Rps17	5.5525317128653E-14	0.255205254558279	0.839	0.71	1.72422767279606E-09
Slc23a2	5.57977543566448E-14	0.267830203122948	0.269	0.161	1.73268766603689E-09
Rnf167	6.52070948388705E-14	-0.361955540184498	0.283	0.38	2.02487591603144E-09
Naglu	6.82941436458614E-14	0.26297945763687	0.457	0.315	2.12073804263493E-09
Ndufa4	7.43317359933091E-14	0.267063341070183	0.757	0.619	2.30822339780023E-09
Atp6v0d1	8.1015251662391E-14	0.256841723680055	0.501	0.342	2.51576660987223E-09
March1	8.27581105347156E-14	-0.365552406584209	0.391	0.479	2.56988760643452E-09
Cox5b	8.46558491892441E-14	0.277483137143121	0.611	0.447	2.6288180848736E-09
Cox5a	8.78197043571543E-14	0.255778217383667	0.586	0.43	2.72706527940271E-09
Rpl31	9.12716164053496E-14	0.265747847984656	0.747	0.595	2.83425750423532E-09
Fry	9.1984410020598E-14	-0.399064182929683	0.149	0.251	2.85639188436963E-09
Arl8a	9.30636242290384E-14	0.25150680734014	0.409	0.27	2.88990472318433E-09
Arid1a	9.53790640384842E-14	-0.354670538769954	0.476	0.543	2.96180607558705E-09
Nos1ap	1.03070669666513E-13	-0.362519811848667	0.115	0.214	3.20065350515423E-09
Hnrnpf	1.13836137974372E-13	0.260906886875476	0.843	0.746	3.53495359251818E-09

(*Continued*)

Table 2. (Continued)

	p_val	avg_log2FC	pct.1	pct.2	p_val_adj
Nfia	1.17748017852189E-13	-0.408056369440299	0.326	0.418	3.65642919836403E-09
Phf14	1.21898825112006E-13	-0.315583931610452	0.532	0.597	3.78532421620312E-09
Vmp1	1.21944254666567E-13	0.280717104537476	0.504	0.358	3.78673494016091E-09
Atxn10	1.24829647065569E-13	0.258684811015794	0.458	0.314	3.87633503032712E-09
Lrpap1	1.25749456382314E-13	0.257589361516729	0.582	0.426	3.90489786903998E-09
Crlf3	1.29849080390834E-13	-0.315694208421083	0.613	0.646	4.03220349337657E-09
Thrsp	1.31436544055218E-13	-0.361849996680576	0.264	0.369	4.08149900254669E-09
Mfng	1.8871840372422E-13	-0.375818280980217	0.309	0.399	5.86027259084819E-09
Dock8	2.00564292462928E-13	-0.386343276761699	0.38	0.449	6.22812297385132E-09
Arhgef40	2.08235610692363E-13	-0.385700119646028	0.303	0.388	6.46634041882996E-09
Ankrd12	2.21658259126232E-13	0.395924993993436	0.474	0.347	6.88315392064687E-09
Cep68	3.58505905729271E-13	-0.358244815516592	0.144	0.244	1.11326838906111E-08
Rcan1	3.79462504112328E-13	0.31594502120239	0.284	0.176	1.17834491402001E-08
Psmb6	5.04650659733684E-13	0.259279992102095	0.599	0.45	1.56709169367101E-08
Chst7	5.11801440964736E-13	-0.363209906220227	0.276	0.371	1.5892970146278E-08
Frmd4b	5.29142728141766E-13	-0.278060792014388	0.694	0.712	1.64314691369863E-08
Soga1	5.40450090652629E-13	-0.353874503760134	0.254	0.351	1.67825966650361E-08
Dpysl2	5.78068558930173E-13	-0.356324351006645	0.423	0.493	1.79507629604587E-08
Mertk	6.35957529969865E-13	-0.273873208453055	0.804	0.813	1.97483891781542E-08
Armc3	6.46876835584872E-13	-0.330035880316145	0.074	0.161	2.0087466375417E-08
Psmd7	6.88748250932346E-13	0.255606129628242	0.585	0.423	2.13876994362021E-08
Mgat4a	7.33268642955137E-13	-0.331794596018824	0.463	0.531	2.27701911696859E-08
Akirin2	7.43793709357552E-13	-0.317072005917028	0.535	0.591	2.30970260566801E-08
mt-Atp8	8.87174971959925E-13	0.252874091257314	0.338	0.222	2.75494444042715E-08
Sult1a1	9.43543911598618E-13	-0.3832758948998	0.248	0.343	2.92998690868719E-08
Snx24	1.02220021930258E-12	0.259419801881412	0.352	0.233	3.1742383410003E-08
Uqcr11	1.12702879465377E-12	0.254647488403128	0.654	0.496	3.49976251603834E-08
1700017B0	1.2071249021999E-12	-0.292974047958738	0.579	0.627	3.74848495880134E-08
Btg1	1.32061728999243E-12	-0.282260309018144	0.76	0.786	4.10091287061351E-08
Soat1	1.3485726701717E-12	0.276635833403159	0.374	0.25	4.18772271268418E-08
Adora3	1.71806282743118E-12	-0.357770048652599	0.347	0.425	5.33510049802206E-08
Anp32b	1.8115591645384E-12	0.28238330071732	0.389	0.267	5.62543467364109E-08
Siglece	2.32433062938259E-12	-0.371961023988845	0.187	0.281	7.21774390342177E-08
Gm32036	2.61605955363153E-12	-0.330051478209053	0.122	0.213	8.12364973189198E-08
Fcrl1	2.93706032511877E-12	-0.312221475664913	0.087	0.175	9.12045342759132E-08
Sft2d2	3.03657087822497E-12	-0.386455262085356	0.227	0.314	9.42946354815201E-08
Snx3	3.29244022761008E-12	0.250095106444104	0.572	0.429	1.02240146387976E-07
Mfap3	3.3969359238781E-12	-0.362783174606334	0.378	0.441	1.05485051244187E-07
Hfe	3.5368718118132E-12	-0.336339887554912	0.4	0.474	1.09830480372235E-07
Evi2a	4.23508467591846E-12	0.284046077537508	0.849	0.756	1.31512084441296E-07
Fam91a1	4.2917903016291E-12	-0.362783322793053	0.26	0.344	1.33272964236489E-07
Myo1b	4.8114936476746E-12	-0.349878576759932	0.132	0.224	1.49411312241239E-07
Rapgef6	5.65288965439106E-12	-0.368775099753797	0.302	0.384	1.75539182437805E-07
BC017643	5.84631313762014E-12	-0.328821511762247	0.409	0.478	1.81545561862518E-07
Ubash3b	5.99421038024171E-12	-0.326270499807639	0.496	0.545	1.86138214937646E-07
Pik3r1	6.33350479393534E-12	-0.308800828559661	0.578	0.614	1.96674324366074E-07
Tmem44	6.5195586825707E-12	-0.326300562511423	0.076	0.158	2.02451855769868E-07

(*Continued*)

Table 2. (Continued)

	p_val	avg_log2FC	pct.1	pct.2	p_val_adj
Tmem100	6.66674616907444E-12	-0.340335796741541	0.331	0.424	2.07022468788269E-07
Pold4	7.42188548763467E-12	-0.323339410081192	0.407	0.477	2.30471810047519E-07
Klhdc8b	7.74592357565568E-12	-0.370925438228524	0.228	0.316	2.40534164794836E-07
Cryl1	1.06624846978481E-11	-0.354023711590468	0.295	0.373	3.31102137322278E-07
Zbtb20	1.14264813480778E-11	-0.425925194116129	0.338	0.423	3.54826525301861E-07
Rtn4rl1	1.15908859032059E-11	-0.313795702018367	0.458	0.523	3.59931779952254E-07
Ckap4	1.16014306543555E-11	0.270591369637953	0.326	0.215	3.60259226109702E-07
Irf2bp2	1.23672785296879E-11	-0.30365330557541	0.499	0.558	3.840411001824E-07
Plcl2	1.32653526615747E-11	-0.358652414706463	0.315	0.391	4.11928996199878E-07
Etv1	2.50252176614799E-11	-0.307576895201074	0.091	0.175	7.77108084041935E-07
Fermt3	2.68431837138697E-11	-0.291950529313464	0.591	0.618	8.33561383866796E-07
Lag3	3.38996223187597E-11	0.255518545051852	0.749	0.619	1.05268497186444E-06
Agmo	3.65982105274457E-11	-0.326326386160307	0.191	0.278	1.13648423150877E-06
Tuba1a	3.66470061363511E-11	-0.313085156619056	0.482	0.538	1.13799948155211E-06
Kmt2e	3.8398873523139E-11	-0.347292190578359	0.458	0.507	1.19240021951404E-06
Ppp1r18	3.840214953127E-11	-0.300392745715527	0.51	0.557	1.19250194939453E-06
Filip1l	4.24320362984864E-11	-0.35325481569522	0.198	0.288	1.3176420231769E-06
Adap2os	4.32867317369491E-11	-0.30225746268662	0.47	0.538	1.34418288062748E-06
Arhgap31	4.35743708673276E-11	-0.343321492673757	0.433	0.49	1.35311493854312E-06
Plxna4	4.83864633828803E-11	-0.341720946807565	0.145	0.233	1.50254484742858E-06
Rhoh	6.28701975795654E-11	-0.269646045304644	0.687	0.72	1.95230824543824E-06
Arhgap27	6.49351636229224E-11	-0.339360939968431	0.184	0.266	2.01643163598261E-06
Prkab1	6.80240112541581E-11	-0.332032795223066	0.233	0.313	2.11234962147537E-06
Kif21b	6.83783527535236E-11	-0.329249464737552	0.295	0.378	2.12335298805517E-06
Cd86	7.19896970323852E-11	0.257365440764221	0.767	0.647	2.23549606194666E-06
Zfp467	8.25737288369693E-11	-0.338324996994412	0.166	0.249	2.56416200157441E-06
Tlr3	1.03403632108671E-10	-0.344453307996895	0.199	0.283	3.21099298787057E-06
Gm26740	1.07053986318923E-10	-0.357099866645611	0.132	0.22	3.32434743716153E-06
Capn3	1.20445186466862E-10	-0.339335918525183	0.204	0.286	3.74018437535547E-06
Gm31243	1.29906956046967E-10	-0.309440708917158	0.113	0.194	4.03400070612645E-06
Ctsf	1.49161496733332E-10	-0.274051039753143	0.598	0.635	4.63191195806014E-06
Abhd6	1.49599371263832E-10	-0.304553701403873	0.407	0.467	4.64550927585578E-06
Ccdc50	1.49625739943834E-10	-0.33601221438744	0.382	0.443	4.64632810247587E-06
Cmtm8	1.57069891881241E-10	-0.329801400710897	0.132	0.213	4.87749135258819E-06
Camk2d	1.67572780664287E-10	-0.295375334217713	0.566	0.605	5.2036375579681E-06
Plxnb2	1.76677322086986E-10	-0.271180330234748	0.547	0.582	5.48636088276717E-06
Tlr2	2.0070829394644E-10	0.365148627193511	0.366	0.258	6.23259465191881E-06
Sik2	2.55658357362055E-10	-0.320084583993081	0.168	0.251	7.93895897116391E-06
Rnase6	2.57097995515787E-10	-0.275402371844687	0.051	0.121	7.98366405475173E-06
Tab2	2.76787220785046E-10	-0.322977711989916	0.357	0.425	8.59507356703805E-06
Serpinf1	2.9252313403133E-10	-0.328831849826937	0.271	0.351	9.08372088107489E-06
St3gal5	2.95376030277258E-10	-0.291506150397422	0.593	0.623	9.1723118681997E-06
Pnn	2.97221239750054E-10	-0.28965587780706	0.613	0.626	9.22961115795842E-06
Garnl3	3.05774102324112E-10	-0.314695046891293	0.164	0.246	9.49520319947067E-06
Wdfy2	3.53155042047174E-10	-0.317315160849578	0.132	0.212	1.09665235206909E-05
G3bp2	4.07566377273629E-10	-0.324232407352645	0.413	0.473	1.2656158713478E-05
Stab1	5.00075085126394E-10	-0.269190258596502	0.596	0.62	1.55288316184299E-05

(*Continued*)

Table 2. (Continued)

	p_val	avg_log2FC	pct.1	pct.2	p_val_adj
1810011H1	5.4741893572433E-10	-0.345300704795401	0.267	0.336	1.69990002110476E-05
Rgs19	6.54843424080239E-10	-0.298723080466954	0.356	0.426	2.03348528479637E-05
Rassf2	6.66620186518655E-10	-0.307689557620538	0.449	0.489	2.07005566519638E-05
Ralgps1	6.88570059642538E-10	-0.319846054456458	0.132	0.208	2.13821660620797E-05
Sall3	7.2100684301764E-10	-0.332077730039377	0.285	0.362	2.23894254962268E-05
Rab3il1	8.25441703034906E-10	-0.255321356899655	0.683	0.703	2.56324412043429E-05
Sema4b	8.77724462414094E-10	-0.306150580593703	0.129	0.207	2.72559777313449E-05
mt-Nd5	8.92775887643216E-10	0.25421372022666	0.668	0.547	2.77233696389848E-05
Gm6277	9.27738412679472E-10	-0.317879039385527	0.233	0.316	2.88090609289356E-05
Pik3cg	9.36388254754199E-10	-0.301240301246207	0.313	0.393	2.90776644748821E-05
Yipf4	9.5970918577271E-10	-0.301900284198654	0.453	0.486	2.98018493458E-05
Mat2a	1.12238953929417E-09	0.297990199837501	0.647	0.534	3.48535623637018E-05
Nrm	1.2003915130591E-09	-0.332245759858035	0.165	0.24	3.72757576550241E-05
Akap13	1.28140817253234E-09	-0.282248131869738	0.627	0.64	3.97915679816468E-05
Ggta1	1.3740174683028E-09	-0.312541637867199	0.159	0.237	4.26673644432067E-05
Eif5	1.50053864322529E-09	0.254011790557805	0.642	0.532	4.65962264880749E-05
Arid4a	1.578265936477E-09	-0.345925775127187	0.27	0.343	4.90098921254204E-05
Tcf7l2	1.58995724011868E-09	-0.349097782965097	0.247	0.316	4.93729421774054E-05
Ier5	1.70322316536736E-09	-0.275338381393287	0.662	0.712	5.28901889541527E-05
Fez2	1.76595936974633E-09	-0.273407185222967	0.509	0.556	5.48383363087329E-05
Hist1h1c	1.95942692953849E-09	-0.372566077479789	0.184	0.263	6.08460844429587E-05
Jmjd1c	2.5547115678097E-09	-0.274847023103296	0.565	0.594	7.93314583151946E-05
3222401L1	2.67947939304363E-09	-0.321430285930938	0.302	0.369	8.3205873592184E-05
Lst1	2.70642616983557E-09	-0.321026851479065	0.456	0.512	8.4042651851904E-05
Snta1	3.04046972609653E-09	-0.30668878769722	0.311	0.373	9.44157064044754E-05
Gp9	3.14779804987945E-09	-0.329360237354145	0.202	0.275	9.77485728429065E-05
Dok3	3.56706647679233E-09	-0.327151945694815	0.142	0.213	0.000110768115303832
Dusp6	3.85249902300743E-09	-0.263184647659365	0.606	0.651	0.00011963165216145
Rtn1	4.07994756406942E-09	-0.283531289630688	0.278	0.354	0.000126694611707048
Thap3	4.17306608039058E-09	-0.305824209631277	0.246	0.312	0.000129586220994369
Slc25a37	4.26781637603559E-09	-0.314852295544989	0.171	0.244	0.000132528501925033
Ulk2	4.29804749750075E-09	-0.305790960168544	0.303	0.37	0.000133467268939891
Rbm5	4.99409704957006E-09	-0.288818911346762	0.547	0.577	0.000155081695680299
Lifr	5.69080121467615E-09	-0.326907778629069	0.153	0.225	0.000176716450119338
Gpr84	5.69361806580752E-09	0.305274892722692	0.464	0.355	0.000176803921797521
Trim12a	5.98290448136089E-09	-0.30733731278951	0.264	0.335	0.0001857871328597
Kat6a	8.69973674686093E-09	-0.324517732144981	0.237	0.309	0.000270152925200273
Cdk5r1	8.98624730331975E-09	-0.316809051500348	0.214	0.287	0.000279049937509988
Jun	9.72891974385823E-09	-0.502742942226946	0.465	0.527	0.00030211214480603
Slc29a3	1.14777218628046E-08	-0.2547779958623	0.64	0.659	0.000356417697005672
Clasp2	1.31805649323952E-08	-0.301406456275779	0.276	0.34	0.00040929608284567
Hmox2	1.36708217816625E-08	-0.275015978552862	0.448	0.488	0.000424520028785966
Wdr44	1.37284708056473E-08	-0.32166310016436	0.175	0.246	0.000426310203927765
Prkcd	1.72084609914569E-08	-0.262432396844864	0.56	0.572	0.00053437433916771
Ninj1	1.73510354497654E-08	0.330546243819882	0.513	0.403	0.000538801703821566
Helz	1.76319713827638E-08	-0.334449057181911	0.246	0.309	0.000547525607348963
Vgll4	1.85711993447595E-08	-0.292733044204024	0.413	0.454	0.000576691453252817

(*Continued*)

Table 2. (Continued)

	p_val	avg_log2FC	pct.1	pct.2	p_val_adj
Cmklr1	1.93408850339667E-08	-0.294728037402751	0.263	0.336	0.000600592502959769
Slc25a45	1.93438409323988E-08	-0.290863520218869	0.295	0.356	0.000600684292473782
4933406I18	2.18394371348499E-08	-0.275261516049534	0.118	0.188	0.000678180041348493
Asb2	2.18671373638281E-08	-0.299346157089326	0.23	0.305	0.000679040216558955
Trio	2.22753220855024E-08	-0.323941419928939	0.221	0.286	0.000691715576721107
Mapk14	2.49750065185523E-08	-0.296487919667262	0.225	0.292	0.000775548877420605
Irf2bpl	2.56931716590577E-08	-0.305391879595496	0.336	0.397	0.000797850059528718
Fcgr2b	2.91806527644632E-08	-0.292263177657661	0.504	0.524	0.000906146810294875
Nfe2l2	3.08390951647958E-08	0.255846904988063	0.701	0.592	0.000957646422152404
Gm32849	3.17602353262688E-08	-0.258035440493209	0.109	0.177	0.000986250587586626
Cdk19	3.8481379302782E-08	-0.289019152418222	0.135	0.201	0.00119496227148929
Kdm2b	4.03006532429599E-08	-0.290002965755192	0.269	0.337	0.00125145618515363
Csad	4.49526931525609E-08	-0.310745062991901	0.323	0.383	0.00139591598046648
Ppcdc	5.81807564676372E-08	-0.265522257315796	0.563	0.584	0.00180668703058954
Zfp691	6.05144940667064E-08	-0.287794053694264	0.222	0.293	0.00187915658425343
Pdk1	6.6108972700 47E-08	-0.301507254693624	0.28	0.337	0.00205288192926769
Abl1	6.6157359156016E-08	-0.281200641230685	0.232	0.297	0.00205438447387176
Arhgap12	6.91442150002903E-08	-0.299920602583469	0.268	0.328	0.00214713530840402
Inpp4b	6.99898231231546E-08	-0.293236091592834	0.212	0.281	0.00217339397744332
Ets1	8.12291339213466E-08	-0.258129291601876	0.265	0.331	0.00252240829565958
Dbnl	8.15076638964446E-08	-0.306365293418463	0.365	0.411	0.00253105748697629
Ddx6	8.63287689751023E-08	-0.286138422873663	0.382	0.43	0.00268076726298385
Fcho2	8.99912031948466E-08	-0.268905607061916	0.422	0.466	0.00279449683280957
Cd2ap	1.16686048984007E-07	-0.27126250567033	0.412	0.454	0.00362345187910038
Gmfg	1.17298689892795E-07	-0.281594406648446	0.327	0.381	0.00364247621724097
Gabarapl2	1.23776220455145E-07	-0.284462602750837	0.509	0.524	0.00384362297379361
Etv5	1.27843959723451E-07	-0.295418034097322	0.213	0.273	0.00396993848129234
Lcp2	1.31690040928617E-07	-0.2723629018795	0.318	0.376	0.00408937084095635
Crebrf	1.34588425133811E-07	-0.276517819739463	0.172	0.24	0.00417937436568022
Tbc1d9	1.38145060290491E-07	-0.266388430315232	0.157	0.221	0.00428981855720062
I830077J02	1.4637366069222E-07	-0.30208590489188	0.228	0.291	0.00454534128547552
Sh2b3	1.49622296908862E-07	-0.280971926905668	0.306	0.36	0.00464622118591089
Lpin2	1.55521845162501E-07	-0.291460760232745	0.336	0.385	0.00482941985783114
Cirbp	1.55771296935472E-07	-0.283304293742543	0.414	0.446	0.0048371660837372
Cbl	1.61780389166837E-07	-0.264558963084066	0.394	0.44	0.00502376642479778
Gm37494	1.63058760011155E-07	-0.287468795740807	0.204	0.27	0.00506346367462639
Gimap1	1.69961687886768E-07	-0.272064366048699	0.136	0.2	0.00527782029394781
Gng2	1.96746260200635E-07	-0.29522924849199	0.316	0.365	0.0061095616180103
Nipa2	1.97417047674926E-07	-0.282142299807652	0.405	0.449	0.00613039158144947
Nr3c1	2.00158840065216E-07	-0.256541721340712	0.435	0.485	0.00621553246054517
Xist	2.17007356334849E-07	-0.359478333487127	0.509	0.557	0.00673872943626608
Arl10	2.17556299101516E-07	-0.263628757101459	0.391	0.433	0.00675577575599939
Cd79b	2.23938168374618E-07	-0.290858792235169	0.161	0.224	0.00695395194253703
Zcchc11	2.2625448077169E-07	-0.298796094943654	0.257	0.318	0.00702588039140329
Hps3	2.34715786241391E-07	-0.304186513367248	0.392	0.424	0.00728862931015391
Fbxl20	2.37536294859142E-07	-0.265026077491498	0.133	0.196	0.00737621456426093
Tmem63a	2.77714222325414E-07	-0.268973762116124	0.333	0.385	0.00862385974587108

(*Continued*)

Table 2. (Continued)

	p_val	avg_log2FC	pct.1	pct.2	p_val_adj
Prex1	2.83525925765431E-07	-0.260451960982122	0.513	0.53	0.00880433057279394
Eva1b	2.87920381952709E-07	-0.254077167852617	0.167	0.232	0.00894079162077747
Fbrsl1	2.97270291232568E-07	-0.274304507436561	0.302	0.355	0.00923113435364493
Acads	3.09890074406194E-07	-0.257886565657563	0.407	0.448	0.00962301648053553
Sort1	3.47223923378202E-07	-0.289851456974882	0.287	0.336	0.0107823444926633
Lrrc3	3.57488321265882E-07	-0.280278370734734	0.302	0.358	0.0111010848402694
Tbc1d23	3.63201324115574E-07	-0.280473449415491	0.271	0.331	0.0112784907177609
Per3	3.75119928883498E-07	-0.251639323204655	0.096	0.156	0.0116485991516193
Cdkn1b	4.24874230795943E-07	-0.252477946346461	0.138	0.2	0.0131936194889064
AI467606	4.6053456777113E-07	-0.259271591383804	0.137	0.199	0.0143009799329969
Ppm1l	5.01054988908223E-07	-0.25323177671416	0.095	0.152	0.015559260570567
Gmip	5.36304216907414E-07	-0.267194910392705	0.289	0.344	0.0166538548476259
Pan3	5.48806520867436E-07	-0.275472289304947	0.336	0.382	0.0170420888924965
Ep300	6.06397927648205E-07	-0.282757640694748	0.333	0.38	0.0188304748472597
Trim26	6.37527759210646E-07	-0.269228386584243	0.299	0.349	0.0197971495067682
Mkrn1	7.33767432973374E-07	-0.261907936073313	0.327	0.377	0.0227856800961222
Borcs6	8.49438171344948E-07	-0.282131008977835	0.204	0.258	0.0263776035347747
Mkln1	8.91067448766098E-07	-0.25150557483357	0.491	0.512	0.0276703174865336
Ralgps2	9.81312479117344E-07	-0.28420563063336	0.191	0.247	0.0304726964140309
Camk2n1	9.81381163537971E-07	-0.271861652410143	0.425	0.467	0.0304748292713446
Arap3	9.92555302065236E-07	-0.268218229797015	0.188	0.246	0.0308218197950318
Gm13889	1.01792145397341E-06	0.38643275581675	0.111	0.068	0.0316095149102364
Hps4	1.08518438324778E-06	-0.257917137610395	0.467	0.478	0.0336982306529932
Usf1	1.09585610937582E-06	-0.279859027515085	0.26	0.309	0.0340296197644473
Spred1	1.11749334199504E-06	-0.278377273266421	0.249	0.303	0.0347015207489719
Abcb4	1.23266801682812E-06	-0.266543229285136	0.137	0.195	0.0382780399265637
Iffo1	1.4803462029996E-06	-0.257780126263516	0.351	0.399	0.0459691906417465
Mgll	1.53873254098203E-06	-0.274564544984353	0.387	0.421	0.0477822615951149
Chsy1	1.55153963505454E-06	-0.264049531225795	0.153	0.21	0.0481799602873486

https://doi.org/10.1371/journal.pone.0296280.t002

subventricular zone, these cells exhibit altered immunoreactivity to some common markers such as Tmem119 and Iba1 [18]. These cells, do however, express Cd68+ puncta, which are generally found only in low levels by microglia that are ramified or surveilling. It has been long known that microglia show spatial patterning in morphology and density across the brain [44]. These morphological differences often correlate with differential phagocytic activity, proliferative potential, and immunoreactivity as different regions of the brain have different needs.

In this study, we characterize the transcriptomic profile of these cells relative to other myeloid cells in the hippocampus at the level of single cell resolution. We identify a greater number of differentially expressed genes by DAM-like microglia, and separate confounding results from CNS-associated macrophages. This approach allows us to computationally separate different subsets of myeloid cells with great precision.

We first noted downregulation of several microglia-specific marker genes in the healthy, adult subgranular zone; strikingly similar to cases of disease and injury [67, 68]. Due to the lower levels of expression of these marker genes, these cells may not be captured by conventional flow cytometry panels, requiring judicious use of marker genes depending on spatial, temporal, and associated disease context. We classify myeloid cells in the SGZ as microglia as

they still retain expression, albeit to a lesser degree, of some microglia-specific genes while maintaining robust expression of other marker genes such as *Hexb* and *Olfm3*. This further corroborates findings which suggest not all microglia-specific markers retain consistent expression and comprehensively label microglia in the brain [67].

Next, we compared genes upregulated in the SGZ to known microglial phenotypes. Studies have reported that microglia described as alternatively activated M2 microglia in the macrophage polarization scheme promote neurogenesis [69–71]. Microglia in the dentate gyrus have also been reported to express a handful of genes in M2 microglia. Our results indicate that this profile does not accurately capture the SGZ transcriptome. Instead, we observe great overlap of genes enriched in our putative SGZ cluster with those upregulated in disease-associated microglia (DAM), which are involved in plaque clearance [8, 72]. This DAM signature is translationally relevant and potentially highly conserved, as it has been observed in postmortem human tissue from patients with AD and MS [9, 10].

Many of these DAM genes are also found in previously described transcriptome profiles or cell states such as proliferation-associated macrophages (PAM) found in developing white matter and early postnatal microglia [8, 15]. These are primarily genes which are associated with lysosomal function. In PAM these genes reflect phagocytosis of oligodendrocyte progenitors, important in myelination, and are no longer present in the mature, adult brain. The presence of these genes in the adult hippocampus may result from engulfment of excess neural progenitors that are undergoing apoptosis [19, 73]. This points to a broader role of DAM genes extending beyond disease, particularly since phagocytic microglia have been shown to support neuronal development in the adult hippocampus [19].

During early postnatal development, developing neurons are pruned through a CD11B-DAP12-dependent mechanism [74]. Interestingly, cluster 8 also shows upregulation of *Dap12* (also known as *Tyrobp*), which is activated downstream of the DAM-specific receptor TREM2. Our data suggest that processes similar to those found in embryonic development of the nervous system as well as in PAMs during postnatal development persist throughout adulthood in the hippocampus. This population specifically may be targeted in diseases in which neurogenesis is perturbed or needs to be altered [21, 27]. Notably, gene networks associated with phagocytic microglia are involved in neurogenic function *in vivo* within the neurogenic niche [19].

We also ruled out whether transcriptomic differences in SGZ microglia could explain how sex-specific differences may contribute to altered risk for neurodevelopment diseases, particularly those affecting hippocampal function and neurogenesis [75–78]. In the healthy adult murine hippocampus, there appear to be no sex-related differences in the transcription of immune -related genes Additionally, no significant differences in genes related to immune function are found specifically in SGZ microglia from male and female mice. Thus, differences in immune function that occur may come into play later in life or are due to post-transcriptional regulation or at the level of protein interactions.

Adult hippocampal neurogenesis is sensitive to various external or environmental factors. As such, the immune cells in this niche are tuned to varying inputs and may be responsible for relaying the state of the outside world to progenitors. Important questions that remain to be answered are whether this specialized microglial phenotype is indicative of a distinct ontogeny, or whether it arises as a response to the environmental cues provided by the niche. Furthermore, whether this signature describes an activated population or a reactive state is not known and of great interest [79]. This is important to uncover because it can elucidate if alterations in adult neurogenesis in pathological contexts result from differential properties of immune cells in the SGZ. Given that these cells express many genes found in the DAM gene signature, the role of these genes specifically in the context of adult neurogenesis need to be examined.

While some genes expressed by microglia have been characterized in various developmental stages and disease models, many of the genes enriched by subgranular zone microglia have unknown functions. Our findings point to a need to separate the SGZ population and examine it separately in disease models. Extracting SGZ-specific differences is a necessary component of understanding hippocampal physiology, particularly from an immune perspective.

Further understanding the mechanisms behind how this population progresses and the trajectory it takes will be fundamentally important, particularly in the context of aging and disease [77, 80] While we highlight one specific subset of cells in this paper, the potential contributions of other populations cannot be excluded from regulation of the neurogenic niche or in disease development and progression. Our data provide a reference point for comparing immune alterations in the hippocampus and its neurogenic niche in the context of disease or other pathology.

Supporting information

S1 Fig. A. Generation of double reporter mouse line. Schematic displaying breeding schemes and selection of breeders to generate mice expressing eGFP in Nestin^{+} neural progenitor cells and tdTomato in cells from fractalkine (Cx3Cr1) expressing cells and their daughter cells. B. Percentage of cells showing dual expression of Tmem119 and tdTomato, Tmem119 only, TdTomato only, or neither. Results are shown for samples derived from transgenic mouse or wildtype mouse (C57/6Bl). "Count" column contains number of cells per sample recorded. C. Percentage of TdTomato+ cells with CD11B and CD45 expression. Unstained samples (WT unstained, TdTomato unstained) are negative controls for antibody staining. D. Isotype control stainings to show nonspecific background binding for FITC and APC conjugated antibodies.
(PDF)

S2 Fig. Quality control (QC) metrics pre-processing. (A) Violin Plots displaying transcript reads, number of unique genes, percentage of reads corresponding to mitochondrial genes, and percentage of reads corresponding to ribosomal genes in each sequencing sample. Dashed line corresponds to lower limit for filtering cells, solid lines represent maximum values for filtering. (B) UMAP plot displaying cell cycle scoring for cells in dataset. (C) UMAP plot displaying predicted doublets based on DoubletFinder. Predicted doublets are highlighted in magenta.
(PDF)

S3 Fig. A. Breakdown of subpopulation frequencies within clusters. B. QC violin plots showing number unique genes (nFeature_RNA) and number of reads (nCount_RNA) in each cluster. C. Elbow plot showing variance represented by principal components. D. Dot Plot of myeloid lineage marker genes.
(PDF)

S4 Fig. Heat Map displaying scaled expression levels of top five or fewer differentially expressed genes based on set thresholds (P_{adj} <0.001 and expressed in at least 70% of cells in cluster). Thirty cells were sampled for each cluster. Each vertical line represents scaled z-score value of gene expression across row.
(PDF)

S5 Fig. Sex-specific differences in hippocampal myeloid cells. (A) Feature plot displaying scaled expression of *Xist* projected onto UMAP. (B) Distribution of cells *Xist*$^{+}$ female cells versus *Xist*—male cells across clusters. (C) Violin Plots displaying genes differentially expressed

between bulk female (F) and Male (M) cells. (D) Violin plots displaying genes differentially expressed between female and male cells in SGZ cluster 8.
(PDF)

S6 Fig. Distribution of differentially expressed genes in cluster 8 in the dentate gyrus. *In situ hybridization* images from the Allen Institute of genes enriched in cluster 8 (top three) and marker genes (*Hexb*) or genes associated with homeostatic microgglia (*Selplg*, *P2ry12*). For enriched genes, hemicortices (left) are shown to display level of specificity of these genes in the SGZ with more zoomed in fields of view alongside them (right).
(PDF)

S7 Fig. Cd9 immunoreactivity in dual reporter mice in individual channels (top) show expression of Cd9, tdTomato+ myeloid cells and eGFP+ neural progenitor cells. Merge images (middle) show colocalization of Cd9 in both tdTomato and GFP positive cells (left middle). Diffuse immunoreactivity in cortex (bottom) Scale = 10 μm.
(PDF)

S8 Fig. A. DAM marker gene expression levels in clusters 8, 12, and 13 of hippocampal myeloid cells. B. Correlation matrix showing split of Cross-dataset comparisons between cluster 8 microglia and reactive microglia. Plot showing relation between clusters 8,12,13 from this study and integrated dataset from Keren-Shaul et. al. 2017. Scale represents fraction of original cluster (from hippocampal myeloid dataset) represented in each integrated cluster from Fig 5E. C. Overlap of upregulated cluster 8, DAM, and early postnatal microglia (Hammond et. al. Cluster 3). D. Feature plots showing localization of *Ccl3*, *Igf1*, *and Lgals3* as examples of genes enriched in reactive microglia from the intersection of genes featured in the venn diagram (part C of this figure).
(PDF)

S1 Table. Quality control (QC) metrics pre and post- processing. Table displaying cells, mean transcript reads, mean number of unique genes, and the mean percentage of reads corresponding to mitochondrial genes in each sequencing sample.
(DOCX)

S2 Table. Gene ontology analysis of genes enriched in SGZ vs homeostatic clusters.
(DOCX)

Author Contributions

Conceptualization: Elizabeth M. Bradshaw, Vilas Menon, Steven G. Kernie.

Data curation: Sana Chintamen, Pallavi Gaur, Vilas Menon.

Formal analysis: Sana Chintamen, Pallavi Gaur, Vilas Menon.

Funding acquisition: Steven G. Kernie.

Investigation: Sana Chintamen.

Methodology: Nicole Vo, Steven G. Kernie.

Supervision: Elizabeth M. Bradshaw, Vilas Menon, Steven G. Kernie.

Writing – original draft: Sana Chintamen.

Writing – review & editing: Sana Chintamen, Pallavi Gaur, Steven G. Kernie.

References

1. Moser EI, Moser MB, McNaughton BL. Spatial representation in the hippocampal formation: a history. Nat Neurosci. 2017; 20(11):1448–64. Epub 2017/10/27. https://doi.org/10.1038/nn.4653 PMID: 29073644.
2. Eichenbaum H, Cohen NJ. Can we reconcile the declarative memory and spatial navigation views on hippocampal function? Neuron. 2014; 83(4):764–70. Epub 2014/08/22. https://doi.org/10.1016/j.neuron.2014.07.032 PMID: 25144874.
3. Burgess N, Maguire EA, O'Keefe J. The human hippocampus and spatial and episodic memory. Neuron. 2002; 35(4):625–41. Epub 2002/08/27. https://doi.org/10.1016/s0896-6273(02)00830-9 PMID: 12194864.
4. Efthymiou AG, Goate AM. Late onset Alzheimer's disease genetics implicates microglial pathways in disease risk. Mol Neurodegener. 2017; 12(1):43. Epub 2017/05/28. https://doi.org/10.1186/s13024-017-0184-x PMID: 28549481.
5. Pluvinage JV, Wyss-Coray T. Systemic factors as mediators of brain homeostasis, ageing and neurodegeneration. Nat Rev Neurosci. 2020; 21(2):93–102. Epub 2020/01/09. https://doi.org/10.1038/s41583-019-0255-9 PMID: 31913356.
6. Wyss-Coray T, Mucke L. Ibuprofen, inflammation and Alzheimer disease. Nat Med. 2000; 6(9):973–4. Epub 2000/09/06. https://doi.org/10.1038/79661 PMID: 10973311.
7. Mosher KI, Wyss-Coray T. Microglial dysfunction in brain aging and Alzheimer's disease. Biochem Pharmacol. 2014; 88(4):594–604. Epub 2014/01/22. https://doi.org/10.1016/j.bcp.2014.01.008 PMID: 24445162.
8. Keren-Shaul H, Spinrad A, Weiner A, Matcovitch-Natan O, Dvir-Szternfeld R, Ulland TK, et al. A Unique Microglia Type Associated with Restricting Development of Alzheimer's Disease. Cell. 2017; 169(7):1276–90 e17. Epub 2017/06/13. https://doi.org/10.1016/j.cell.2017.05.018 PMID: 28602351.
9. Olah M, Menon V, Habib N, Taga MF, Ma Y, Yung CJ, et al. Single cell RNA sequencing of human microglia uncovers a subset associated with Alzheimer's disease. Nat Commun. 2020; 11(1):6129. Epub 2020/12/02. https://doi.org/10.1038/s41467-020-19737-2 PMID: 33257666.
10. Masuda T, Sankowski R, Staszewski O, Bottcher C, Amann L, Sagar, et al. Spatial and temporal heterogeneity of mouse and human microglia at single-cell resolution. Nature. 2019; 566(7744):388–92. Epub 2019/02/15. https://doi.org/10.1038/s41586-019-0924-x PMID: 30760929.
11. Prinz M, Masuda T, Wheeler MA, Quintana FJ. Microglia and Central Nervous System-Associated Macrophages-From Origin to Disease Modulation. Annu Rev Immunol. 2021; 39:251–77. Epub 2021/02/09. https://doi.org/10.1146/annurev-immunol-093019-110159 PMID: 33556248.
12. Van Hove H, Martens L, Scheyltjens I, De Vlaminck K, Pombo Antunes AR, De Prijck S, et al. A single-cell atlas of mouse brain macrophages reveals unique transcriptional identities shaped by ontogeny and tissue environment. Nat Neurosci. 2019; 22(6):1021–35. Epub 2019/05/08. https://doi.org/10.1038/s41593-019-0393-4 PMID: 31061494.
13. Utz SG, See P, Mildenberger W, Thion MS, Silvin A, Lutz M, et al. Early Fate Defines Microglia and Non-parenchymal Brain Macrophage Development. Cell. 2020; 181(3):557–73 e18. Epub 2020/04/08. https://doi.org/10.1016/j.cell.2020.03.021 PMID: 32259484.
14. Li Q, Cheng Z, Zhou L, Darmanis S, Neff NF, Okamoto J, et al. Developmental Heterogeneity of Microglia and Brain Myeloid Cells Revealed by Deep Single-Cell RNA Sequencing. Neuron. 2019; 101(2):207–23.e10. Epub 2019/01/05. https://doi.org/10.1016/j.neuron.2018.12.006 PMID: 30606613.
15. Hammond TR, Dufort C, Dissing-Olesen L, Giera S, Young A, Wysoker A, et al. Single-Cell RNA Sequencing of Microglia throughout the Mouse Lifespan and in the Injured Brain Reveals Complex Cell-State Changes. Immunity. 2019; 50(1):253–71.e6. Epub 2018/11/26. https://doi.org/10.1016/j.immuni.2018.11.004 PMID: 30471926.
16. Kreisel T, Wolf B, Keshet E, Licht T. Unique role for dentate gyrus microglia in neuroblast survival and in VEGF-induced activation. Glia. 2019; 67(4):594–618. Epub 2018/11/20. https://doi.org/10.1002/glia.23505 PMID: 30453385.
17. Marshall GP 2nd, Deleyrolle LP, Reynolds BA, Steindler DA, Laywell ED. Microglia from neurogenic and non-neurogenic regions display differential proliferative potential and neuroblast support. Front Cell Neurosci. 2014; 8:180. Epub 2014/08/01. https://doi.org/10.3389/fncel.2014.00180 PMID: 25076873.
18. Ribeiro Xavier AL, Kress BT, Goldman SA, Lacerda de Menezes JR, Nedergaard M. A Distinct Population of Microglia Supports Adult Neurogenesis in the Subventricular Zone. J Neurosci. 2015; 35(34):11848–61. Epub 2015/08/28. https://doi.org/10.1523/JNEUROSCI.1217-15.2015 PMID: 26311768.
19. Diaz-Aparicio I, Paris I, Sierra-Torre V, Plaza-Zabala A, Rodriguez-Iglesias N, Marquez-Ropero M, et al. Microglia Actively Remodel Adult Hippocampal Neurogenesis through the Phagocytosis

Secretome. J Neurosci. 2020; 40(7):1453–82. Epub 2020/01/04. https://doi.org/10.1523/JNEUROSCI.0993-19.2019 PMID: 31896673.

20. Chintamen S, Imessadouene F, Kernie SG. Immune Regulation of Adult Neurogenic Niches in Health and Disease. Front Cell Neurosci. 2020; 14:571071. Epub 2021/02/09. https://doi.org/10.3389/fncel.2020.571071 PMID: 33551746.

21. Willis EF, MacDonald KPA, Nguyen QH, Garrido AL, Gillespie ER, Harley SBR, et al. Repopulating Microglia Promote Brain Repair in an IL-6-Dependent Manner. Cell. 2020; 180(5):833–46.e16. Epub 2020/03/07. https://doi.org/10.1016/j.cell.2020.02.013 PMID: 32142677.

22. Blaiss CA, Yu TS, Zhang G, Chen J, Dimchev G, Parada LF, et al. Temporally specified genetic ablation of neurogenesis impairs cognitive recovery after traumatic brain injury. J Neurosci. 2011; 31(13):4906–16. Epub 2011/04/01. https://doi.org/10.1523/JNEUROSCI.5265-10.2011 PMID: 21451029.

23. Scopa C, Marrocco F, Latina V, Ruggeri F, Corvaglia V, La Regina F, et al. Impaired adult neurogenesis is an early event in Alzheimer's disease neurodegeneration, mediated by intracellular Abeta oligomers. Cell Death Differ. 2020; 27(3):934–48. Epub 2019/10/09. https://doi.org/10.1038/s41418-019-0409-3 PMID: 31591472.

24. Moreno-Jimenez EP, Flor-Garcia M, Terreros-Roncal J, Rabano A, Cafini F, Pallas-Bazarra N, et al. Adult hippocampal neurogenesis is abundant in neurologically healthy subjects and drops sharply in patients with Alzheimer's disease. Nat Med. 2019; 25(4):554–60. Epub 2019/03/27. https://doi.org/10.1038/s41591-019-0375-9 PMID: 30911133.

25. Dranovsky A, Hen R. Hippocampal neurogenesis: regulation by stress and antidepressants. Biol Psychiatry. 2006; 59(12):1136–43. Epub 2006/06/27. https://doi.org/10.1016/j.biopsych.2006.03.082 PMID: 16797263.

26. Choi SH, Bylykbashi E, Chatila ZK, Lee SW, Pulli B, Clemenson GD, et al. Combined adult neurogenesis and BDNF mimic exercise effects on cognition in an Alzheimer's mouse model. Science. 2018; 361(6406). Epub 2018/09/08. https://doi.org/10.1126/science.aan8821 PMID: 30190379.

27. Berdugo-Vega G, Arias-Gil G, Lopez-Fernandez A, Artegiani B, Wasielewska JM, Lee CC, et al. Increasing neurogenesis refines hippocampal activity rejuvenating navigational learning strategies and contextual memory throughout life. Nat Commun. 2020; 11(1):135. Epub 2020/01/11. https://doi.org/10.1038/s41467-019-14026-z PMID: 31919362.

28. Artegiani B, Lyubimova A, Muraro M, van Es JH, van Oudenaarden A, Clevers H. A Single-Cell RNA Sequencing Study Reveals Cellular and Molecular Dynamics of the Hippocampal Neurogenic Niche. Cell Rep. 2017; 21(11):3271–84. Epub 2017/12/16. https://doi.org/10.1016/j.celrep.2017.11.050 PMID: 29241552.

29. Yu TS, Zhang G, Liebl DJ, Kernie SG. Traumatic brain injury-induced hippocampal neurogenesis requires activation of early nestin-expressing progenitors. J Neurosci. 2008; 28(48):12901–12. Epub 2008/11/28. https://doi.org/10.1523/JNEUROSCI.4629-08.2008 PMID: 19036984.

30. Bohlen CJ, Bennett FC, Bennett ML. Isolation and Culture of Microglia. Curr Protoc Immunol. 2019; 125(1):e70. Epub 2018/11/11. https://doi.org/10.1002/cpim.70 PMID: 30414379.

31. Yona S, Kim KW, Wolf Y, Mildner A, Varol D, Breker M, et al. Fate mapping reveals origins and dynamics of monocytes and tissue macrophages under homeostasis. Immunity. 2013; 38(1):79–91. Epub 2013/01/01. https://doi.org/10.1016/j.immuni.2012.12.001 PMID: 23273845.

32. Reu P, Khosravi A, Bernard S, Mold JE, Salehpour M, Alkass K, et al. The Lifespan and Turnover of Microglia in the Human Brain. Cell Rep. 2017; 20(4):779–84. Epub 2017/07/27. https://doi.org/10.1016/j.celrep.2017.07.004 PMID: 28746864.

33. Elmore MR, Najafi AR, Koike MA, Dagher NN, Spangenberg EE, Rice RA, et al. Colony-stimulating factor 1 receptor signaling is necessary for microglia viability, unmasking a microglia progenitor cell in the adult brain. Neuron. 2014; 82(2):380–97. Epub 2014/04/20. https://doi.org/10.1016/j.neuron.2014.02.040 PMID: 24742461.

34. Butovsky O, Jedrychowski MP, Moore CS, Cialic R, Lanser AJ, Gabriely G, et al. Identification of a unique TGF-beta-dependent molecular and functional signature in microglia. Nat Neurosci. 2014; 17(1):131–43. Epub 2013/12/10. https://doi.org/10.1038/nn.3599 PMID: 24316888.

35. Kim JS, Kolesnikov M, Peled-Hajaj S, Scheyltjens I, Xia Y, Trzebanski S, et al. A Binary Cre Transgenic Approach Dissects Microglia and CNS Border-Associated Macrophages. Immunity. 2021; 54(1):176–90 e7. Epub 2020/12/18. https://doi.org/10.1016/j.immuni.2020.11.007 PMID: 33333014.

36. Bennett ML, Bennett FC, Liddelow SA, Ajami B, Zamanian JL, Fernhoff NB, et al. New tools for studying microglia in the mouse and human CNS. Proc Natl Acad Sci U S A. 2016; 113(12):E1738–46. Epub 2016/02/18. https://doi.org/10.1073/pnas.1525528113 PMID: 26884166.

37. Brunschwig EB, Wilson K, Mack D, Dawson D, Lawrence E, Willson JK, et al. PMEPA1, a transforming growth factor-beta-induced marker of terminal colonocyte differentiation whose expression is

maintained in primary and metastatic colon cancer. Cancer Res. 2003; 63(7):1568–75. Epub 2003/04/03. PMID: 12670906.

38. Goldmann T, Wieghofer P, Jordao MJ, Prutek F, Hagemeyer N, Frenzel K, et al. Origin, fate and dynamics of macrophages at central nervous system interfaces. Nat Immunol. 2016; 17(7):797–805. Epub 2016/05/03. https://doi.org/10.1038/ni.3423 PMID: 27135602.

39. Li Q, Barres BA. Microglia and macrophages in brain homeostasis and disease. Nat Rev Immunol. 2018; 18(4):225–42. Epub 2017/11/21. https://doi.org/10.1038/nri.2017.125 PMID: 29151590.

40. Mrdjen D, Pavlovic A, Hartmann FJ, Schreiner B, Utz SG, Leung BP, et al. High-Dimensional Single-Cell Mapping of Central Nervous System Immune Cells Reveals Distinct Myeloid Subsets in Health, Aging, and Disease. Immunity. 2018; 48(3):599. Epub 2018/03/22. https://doi.org/10.1016/j.immuni.2018.02.014 PMID: 29562204.

41. Zhan L, Fan L, Kodama L, Sohn PD, Wong MY, Mousa GA, et al. A MAC2-positive progenitor-like microglial population is resistant to CSF1R inhibition in adult mouse brain. Elife. 2020; 9. Epub 2020/10/16. https://doi.org/10.7554/eLife.51796 PMID: 33054973.

42. Tansley S, Uttam S, Urena Guzman A, Yaqubi M, Pacis A, Parisien M, et al. Single-cell RNA sequencing reveals time- and sex-specific responses of mouse spinal cord microglia to peripheral nerve injury and links ApoE to chronic pain. Nat Commun. 2022; 13(1):843. Epub 2022/02/13. https://doi.org/10.1038/s41467-022-28473-8 PMID: 35149686.

43. Mendes MS, Majewska AK. An overview of microglia ontogeny and maturation in the homeostatic and pathological brain. Eur J Neurosci. 2021; 53(11):3525–47. Epub 2021/04/10. https://doi.org/10.1111/ejn.15225 PMID: 33835613.

44. Lawson LJ, Perry VH, Dri P, Gordon S. Heterogeneity in the distribution and morphology of microglia in the normal adult mouse brain. Neuroscience. 1990; 39(1):151–70. Epub 1990/01/01. https://doi.org/10.1016/0306-4522(90)90229-w PMID: 2089275.

45. Ayata P, Badimon A, Strasburger HJ, Duff MK, Montgomery SE, Loh YE, et al. Epigenetic regulation of brain region-specific microglia clearance activity. Nat Neurosci. 2018; 21(8):1049–60. Epub 2018/07/25. https://doi.org/10.1038/s41593-018-0192-3 PMID: 30038282.

46. Chistiakov DA, Killingsworth MC, Myasoedova VA, Orekhov AN, Bobryshev YV. CD68/macrosialin: not just a histochemical marker. Lab Invest. 2017; 97(1):4–13. Epub 2016/11/22. https://doi.org/10.1038/labinvest.2016.116 PMID: 27869795.

47. Lein ES, Hawrylycz MJ, Ao N, Ayres M, Bensinger A, Bernard A, et al. Genome-wide atlas of gene expression in the adult mouse brain. Nature. 2007; 445(7124):168–76. Epub 2006/12/08. https://doi.org/10.1038/nature05453 PMID: 17151600.

48. Stevens B, Allen NJ, Vazquez LE, Howell GR, Christopherson KS, Nouri N, et al. The classical complement cascade mediates CNS synapse elimination. Cell. 2007; 131(6):1164–78. Epub 2007/12/18. https://doi.org/10.1016/j.cell.2007.10.036 PMID: 18083105.

49. Schafer DP, Lehrman EK, Kautzman AG, Koyama R, Mardinly AR, Yamasaki R, et al. Microglia sculpt postnatal neural circuits in an activity and complement-dependent manner. Neuron. 2012; 74(4):691–705. Epub 2012/05/29. https://doi.org/10.1016/j.neuron.2012.03.026 PMID: 22632727.

50. Rahpeymai Y, Hietala MA, Wilhelmsson U, Fotheringham A, Davies I, Nilsson AK, et al. Complement: a novel factor in basal and ischemia-induced neurogenesis. EMBO J. 2006; 25(6):1364–74. Epub 2006/02/25. https://doi.org/10.1038/sj.emboj.7601004 PMID: 16498410.

51. Marques-Torrejon MA, Williams CAC, Southgate B, Alfazema N, Clements MP, Garcia-Diaz C, et al. LRIG1 is a gatekeeper to exit from quiescence in adult neural stem cells. Nat Commun. 2021; 12(1):2594. Epub 2021/05/12. https://doi.org/10.1038/s41467-021-22813-w PMID: 33972529 that is developing cancer therapeutics, including glioblastoma. The other authors declare no competing interests.

52. Parkhurst CN, Gan WB. Microglia dynamics and function in the CNS. Curr Opin Neurobiol. 2010; 20(5):595–600. Epub 2010/08/14. https://doi.org/10.1016/j.conb.2010.07.002 PMID: 20705452.

53. Haynes SE, Hollopeter G, Yang G, Kurpius D, Dailey ME, Gan WB, et al. The P2Y12 receptor regulates microglial activation by extracellular nucleotides. Nat Neurosci. 2006; 9(12):1512–9. Epub 2006/11/23. https://doi.org/10.1038/nn1805 PMID: 17115040.

54. Stence N, Waite M, Dailey ME. Dynamics of microglial activation: a confocal time-lapse analysis in hippocampal slices. Glia. 2001; 33(3):256–66. Epub 2001/03/10. PMID: 11241743.

55. Butovsky O, Weiner HL. Microglial signatures and their role in health and disease. Nat Rev Neurosci. 2018; 19(10):622–35. Epub 2018/09/13. https://doi.org/10.1038/s41583-018-0057-5 PMID: 30206328.

56. Ransohoff RM, Perry VH. Microglial physiology: unique stimuli, specialized responses. Annu Rev Immunol. 2009; 27:119–45. Epub 2009/03/24. https://doi.org/10.1146/annurev.immunol.021908.132528 PMID: 19302036.

57. Kierdorf K, Masuda T, Jordao MJC, Prinz M. Macrophages at CNS interfaces: ontogeny and function in health and disease. Nat Rev Neurosci. 2019; 20(9):547–62. Epub 2019/07/31. https://doi.org/10.1038/s41583-019-0201-x PMID: 31358892.

58. Safaiyan S, Besson-Girard S, Kaya T, Cantuti-Castelvetri L, Liu L, Ji H, et al. White matter aging drives microglial diversity. Neuron. 2021; 109(7):1100–17 e10. Epub 2021/02/20. https://doi.org/10.1016/j.neuron.2021.01.027 PMID: 33606969.

59. Mathys H, Adaikkan C, Gao F, Young JZ, Manet E, Hemberg M, et al. Temporal Tracking of Microglia Activation in Neurodegeneration at Single-Cell Resolution. Cell Rep. 2017; 21(2):366–80. Epub 2017/10/12. https://doi.org/10.1016/j.celrep.2017.09.039 PMID: 29020624.

60. Jordao MJC, Sankowski R, Brendecke SM, Sagar, Locatelli G, Tai YH, et al. Single-cell profiling identifies myeloid cell subsets with distinct fates during neuroinflammation. Science. 2019; 363(6425). Epub 2019/01/27. https://doi.org/10.1126/science.aat7554 PMID: 30679343.

61. Glass CK, Saijo K, Winner B, Marchetto MC, Gage FH. Mechanisms underlying inflammation in neurodegeneration. Cell. 2010; 140(6):918–34. Epub 2010/03/23. https://doi.org/10.1016/j.cell.2010.02.016 PMID: 20303880.

62. Liddelow SA, Guttenplan KA, Clarke LE, Bennett FC, Bohlen CJ, Schirmer L, et al. Neurotoxic reactive astrocytes are induced by activated microglia. Nature. 2017; 541(7638):481–7. Epub 2017/01/19. https://doi.org/10.1038/nature21029 PMID: 28099414.

63. Cribbs DH, Berchtold NC, Perreau V, Coleman PD, Rogers J, Tenner AJ, et al. Extensive innate immune gene activation accompanies brain aging, increasing vulnerability to cognitive decline and neurodegeneration: a microarray study. J Neuroinflammation. 2012; 9:179. Epub 2012/07/25. https://doi.org/10.1186/1742-2094-9-179 PMID: 22824372.

64. Villeda SA, Luo J, Mosher KI, Zou B, Britschgi M, Bieri G, et al. The ageing systemic milieu negatively regulates neurogenesis and cognitive function. Nature. 2011; 477(7362):90–4. Epub 2011/09/03. https://doi.org/10.1038/nature10357 PMID: 21886162.

65. Elmore MRP, Hohsfield LA, Kramar EA, Soreq L, Lee RJ, Pham ST, et al. Replacement of microglia in the aged brain reverses cognitive, synaptic, and neuronal deficits in mice. Aging Cell. 2018; 17(6):e12832. Epub 2018/10/03. https://doi.org/10.1111/acel.12832 PMID: 30276955.

66. Rogers JT, Morganti JM, Bachstetter AD, Hudson CE, Peters MM, Grimmig BA, et al. CX3CR1 deficiency leads to impairment of hippocampal cognitive function and synaptic plasticity. J Neurosci. 2011; 31(45):16241–50. Epub 2011/11/11. https://doi.org/10.1523/JNEUROSCI.3667-11.2011 PMID: 22072675.

67. Masuda T, Amann L, Sankowski R, Staszewski O, Lenz M, P DE, et al. Novel Hexb-based tools for studying microglia in the CNS. Nat Immunol. 2020; 21(7):802–15. Epub 2020/06/17. https://doi.org/10.1038/s41590-020-0707-4 PMID: 32541832.

68. van Wageningen TA, Vlaar E, Kooij G, Jongenelen CAM, Geurts JJG, van Dam AM. Regulation of microglial TMEM119 and P2RY12 immunoreactivity in multiple sclerosis white and grey matter lesions is dependent on their inflammatory environment. Acta Neuropathol Commun. 2019; 7(1):206. Epub 2019/12/13. https://doi.org/10.1186/s40478-019-0850-z PMID: 31829283.

69. Yuan J, Ge H, Liu W, Zhu H, Chen Y, Zhang X, et al. M2 microglia promotes neurogenesis and oligodendrogenesis from neural stem/progenitor cells via the PPARgamma signaling pathway. Oncotarget. 2017; 8(12):19855–65. Epub 2017/04/21. https://doi.org/10.18632/oncotarget.15774 PMID: 28423639.

70. Yang Y, Ye Y, Kong C, Su X, Zhang X, Bai W, et al. MiR-124 Enriched Exosomes Promoted the M2 Polarization of Microglia and Enhanced Hippocampus Neurogenesis After Traumatic Brain Injury by Inhibiting TLR4 Pathway. Neurochem Res. 2019; 44(4):811–28. Epub 2019/01/11. https://doi.org/10.1007/s11064-018-02714-z PMID: 30628018.

71. Choi JY, Kim JY, Kim JY, Park J, Lee WT, Lee JE. M2 Phenotype Microglia-derived Cytokine Stimulates Proliferation and Neuronal Differentiation of Endogenous Stem Cells in Ischemic Brain. Exp Neurobiol. 2017; 26(1):33–41. Epub 2017/03/01. https://doi.org/10.5607/en.2017.26.1.33 PMID: 28243165.

72. Krasemann S, Madore C, Cialic R, Baufeld C, Calcagno N, El Fatimy R, et al. The TREM2-APOE Pathway Drives the Transcriptional Phenotype of Dysfunctional Microglia in Neurodegenerative Diseases. Immunity. 2017; 47(3):566–81 e9. Epub 2017/09/21. https://doi.org/10.1016/j.immuni.2017.08.008 PMID: 28930663.

73. Sierra A, Encinas JM, Deudero JJ, Chancey JH, Enikolopov G, Overstreet-Wadiche LS, et al. Microglia shape adult hippocampal neurogenesis through apoptosis-coupled phagocytosis. Cell Stem Cell. 2010; 7(4):483–95. Epub 2010/10/05. https://doi.org/10.1016/j.stem.2010.08.014 PMID: 20887954.

74. Wakselman S, Bechade C, Roumier A, Bernard D, Triller A, Bessis A. Developmental neuronal death in hippocampus requires the microglial CD11b integrin and DAP12 immunoreceptor. J Neurosci. 2008; 28(32):8138–43. Epub 2008/08/08. https://doi.org/10.1523/JNEUROSCI.1006-08.2008 PMID: 18685038.

75. Yagi S, Galea LAM. Sex differences in hippocampal cognition and neurogenesis. Neuropsychopharmacology. 2019; 44(1):200–13. Epub 2018/09/15. https://doi.org/10.1038/s41386-018-0208-4 PMID: 30214058.

76. Yagi S, Splinter JEJ, Tai D, Wong S, Wen Y, Galea LAM. Sex Differences in Maturation and Attrition of Adult Neurogenesis in the Hippocampus. eNeuro. 2020; 7(4). Epub 2020/06/27. https://doi.org/10.1523/ENEURO.0468-19.2020 PMID: 32586842.

77. Sala Frigerio C, Wolfs L, Fattorelli N, Thrupp N, Voytyuk I, Schmidt I, et al. The Major Risk Factors for Alzheimer's Disease: Age, Sex, and Genes Modulate the Microglia Response to Abeta Plaques. Cell Rep. 2019; 27(4):1293–306 e6. Epub 2019/04/25. https://doi.org/10.1016/j.celrep.2019.03.099 PMID: 31018141.

78. Villa A, Gelosa P, Castiglioni L, Cimino M, Rizzi N, Pepe G, et al. Sex-Specific Features of Microglia from Adult Mice. Cell Rep. 2018; 23(12):3501–11. Epub 2018/06/21. https://doi.org/10.1016/j.celrep.2018.05.048 PMID: 29924994.

79. Bennett ML, Viaene AN. What are activated and reactive glia and what is their role in neurodegeneration? Neurobiol Dis. 2021; 148:105172. Epub 2020/11/11. https://doi.org/10.1016/j.nbd.2020.105172 PMID: 33171230.

80. Eggen BJ, Raj D, Hanisch UK, Boddeke HW. Microglial phenotype and adaptation. J Neuroimmune Pharmacol. 2013; 8(4):807–23. Epub 2013/07/25. https://doi.org/10.1007/s11481-013-9490-4 PMID: 23881706.